Studies on subcellular localization of a moonlighting protein, enolase, and its foci formation

Natsuko MIURA

2013

CONTENTS

GENERAL INTRODUCTION

In the post-genomic era, it is becoming increasingly important to analyze how molecules in a single cell play individual roles on each specific occasion. Proteins, one of the cellular components, were previously believed to have only a single function. Therefore, other molecules, such as RNAs or peptides, were believed to have multiple functions and to compensate for the small numbers of protein-coding genes in a cell. However, it is now clear that some proteins have more than one function. The discoveries in the 1980s that the lens protein crystallin is similar to glycolytic enzymes opened up the potentiality of proteins once again. The examples of multifunctional proteins, called "moonlighting proteins" by Jeffery in 1999, are increasing year by year. It is now reported that 10 of 10 glycolytic enzymes and 7 of 8 TCA cycle enzymes, as well as chaperones and histone proteins, are moonlighting proteins. Moonlighting proteins have different functions depending on their time or location of production. Therefore, analyzing changes in the localization of moonlighting proteins is highly important. Revealing how moonlighting proteins perform more than one function will disclose the hidden living machinery of the cell. Although some moonlighting proteins are reported to be functional outside the cell, their secretion machineries are not known in all organisms. Determining the translocation pathway of glycolytic enzymes will be a feasible approach to analyze the molecular basis of moonlighting. In addition, development of suitable cultivation methods for analyzing intercellular proteins is necessary for further research.

Moonlighting proteins—history, molecular mechanisms, and evolution

The word "moonlighting" had been used to mean "commit crimes at night" in 19th-century Ireland[1,2], and now, this term is used as an informal intransitive verb to describe taking on a second job [2]. The compound term moonlighting proteins was first defined by Jeffery in 1999 (Jeffery 1999). According to Jeffery, moonlighting proteins are proteins with more than one function. These proteins are not cleaved or post-translationally modified, but they perform different functions in the same or in different locations (Jeffery 1999, Fig. 1).

---

[1]moonlight. (n.d.). *Online Etymology Dictionary*. Retrieved August 26, 2012, from Dictionary.com website: http://dictionary.reference.com/browse/moonlight

[2]moonlight. (n.d.). *Collins English Dictionary - Complete & Unabridged 10th Edition*. Retrieved August 26, 2012, from Dictionary.com website: http://dictionary.reference.com/browse/moonlight

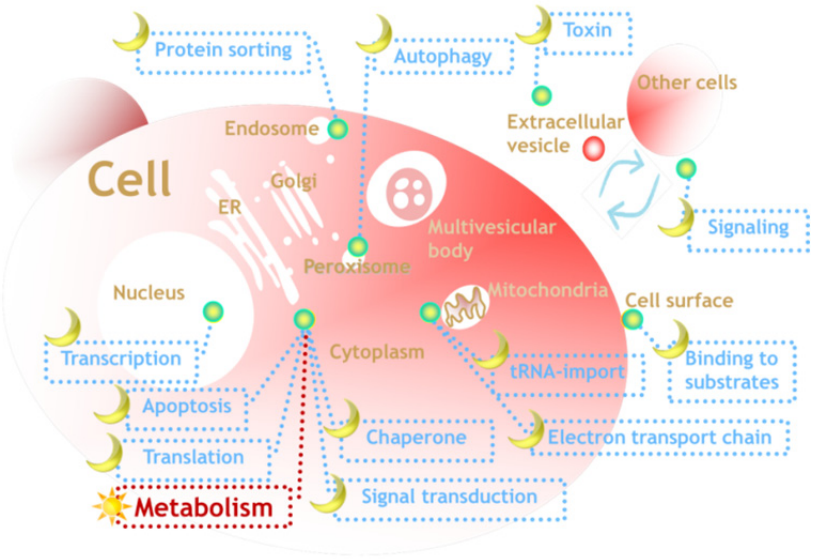

Fig.1 Moonlighting proteins

The first examples of moonlighting proteins were lens crystallins, three of which were found to be identical to metabolic enzymes, namely lactate dehydrogenase, enolase, and aldolase (Wistow and Piatigorsky 1987, Piatigorsky and Wistow 1989, Piatigorsky 1998, Wistow et al. 1988). Surprisingly, these enzymes were purified from lens that retained enzymatic activity, suggesting that these proteins function as both structural proteins and metabolic enzymes (True and Carroll 2002, Graw 2009). A number of proteins have been subsequently found to have more than one function. A remarkable feature of moonlighting proteins is that, as a primary function, they often take part in central cellular processes such as transcription, translation, signaling, and metabolism (Fig. 2, Pancholi 2001). These proteins are also essential in the synthetic minimal genome created by Glass and colleagues (Glass et al. 2006).

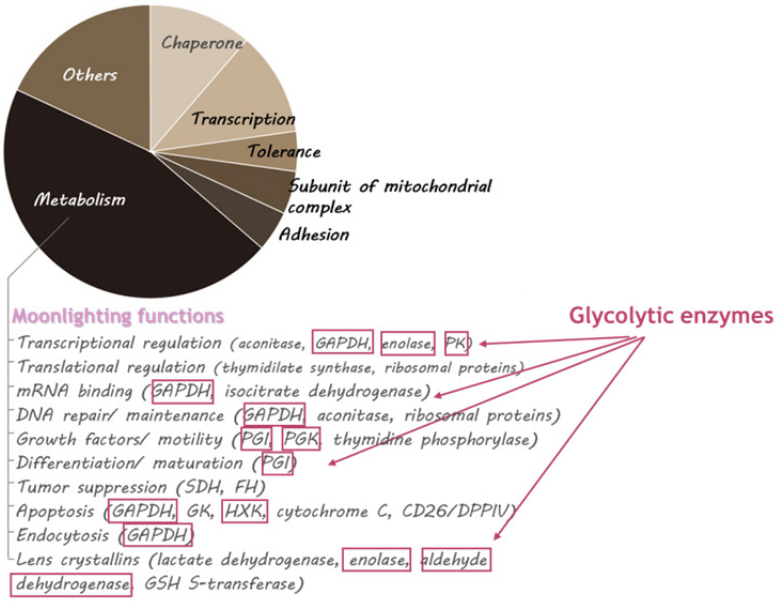

Fig. 2 Previously-known roles of moonlighting proteins (modified from Sriram et al. 2005)

Two important points arise when considering the importance of moonlighting proteins. First, because of the presence of moonlighting proteins, the living system can reduce the number of protein-coding genes. It is known that *Escherichia coli* has fewer number of protein-coding genes than the number of biological processes needed for survival (Thiele et al. 2009). With the help of moonlighting proteins, organisms can fill the gap and save energy to maintain a large number of gene sets. Second, these proteins possibly reflect the primitive form of proteins. The moonlighting abilities of proteins may have evolved over generations and diverged as homologs in the late stages of life (Piatigorsky et al. 2003). Indeed, most mammalian proteins have homologs that have different functions or localization sites in the cell. In some cases, the number of homologs is greater in "later" organisms, such as mammals, than in "earlier" organisms, such as prokaryotes (Jensen 1976, Parsot et al. 1987). Investigating how moonlighting proteins could have more than one function may reveal the features of polypeptides necessary to form organisms, to evolve, and to stand the test of immense amount of time.

The reason why moonlighting proteins can have more than one function or the molecular basis of moonlighting proteins is not completely understood. Some insights have been gained from the following two examples: tau protein and moonlighting peptides (Rodríguez et al. 2012). Tau protein, which is unfolded in its native state (Jeganathan et al. 2008), is known to change its conformation to bind to neuronal axons or form aggregates that cause neuronal diseases (Kolarva et al. 2012). In addition, it has been demonstrated that a single amino acid residue can govern the folding of tau (Margittai and Langen, 2006). Rodríguez and colleagues (2012) demonstrated that a part of proteins (in their case, peptides) govern multiple functions. From these examples, it might be said that a single protein is likely to regulate multiple functions by changing its conformation to change the exposed surface of individual domains.

Some researchers consider that moonlighting is not a special feature. Proteins can change their three-dimensional folding to change their interactions with other proteins. In association with proper proteins, the moonlighting protein can play a role in some biological events (Tompa et al. 2005, Sugase et al. 2007). These proteins are sometimes called "intrinsically unstructured proteins (IUPs)" (Dunker et al. 2001) and can be considered as a subset of moonlighting proteins, although the differences between IUPs and moonlighting proteins are under debate (Hernández et al. 2012). It may be said that changing protein structure to accommodate associated biomolecules (Sinthuvanich et al. 2012) is the molecular mechanism of moonlighting. In that case, a part of the moonlighting protein domain can be attributed to moonlighting properties, and the domain can change its conformation easily. The important question here is whether the specific amino acid sequence, which participates in a certain function exists.

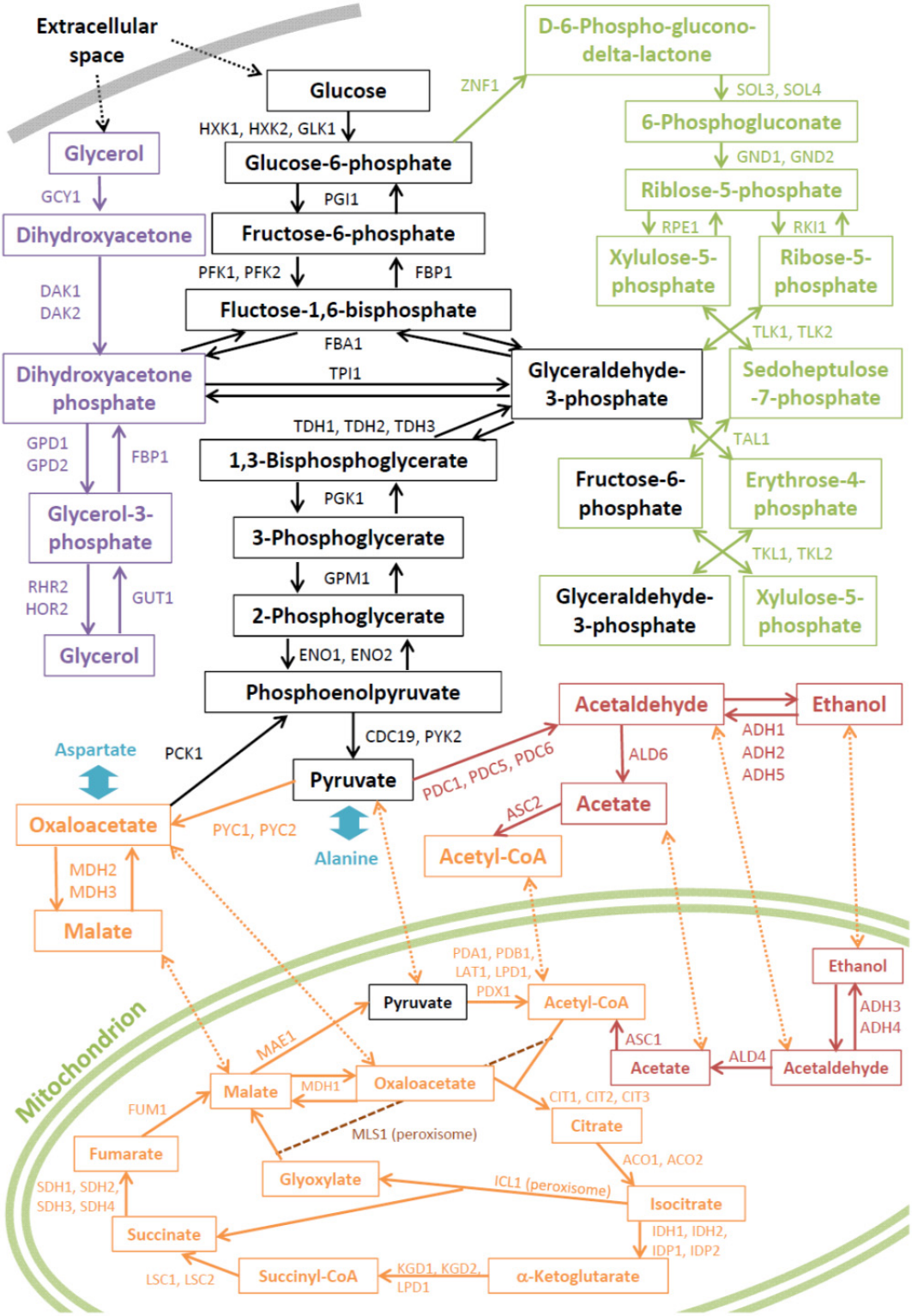

Fig. 3 Glycolysis and the associated pathways

Violet: Glycerol synthetic pathway, Black: Glycolytic pathway, Green: Pentose-5-phosphate pathway, Red: Ethanol or acetate fermentation, Orange: TCA cycle.

Glycolytic enzymes and their moonlighting functions

Glycolytic enzymes are conserved proteins in most biological species. They are also present in *Achaea*, *Mycoplasma* (free living organism with the smallest genome), cyanobacteria, and algae. Glycolytic enzymes are an important class of proteins that produce energy from carbon sources under anaerobic conditions. The glycolytic pathway is connected to and crossed with important metabolic pathways such as the pentose phosphate pathway, TCA cycle, amino acid synthesis, and lipid metabolism (Fig. 3). Thus, they are vital cellular components.

Of the 43 moonlighting proteins reported before 2005, 47% of them were previously known as glycolytic enzymes (Pancholi 2001, Sriram et al. 2005). It is known today that all glycolytic enzymes are moonlighting proteins (Table 1). The moonlighting functions of glycolytic enzymes are often related to important cellular machineries such as transcription, translation, signal transduction, cell movement, and trafficking.

Table 1 Glycolytic enzymes and examples of their moonlighting functions

Glycolytic enzymes	Genes (*S. cerevisiae*)	Moonlighting functions	organisms	References
Hexokinase	*HXK1, HXK2,GLK1*	porin binding	rat	Fiek et al. 1982, Linden et al. 1982
		appoptosis	mouse	Majewski et al. 2004
Phosphoglucose isomerase	*PGI1*	neuroleukin	mouse	Chaput et al. 1988, Faik et al. 1988
		autocrine motility factor	human	Watanabe et al. 1996
		diff./maturation mediator	mouse	Gurney et al. 1986
		nerve growth factor	human	Xu et al. 1996
Phosphofructokinase	*PFK1, PFK2*	microautophagy	*Pichia pastoris*	Gancedo and Flores, 2008
		RNA processing	*B. subtilis* and *S. aureus*	Commichau et al. 2009, Roux et al. 2011
Fructose bisphosphate aldolase	*FBA1*	V-ATPase assembly	human	Lu et al. 2001, Lu et al. 2004
		actin binding	*in vitro*, rabbit, apicomplexan parasites	Arnold and Pette 1968, Wang et al. 1996, Jewett and Sibley, 2003
Trisephosphate isomerase	*TPI1*	adhesin	*C. neoformans*	Furuya and Ikeda 2009
Glyceraldehyde phosphate	*TDH1, TDH2, TDH3*	uracil DNAglycosylase	human	Meyer-Siegler et al. 1991
		apoptosis	human	Berry and Boulton 2000, Tatton et al. 2000
		endocytosis	rat	Robbins et al. 1995
		microtuble bundling	rabbit	Kumagai and Sakai 1983
		transcriptional activation	human	Zheng et al. 2003
		sperm motility	mouse	Miki et al. 2004
		RNA binding	human	Nagy and Rigby 1995
Phosphoglycerate kinase	*PGK1*	plasmin reductase	human	Lay et al. 2000
		primer-recognition protein	*P. sativum*	Bryant et al. 2000
Phosphoglycerate mutase	*GPM1*	plasminogen receptor	*C. albicans*	Poltermann et al. 2007
Enolase	*ENO1, ENO2*	lens crystallin	turtle, duck, mouse	Wistow et al. 1988, Piatigorsky and Wisdow, 1989
		plasminogen receptor	human	Miles et al. 1991
		heat-shock protein	*S. cerevisiae*	Iida and Yahara 1985
		binding to cytoskeleton	rabbit	Walsh et al. 1989
		transcriptional activation	*A. thaliana*	Lee et al. 2002
		homotypic vacuole fusion	*S. cerevisiae*	Decker and Wickner 2006
		nutichondrial tRNA import	*S. cerevisiae*	Entelis et al. 2006
		RNA processing	*B. subtilis* and *S. aureus*	Commichau et al. 2009, Roux et al. 2011
Pyruvate kinase	*CDC19, PYK2*	thyroid hormone binding	rat	Kato et al. 1989
		adhesion for yeast mannan	*L. lactis*	Katakura et al. 2010
		transcriptional activation	human	Gao et al. 2012
		NTP synthesis	*P. aeruginosa*	Chopade et al. 1997

Moonlighting glycolytic enzymes often need to change their location to perform their moonlighting functions. For example, enolase has at least seven moonlighting functions (Table 1) both inside and outside the cell. Extracellular enolase, which is a glycolytic enzyme, is a virulence factor in *Candida albicans* and some parasites (Jong et al. 2003, Avilan et al. 2011). Enolase has been found in small vesicles outside the cell (Oliveira et al. 2010, Oliveira et al. 2010) and in the cell

wall (Edwards et al. 1999). In addition, enolase is secreted in a sequence-dependent manner (Lopez-Villar et al. 2006, Yang et al. 2011) and is present in the cell wall with no enzymatic activity, but it binds to plasminogen and helps pathogens invade (Swenerton et al. 2011). Enolase is also found in viral particles (Bechtel et al. 2005, Chertova et al. 2006, Shaw et al. 2008) and is required for transcription in Sendai virus (Ogino et al. 2001). Therefore, enolase is a therapeutic target for many diseases, including candidiasis (van Deventer et al. 1996, Capello et al. 2011). Another extracellular glycolytic enzyme, phosphoglucose isomerase, enhances the motility of tumor cells (Dobashi et al. 2006) and acts like a cytokine (Torimura et al. 2001), although it possesses no enzymatic activity outside the cell (Tsutsumi et al. 2003). However, the secretory pathway of glycolytic enzymes such as enolase and phosphoglucose isomerase remains to be revealed. This pathway appears to be unconventional because glycolytic enzymes have no known secretion signals. Therefore, in this study, we analyze the secretory pathway of glycolytic enzymes.

Conventional secretion pathways of proteins have been extensively studied using *Saccharomyces cerevisiae* (Schekman 2010). In addition, we may reveal unknown secretion pathways of proteins; however, it remains challenging because the trafficking patterns inside the organism are not completely known.

Secretion pathways of *S. cerevisiae*

S. cerevisiae is a model organism for determining the secretion pathways of proteins and lipids because it has known gene sets that work in various protein transport pathways. Schekman (Novick and Schekman 1979, Novick et al. 1980, Schekman 2010), Ohsumi (Nagatogawa et al. 2009, Mizushima et al, 2011), and numerous other researchers (Bryant and Stevens 1998, Hua et al. 2002, Gall et al. 2002) have developed various temperature-sensitive and/or knockout mutants of *S. cerevisiae* to investigate protein transport pathways. The outline of *S. cerevisiae* secretion pathways is shown in Fig. 4.

Protein transport mediated by membrane cargoes is regulated by various membrane-associated proteins or protein complexes (Whyte and Munro 2002, Bröcker et al. 2010). Among the proteins involved in transport machineries, soluble N-ethylmaleimide-sensitive factor attachment protein receptor (SNARE) proteins are the most extensively studied (Ungar and Hughson, 2003, Duman and Forte 2003, Jahn and Scheller 2006, Table 2). As shown in Table 2, 13 of 23 SNAREs are essential, and at least 9 proteins are used in more than two of the pathways described in Fig. 4. Of these, pathways 5 and 6 are considered conventional secretion pathways, while the others (17 and secretion via early endosome) are unconventional. The pathway used by unconventionally secreted moonlighting glycolytic enzymes remains unknown.

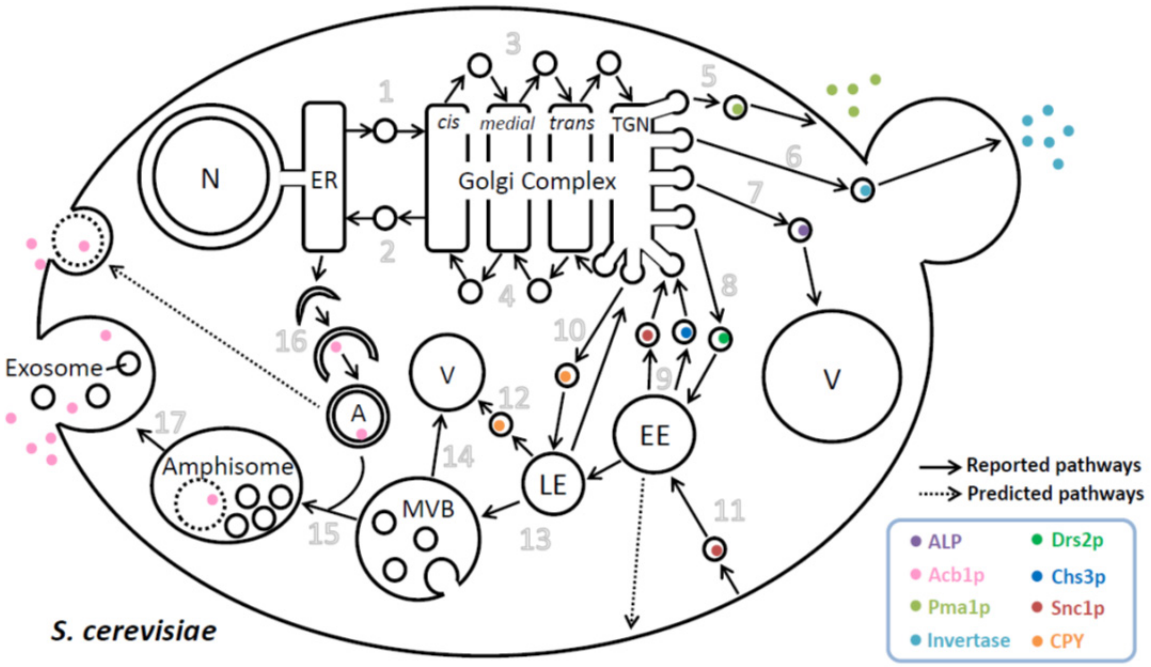

Fig. 4 Overview of protein secretion pathways in *S. cerevisiae* (modified figure from Brocker et al. 2010 and Muthusamy et al. 2009) N: Nucleus, ER: Endoplasmic reticulum, TGN: Trans-Golgi network, V: Vacuole, EE: Early endosome, LE: Late endosome, MVB: Multi vesicular vody, A: Autophagosome. See also Table 2 for detailed names of pathways numbered.

Spatial arrangement of glycolytic enzymes

Fluorescent protein tags have been used to determine the subcellular localization of proteins (Phillips 2001, Rudner and Losick 2010, Chudakov et al. 2010), especially in *S. cerevisiae*. Dr. Erin O'Shea and Dr. Jonathan Weissman at UCSF generated a collection of *S. cerevisiae* open reading frames that were tagged at the carboxy terminal using the coding sequence of *Aequorea victoria* GFP (S65T) (Huh et al. 2003). A database of GFP-fused protein localization (yeast GFP localization database, http://yeastgfp.yeastgenome.org/) is now available. In addition, many other databases for the subcellular localization of proteins are available (LOCATE, subcellular localization database for mouse and human, http://locate.imb.uq.edu.au/; eSLAB, a database of protein subcellular localization annotation for eukaryotic organisms, http://gpcr.biocomp.unibo.it/esldb/; Organelle DB, a database of organelle proteins and subcellular structures/complexes, http://organelledb.lsi.umich.edu/; locDB, collection of experimental annotations for the subcellular localization of proteins in human and weed, http://www.rostlab.org/services/locDB/). Apart from its property to accumulate in the nucleus to some extent (Seibel et al. 2007) and that its fluorescence intensity is affected by oxygen concentration (Yang et al. 1996, Takahashi et al. 2006), GFP is useful

and is one of the frequently used fluorescent proteins. Accumulation, aggregation, and association of proteins inside the cell often indicate some cellular machineries or protein functions (Kanda et al. 1998, Bence et al. 2001, Tilsner and Oparka 2010). Therefore, protein localization in response to certain stimuli has been extensively researched to discover novel cellular machineries (Sakai et al. 1997, Dastoor and Dreyer 2001, An et al. 2008, Narayanaswamy et al. 2009, Noree et al. 2010).

Spatial rearrangement of moonlighting proteins, including glycolytic enzymes, is highly important for their various functions. In several organisms and cells, some glycolytic enzymes have been reported to associate with the cytoskeleton (Masters 1984, Stephan et al. 1986), erythrocyte membrane (Campanella et al. 2005), or muscle (Brooks and Storey 1988), or to associate with each other (Mowbray and Moses 1976, Anderson et al. 1995, Mazzola and Sirover 2003). In a few species of protozoa, including *Trypanosoma brucei*, glycolytic enzymes are contained in a membrane-enclosed organelle called glycosome (Hannaert and Michels 1994, Bakker et al. 2000). Association of glycolytic enzymes is believed to facilitate metabolism (Beeckmans et al. 1990, Amar et al. 2008). In addition, changes in the localization of glycolytic enzymes suggest other moonlighting functions (Dastoor and Dreyer 2001, Decker and Wickner 2006).

The intracellular assembly of glycolytic enzymes has been observed in mammalian cells; one of the glycolytic enzymes, i.e., GAPDH conjugated with GFP, was found to form fluorescent foci under hypoxia (Agbor et al. 2011). Agbor and colleagues (2011) demonstrated that the spatial rearrangement was dependent on modification by small ubiquitin-like modifier (SUMOylation). However, its function and sensing machineries involved in the initiation of spatial reorganization of the glycolytic enzyme under hypoxia remain known. It is important to determine the location of the foci because GAPDH has been reported to translocate into the nucleus under hypoxia (Stannard et al. 2004). Moreover, according to the *S. cerevisiae* database (yeast GFP localization database, http://yeastgfp.yeastgenome.org/), subcellular localization of glycolytic enzymes fused with GFP (GFP clones, Invitrogen) is uniform in the cytoplasm. Therefore, it is uncertain whether glycolytic enzymes change their localization in response to hypoxia, especially in yeast cells. When the spatial rearrangement of glycolytic enzymes occurs under hypoxia, the relocalization of enzymes may affect cell physiology.

Table 2 SNARE proteins involved in secretion pathway

	Pathway	SNARE protein-coding genes	Essential / or nonessential	Description
1	ER to Golgi	**SED5**	essential	cis-Golgi t-SNARE syntaxin required for vesicular transport between the ER and the Golgi complex, binds at least 9 SNARE proteins
		YKT6	essential	Vesicle membrane protein (v-SNARE) with acyltransferase activity; involved in trafficking to and within the Golgi, endocytic trafficking to the vacuole, and vacuolar fusion; membrane localization due to prenylation at the carboxy-terminus
		SEC22	nonessential	R-SNARE protein; assembles into SNARE complex with Bet1p, Bos1p and Sed5p; cycles between the ER and Golgi complex; involved in anterograde and retrograde transport between the ER and Golgi; synaptobrevin homolog
		BOS1	essential	v-SNARE (vesicle specific SNAP receptor), localized to the endoplasmic reticulum membrane and necessary for vesicular transport from the ER to the Golgi
		BET1	essential	Type II membrane protein required for vesicular transport between the endoplasmic reticulum and Golgi complex; v-SNARE with similarity to synaptobrevins
2	Golgi to ER	**SEC22**	nonessential	-
		UFE1	essential	t-SNARE required for retrograde vesicular traffic and homotypic ER membrane fusion; forms a complex with the SNAREs Sec22p, Sec20p and Use1p to mediate fusion of Golgi-derived vesicles at the ER
		SEC20	essential	Membrane glycoprotein v-SNARE involved in retrograde transport from the Golgi to the ER; required for N- and O-glycosylation in the Golgi but not in the ER; interacts with the Dsl1p complex through Tip20p
		USE1	essential	Essential SNARE protein localized to the ER, involved in retrograde traffic from the Golgi to the ER; forms a complex with the SNAREs Sec22p, Sec20p and Ufe1p
		GOS1	nonessential	v-SNARE protein involved in Golgi transport, homolog of the mammalian protein GOS-28/GS28
		YKT6	essential	Vesicle membrane protein (v-SNARE) with acyltransferase activity; involved in trafficking to and within the Golgi, endocytic trafficking to the vacuole, and vacuolar fusion; membrane localization due to prenylation at the carboxy-terminus
3	Golgi (cis to TGN)	**GOS1**	nonessential	-
		SFT1	essential	Intra-Golgi v-SNARE, required for transport of proteins between an early and a later Golgi compartment
4	Golgi (TGN to cis)	**YKT6**	essential	-
		SED5	essential	-
		VTI1	essential	Protein involved in cis-Golgi membrane traffic; v-SNARE that interacts with two t-SNARES, Sed5p and Pep12p; required for multiple vacuolar sorting pathways
		SLT1	essential	Essential SNARE protein localized to the ER, involved in retrograde traffic from the Golgi to the ER; forms a complex with the SNAREs Sec22p, Sec20p and Ufe1p
5	TGN to CM (light)	SSO1/2	nonessential	Plasma membrane t-SNAREs involved in fusion of secretory vesicles at the plasma membrane
		SNC1/2	nonessential	Vesicle membrane receptor protein (v-SNARE); involved in the fusion between Golgi-derived secretory vesicles with the plasma membrane; proposed to be involved in endocytosis; member of the synaptobrevin/VAMP family of R-type v-SNARE proteins

Table 2 SNARE proteins involved in secretion pathway (continued)

5	TGN to CM (light)	SEC9	essential	t-SNARE protein important for fusion of secretory vesicles with the plasma membrane; similar to but not functionally redundant with Spo20p; SNAP-25 homolog
6	TGN to CM (hevy)	**YKT6**	essential	-
7	TGN to V	VAM3	nonessential	Syntaxin-like vacuolar t-SNARE that functions with Vam7p in vacuolar protein trafficking; mediates docking/fusion of late transport intermediates with the vacuole; has an acidic di-leucine sorting signal and C-terminal transmembrane region
		VTI1	essential	-
		VAM7	nonessential	Vacuolar SNARE protein that functions with Vam3p in vacuolar protein trafficking; has an N-terminal PX domain (phosphoinositide-binding module) that binds PtdIns-3-P and mediates membrane binding; SNAP-25 homolog
		NYV1	nonessential	v-SNARE component of the vacuolar SNARE complex involved in vesicle fusion; inhibits ATP-dependent Ca(2+) transport activity of Pmc1p in the vacuolar membrane
8	TGN to EE	**SNC1/2**	nonessential	-
9	EE to TGN	TLG2	nonessential	Syntaxin-like t-SNARE that forms a complex with Tlg1p and Vti1p and mediates fusion of endosome-derived vesicles with the late Golgi; binds Vps45p, which prevents Tlg2p degradation and also facilitates t-SNARE complex formation; homologous to mammalian SNARE protein syntaxin 16 (Sx16)
		VTI1	essential	-
		TLG1	essential	Essential t-SNARE that forms a complex with Tlg2p and Vti1p and mediates fusion of endosome-derived vesicles with the late Golgi; binds the docking complex VFT (Vps fifty-three) through interaction with Vps51p
		YKT6	essential	-
10	TGN to LE	PEP12	nonessential	Target membrane receptor (t-SNARE) for vesicular intermediates traveling between the Golgi apparatus and the vacuole; controls entry of biosynthetic, endocytic, and retrograde traffic into the prevacuolar compartment; syntaxin
		VTI1	essential	-
		SYN8	nonessential	Endosomal SNARE related to mammalian syntaxin 8
11	CM to EE	**SYN8**	nonessential	-
		SNC1/2	nonessential	-
12	LE to V	**VTI1**	essential	-
		VAM7	nonessential	-
13	LE to MVB			
14	MVB to V			
15	MVB to Amphisome			
16	ER to A			
17	Amphisome to CM			

N: Nucleus, ER: Endoplasmic reticulum, TGN: Trans-Golgi network, V: Vacuole, EE: Early endosome, LE: Late endosome, MVB: Multi vesicular body, A: Autophagosome, CM: Cell membrane. Under line: unessential. Bold: used in several pathways

Cell physiology under hypoxia

Hypoxia is a condition in which the cell is deprived of adequate oxygen supply. Many studies define hypoxia at ≤2 mg/L of dissolved oxygen (DO) in an aqueous environment (Eby et al. 2002, Buzzelli et al. 2002). In cultured mammalian cells, 1% atmospheric oxygen is regarded to be a hypoxic state, while 21% is regarded to be the normal oxygen concentration (normoxia) (Hagen et al. 2003, Frezza et al. 2011). A hypoxic state for mammalian cells often occurs *in vivo* when the oxygen supply is limited (Denko 2008). Hypoxia is reported to correlate with many diseases including heart attack, cancer, and stroke (Lyer et al. 1998). Some tumor cells are known to response to hypoxia and obtain increased metastatic activity (Zhong et al. 1999), radiation resistance (Eyler and Rich 2008), and drug resistance (Teicher 1994). Baker's yeast, *S. cerevisiae* is also well known to response to hypoxia during fermentation (Simeonidis et al. 2010). When sufficient amounts of nutrients are supplied, *S. cerevisiae* produces CO_2 in metabolic processes, which decreases the oxygen concentration in the medium (Rosenfeld et al. 2003). The hypoxic responses of yeast cells have attracted attention because researchers have proved that these responses have some roles in infection by pathogenic fungi including *C. albicans* (Grahl and Cramer, 2010) and *Aspergillus fumigatus* (Grahl et al. 2011, Fller and Rhodes, 2012).

The hypoxic responses of mammalian cells and yeasts are common to some extent (Fig. 5). Because molecular oxygen is required for heme and sterol biosynthesis, the production of these molecules is reduced under hypoxia (Hickman et al. 2011, Siso et al. 2012). In addition, oxygen deprivation triggers the release of reactive oxygen species (ROS) from mitochondria (Chandel et al. 1998, Chandel et al. 2000, Blokhina et al. 2003, Guzy et al. 2005, Bell et al. 2007, Murphy 2009) by unknown mechanisms (Guzy and Schumacker 2006). These primary hypoxic responses trigger the following secondary responses. In mammalian cells, cytosolic ROS stabilize hypoxia-inducible factor 1α (HIF-1α) (Guzy and Schumacker 2006), which is a major regulator for the hypoxic response. ROS (Gillespie et al. 2009, Ruchko et al., 2009, Poyton et al. 2009, Gillespie et al. 2010), and HIF-1α (Ortiz-Barahona et al. 2010, Tanimoto et al. 2010, Schödel et al. 2011, Liu et al. 2012) oxidizes or binds several specific bases in hypoxia-responsive elements (HRE). Genes containing HRE in their promoters include those that encode aldolase, enolase, and lactate dehydrogenase (Semenza et al. 1996). In mammalian cells, transcription of *PKM2*, a gene that encodes one of the glycolytic enzymes, is activated by HIF-1α (Luo et al. 2011). Interestingly, Pkm2p interacts directly with the HIF-1α subunit and acts as a coactivator (Luo et al. 2011). In addition to HRE oxidization, mitochondria-generated ROS trigger AMP-activated protein kinase signaling (Jung et al. 2008, Emerling et al. 2009, Mungai et al. 2011, Kim et al. 2011) through several reaction steps (Mungai et al. 2011). Yeast cells have no HIF-1α homologs (Rytkönen and Storz 2011); however, yeast has HRE clusters in the promoters of *TDH2*, *ALD6,* and genes involved in amino acid metabolism (Ferreira et al. 2007). It is also reported that hexose transporters are affected under a hypoxic condition,

accelerating the uptake of extracellular hexoses (Rintala et al. 2008). Because of the resemblance of responses to hypoxia between *S. cerevisiae* and mammalian cells, some researchers regard *S. cerevisiae* as one of the model organisms for studying a hypoxic response (Netzar and Breitenbach 2010). Mitochondrial ROS production can also be measured in yeast cells. Using dihydroethidium and MitoSOX Red, cellular and mitochondria-specific reactive oxygen can be measured *in vivo* (Quaranta et al. 2011). 2′, 7′-dichlorofluorescin diacetate can also be used as a cytosolic indicator of ROS (Gomes et al. 2005, Bonini et al. 2006, Al-Mehdi et al. 2012).

Hypoxic response mechanisms have been extensively studied by culturing yeast cells in a media depleted in oxygen by sparging with N_2 (Kwast et al. 2002, Lai et al. 2008). Kwast and colleagues (2002) have shown that N_2-induced hypoxia triggers global changes in metabolic gene induction. Interestingly, these two researches do not report enolase gene induction, in contrast to that in mammalian cells (Kwast et al. 2002, Lai et al. 2008). In *S. cerevisiae*, a decrease in heme and sterol levels induces the activation of transcription by Upc2p, while a decrease in only heme levels inhibits Rox1p and Mot3p to repress hypoxic genes, thus inducing hypoxia-responsive genes (Grahl and Cramer, 2010). The connection between sterol- and heme-regulated responses to hypoxia, and their correlation with mitochondrial ROS production have not been described.

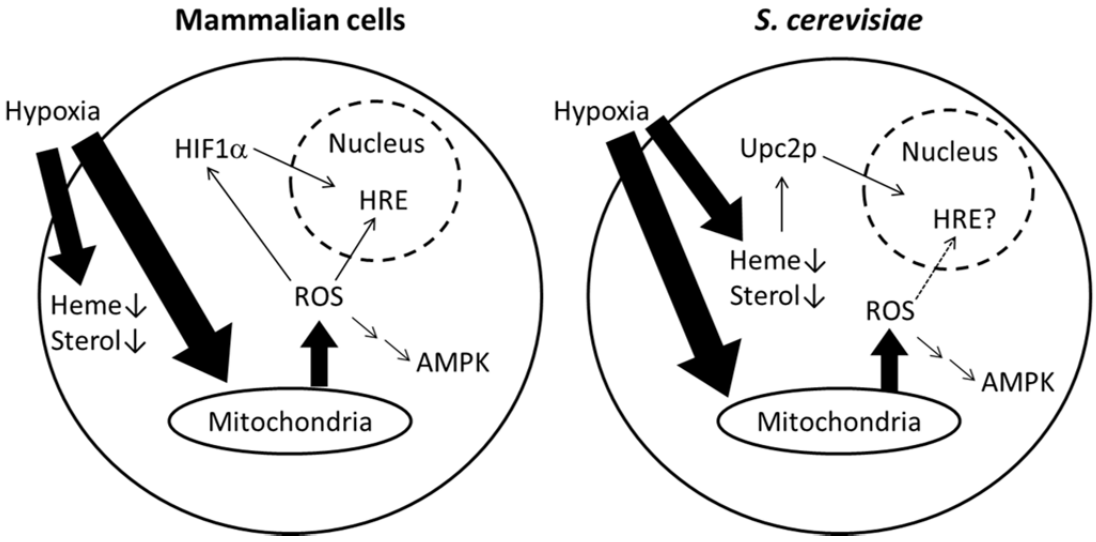

Fig. 5 Outline of similar hypoxic responses in mammalian and yeast cells

In response to hypoxia, cultured mammalian cells produce large amounts of lactate, alanine (Brecht and Groot 1994, Chateil et al. 2001), and acetate. On the other hand, *S. cerevisiae* cells grown under hypoxic conditions are known to produce ethanol, glycerol, succinic acid, and alanine (Chico et al. 1978, Gleason et al. 2011) as end products of glycolysis. These changes in metabolites, especially overproduction of alanine under hypoxia, are also known in flies (Feala et al. 2007) and

plants (Rocha et al. 2010). In rat heart, aspartate production is significantly increased under hypoxia relative to normoxia (Rumsey et al. 1999). Alanine, aspartate, and other amino acids are considered to protect cells from hypoxic injury (Weinberg et al. 1990, Brecht and Groot 1994). In yeasts, conversion of pyruvate to oxaloacetate and aspartate is a part of gluconeogenesis, which enables yeast cells to grow on non-sugar carbon sources such as ethanol, glycerol, or peptone (Foy and Bhattacharjee 1977, Eschrich et al. 2002).

In case of gluconeogenesis in yeast, acetyl-CoA carboxylase produces malonyl-CoA under regulation by SNF1, which is a yeast functional homolog of mammalian AMP kinase (Woods et al. 1994). Malonyl-CoA is the first precursor of long fatty acids (Fig. 6). Without acetyl-CoA carboxylase, yeasts need fatty acids to survive and arrest the G2/M phase of the cell cycle (Al-Feel et al. 2003). Acetyl-CoA carboxylase is also vital in mammalian cells, as RNAi of acetyl-CoA carboxylase inhibits the growth of prostate cancer cells and mouse embryos (Abu-Elheiga et al. 2005, Brusselmans et al. 2005).

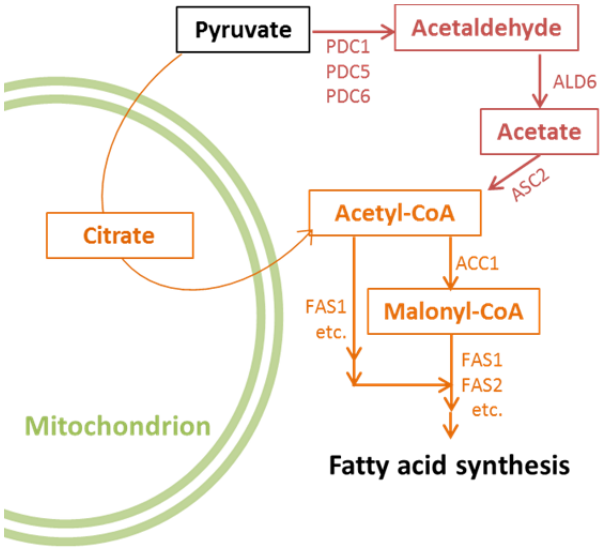

Fig. 6 Fatty acid synthesis from pyruvate in *S. cerevisiae*

There had been several reports demonstrating that cobalt and other metal ions induce cellular responses, which resemble the hypoxic response. However, reports also suggest that there are some differences between these two stimuli. For example, overproduction of alanine is observed under hypoxia but not in the presence of cobalt (Gleason et al. 2011). In addition, ROS generation by hypoxia and by $CoCl_2$ addition is differently inhibited by adding mitochondria-inhibiting agents to mammalian cells (Chandel et al. 2000).

Although the role of the spatial relocalization of glycolytic enzymes under hypoxia is not revealed, there is a report suggesting the importance of spatial localization of cellular components. Recently, Al-Mehdi and colleagues (2012) have revealed that mitochondria localize near the nucleus

under hypoxia to translocate ROS into the nucleus and oxidize guanine nucleotides of specific promoter DNA sequences in order to induce the expression of the vascular endothelial growth factor-encoding gene (*VFGF*) (Murphy 2012). The results suggest that regulating intracellular localization of mitochondria has an important role in the hypoxic response. If glycolytic enzymes change their localization in the cell, the role this relocation plays in cellular metabolism and the mechanisms that regulate this translocation should be investigated.

Culture instruments for cultivation of yeast cells

Suitable culture vials are needed to study hypoxia in yeast cells. A novel culture device, which can separate and co-cultivate different types of cells at the same time, is needed to investigate unknown functions of unconventionally secreted proteins.

Because yeast cells experience a hypoxic environment during fermentation, vials for fermentation can be used to investigate their hypoxic responses. Glass vials have been developed by Matsumoto et al. (2002) for laboratory-scale fermentation. A small pump can be used to create normoxia (sufficient oxygen concentration) in these vials.

Several different culture vials, including Millicell culture inserts (Millipore, Germany), IdMOC (Kurabo, Osaka, Japan), and Alvetex (TaKaRa Bio, Otsu, Japan), have been developed for the investigation of intercellular proteins. Because these chambers developed are for mammalian cells, only a small volume of microbial cells can be cultured using these chambers. These chambers can be used for co-cultivation of different cells, but first, a model system to investigate the intercellular function of extracellular proteins should be constructed. Following which, large-scale culture vials for separated co-cultivation should be developed.

To determine the molecular machineries that enable proteins to perform moonlighting functions, investigating the mechanism regulating the localization of moonlighting proteins is a plausible approach. In this regard, the following questions arise:

- Is there a specific amino acid sequence that participates in certain localizations?
- Through which transporting pathway is the change in localization achieved?
- By which cellular mechanism or sensing pathway is the change in localization regulated?
- Does the change in localization correlate with cell physiology?

These issues were addressed in this study using the moonlighting glycolytic enzyme, enolase, as a model.

REFERENCES

1. Abu-Elheiga L, Matzuk MM, Kordari P, Oh W, Shaikenov T, Gu Z, Wakil SJ (2005) Mutant mice lacking acetyl-CoA carboxylase 1 are embryonically lethal. Proc. Natl. Acad. Sci. USA. 102:12011-12016.
2. Agbor TA, Cheong A, Comerford KM, Scholz CC, Bruning U, Clarke A, Cummins EP, Cagney G, Taylor CT (2011) Small ubiquitin-related modifier (SUMO)-1 promotes glycolysis in hypoxia. J. Biol. Chem. 286:4718-4726.
3. Al-Feel W, DeMar JC, Wakil SJ (2003) A Saccharomyces cerevisiae mutant strain defective in acetyl-CoA carboxylase arrests at the G2/M phase of the cell cycle. Proc. Natl. Acad. Sci. USA. 100:3095-3100.
4. Al-Mehdi AB, Pastukh VM, Swiger BM, Reed DJ, Patel MR, Bardwell GC, Pastukh VV, Alexeyev MF, Gillespie MN (2012) Perinuclear mitochondrial clustering creates an oxidant-rich nuclear domain required for hypoxia-induced transcription. Sci. Signal. 5:ra47.
5. Amar P, Legent G, Thellier M, Ripoll C, Bernot G, Nystrom T, Saier MH Jr, Norris V (2008) A stochastic automaton shows how enzyme assemblies may contribute to metabolic efficiency. BMC Syst. Biol. 2:27.
6. An S, Kumar R, Sheets ED, Benkovic SJ (2008) Reversible compartmentalization of de novo purine biosynthetic complexes in living cells. Science. 320:103-106.
7. Anderson LE, Goldhaber-Gordon IM, Li D, Tang XY, Xiang M, Prakash N (1995) Enzyme-enzyme interaction in the chloroplast: glyceraldehyde-3-phosphate dehydrogenase, triose phosphate isomerase and aldolase. Planta 196:245-255.
8. Arnold H, Pette D (1968) Binding of glycolytic enzymes to structure proteins of the muscle. Eur. J. Biochem. 6:163–171.
9. Avilán L, Gualdrón-López M, Quiñones W, González-González L, Hannaert V, Michels PA, Concepción JL (2011) Enolase: a key player in the metabolism and a probable virulence factor of trypanosomatid parasites: perspectives for its use as a therapeutic target. Enzyme Res. 2011:932549.
10. Bakker BM, Mensonides FI, Teusink B, van Hoek P, Michels PA, Westerhoff HV (2000) Compartmentation protects trypanosomes from the dangerous design of glycolysis. Proc. Natl. Acad. Sci. USA. 97:2087-2092.
11. Bechtel JT, Winant RC, Ganem D (2005) Host and viral proteins in the virion of Kaposi's sarcoma-associated herpesvirus. J. Virol. 79:4952-4964.
12. Beeckmans S, Van Driessche E, Kanarek L (1990) Clustering of sequential enzymes in the glycolytic pathway and the citric acid cycle. J. Cell Biochem. 43:297-306.
13. Bell EL, Klimova TA, Eisenbart J, Moraes CT, Murphy MP, Budinger GR, Chandel NS (2007) The Qo site of the mitochondrial complex III is required for the transduction of

hypoxic signaling via reactive oxygen species production. J. Cell Biol. 177:1029-1036.

14. Bence NF, Sampat RM, Kopito RR (2001) Impairment of the ubiquitin-proteasome system by protein aggregation. Science. 292:1552-1555.
15. Berry MD, Boulton AA (2000) Glyceraldehyde-3-phosphate dehydrogenase and apoptosis. J. Neurosci. Res. 60:150–154.
16. Blokhina O, Virolainen E, Fagerstedt KV (2003) Antioxidants, oxidative damage and oxygen deprivation stress: a review. Ann. Bot. 91:179-194.
17. Bonini MG, Rota C, Tomasi A, Mason RP (2006) The oxidation of 2',7'-dichlorofluorescin to reactive oxygen species: a self-fulfilling prophesy? Free Radic. Biol. Med. 40:968-975.
18. Brecht M, Groot H (1994) Protection from hypoxic injury in cultured hepatocytes by glycine, alanine, and serine. Amino Acids 6:25-35.
19. Bröcker C, Engelbrecht-Vandré S, Ungermann C (2010) Multisubunit tethering complexes and their role in membrane fusion. Curr. Biol. 20:R943-952.
20. Brooks SP, Storey KB (1988) Subcellular enzyme binding in glycolytic control: in vivo studies with fish muscle. Am. J. Physiol. 255:R289-94.
21. Brusselmans K, De Schrijver E, Verhoeven G, Swinnen JV (2005) RNA interference-mediated silencing of the acetyl-CoA-carboxylase-alpha gene induces growth inhibition and apoptosis of prostate cancer cells. Cancer Res. 65:6719-6725.
22. Bryant JA, Brice DC, Fitchett PN, Anderson LE (2000) A novel DNA-binding protein associated with DNA polymerase-alpha in pea stimulates polymerase activity on infrequently primed templates. J. Exp. Bot. 51:1945-1947.
23. Buzzelli CP, Luettich RA, Powers SP, Peterson CH, McNinch JE, Pinckney JL, Paerl HW (2002) Estimating the spatial extent of bottom-water hypoxia and habitat degradation in a shallow estuary. Mar. Eco. Prog. Seri. 230:103-112.
24. Campanella ME, Chu H, Low PS (2005) Assembly and regulation of a glycolytic enzyme complex on the human erythrocyte membrane. Proc. Natl. Acad. Sci. USA. 102:2402-2407.
25. Chandel NS, Maltepe E, Goldwasser E, Mathieu CE, Simon MC, Schumacker PT (1998) Mitochondrial reactive oxygen species trigger hypoxia-induced transcription. Proc. Natl. Acad. Sci. USA. 95:11715-11720.
26. Chandel NS, McClintock DS, Feliciano CE, Wood TM, Melendez JA, Rodriguez AM, Schumacker PT (2000) Reactive oxygen species generated at mitochondrial complex III stabilize hypoxia-inducible factor-1alpha during hypoxia: a mechanism of O_2 sensing. J. Biol. Chem. 275:25130-25138.
27. Chaput M, Claes V, Portetelle D, Cludts I, Cravador A, Burny A, Gras H, Tartar A (1988) The neurotrophic factor neuroleukin is 90% homologous with phosphohexose isomerase. Nature 332:454–455.

28. Chateil J, Biran M, Thiaudière E, Canioni P, Merle M (2001) Metabolism of [1-^{13}C]glucose and [2-^{13}C]acetate in the hypoxic rat brain. Neurochem. Int. 38:399-407.
29. Chertova E, Chertov O, Coren LV, Roser JD, Trubey CM, Bess JW Jr, Sowder RC 2nd, Barsov E, Hood BL, Fisher RJ, Nagashima K, Conrads TP, Veenstra TD, Lifson JD, Ott DE (2006) Proteomic and biochemical analysis of purified human immunodeficiency virus type 1 produced from infected monocyte-derived macrophages. J. Virol. 80:9039 -9052.
30. Chico E, Olavarría JS, Núnez de Castro I (1978) L-Alanine as an end product of glycolysis in *Saccharomyces cerevisiae* growing under different hypoxic conditions. Antonie. Van. Leeuwenhoek 44:193-201.
31. Chopade BA, Shankar S, Sundin GW, Mukhopadhyay S, Chakrabarty AM (1997) Characterization of membrane-associated *Pseudomonas aeruginosa* Ras-like protein Pra, a GTP-binding protein that forms complexes with truncated nucleoside diphosphate kinase and pyruvate kinase to modulate GTP synthesis. J. Bacteriol. 179:2181-2188.
32. Chudakov DM, Matz MV, Lukyanov S, Lukyanov KA (2010) Fluorescent proteins and their applications in imaging living cells and tissues. Physiol. Rev. 90:1103-1163.
33. Commichau FM, Rothe FM, Herzberg C, Wagner E, Hellwig D, Lehnik-Habrink M, Hammer E, Völker U, Stülke J (2009) Mol. Cell. Proteomics 8:1350-1360.
34. Dastoor Z, Dreyer JL (2001) Potential role of nuclear translocation of glyceraldehyde-3-phosphate dehydrogenase in apoptosis and oxidative stress. J. Cell Sci. 114:1643-1653.
35. Decker BL, Wickner WT (2006) Enolase activates homotypic vacuole fusion and protein transport to the vacuole in yeast. J. Biol. Chem. 281:14523-14528.
36. Denko NC (2008) Hypoxia, HIF1 and glucose metabolism in the solid tumor. Nat. Rev. Cancer 8:705-713.
37. Dobashi Y, Watanabe H, Matsubara M, Yanagawa T, Raz A, Shimamiya T, Ooi A (2006) Autocrine motility factor/glucose-6-phosphate isomerase is a possible predictor of metastasis in bone and soft tissue tumours. J. Pathol. 208:44 -53.
38. Dunker AK, Lawson JD, Brown CJ, Williams RM, Romero P, Oh JS, Oldfield CJ, Campen AM, Ratliff CM, Hipps KW, Ausio J, Nissen MS, Reeves R, Kang C, Kissinger CR, Bailey RW, Griswold MD, Chiu W, Garner EC, Obradovic Z (2001) Intrinsically disordered protein. J. Mol. Graph. Model. 19:26-59.
39. Duman JG, Forte JG (2003) What is the role of SNARE proteins in membrane fusion? Am. J. Physiol. Cell Physiol. 285:C237-249.
40. Eby LA, Crowder LB (2002) Hypoxia-based habitat compression in the Neuse River Estuary: context-dependent shifts in behavioral avoidance thresholds. Can. J. Fish. Aquat. Sci. 59:952-965.

41. Edwards SR, Braley R, Chaffin WL (1999) Enolase is present in the cell wall of *Saccharomyces cerevisiae*. FEMS Microbiol. Lett. 177:211-216.
42. Emerling BM, Weinberg F, Snyder C, Burgess Z, Mutlu GM, Viollet B, Budinger GR, Chandel NS (2009) Hypoxic activation of AMPK is dependent on mitochondrial ROS but independent of an increase in AMP/ATP ratio. Free Radic. Biol. Med. 46:1386-1391.
43. Entelis N, Brandia I, Kamenski P, Krasheninnikov IA, Martin RP, Tarassov I (2006) A glycolytic enzyme, enolase, is recruited as a cofactor of tRNA targeting toward mitochondria in *Saccharomyces cerevisiae*. Genes Dev. 20:1609-1620.
44. Eschrich D, Kötter P, Entian KD (2002) Gluconeogenesis in Candida albicans. FEMS Yeast Res. 2:315-25.
45. Eyler CE, Rich JN (2008) Survival of the fittest: cancer stem cells in therapeutic resistance and angiogenesis. J. Clin. Oncol. 26:2839-2845.
46. Faik P, Walker JI, Redmill AA, Morgan MJ (1988) Mouse glucose-6-phosphate isomerase and neuroleukin have identical 3' sequences. Nature 332:455‑457.
47. Feala JD, Coquin L, McCulloch AD, Paternostro G (2007) Flexibility in energy metabolism supports hypoxia tolerance in *Drosophila* flight muscle: metabolomic and computational systems analysis. Mol. Syst. Biol. 3:99.
48. Ferreira TC, Hertzberg L, Gassmann M, Campos EG (2007) The yeast genome may harbor hypoxia response elements (HRE). Comp. Biochem. Physiol. C. Toxicol. Pharmacol. 46:255-263.
49. Fiek C, Benz R, Roos N, Brdiczka D (1982) Evidence for identity between the hexokinase-binding protein and the mitochondrial porin in the outer membrane of rat liver mitochondria. Biochim. Biophys. Acta. 688:429–440.
50. Foy JJ, Bhattacharjee JK (1977) Gluconeogenesis in Saccharomyces cerevisiae: determination of fructose-1,6-bisphosphatase activity in cells grown in the presence of glycolytic carbon sources. J. Bacteriol. 129:978-982.
51. Frezza C, Zheng L, Tennant DA, Papkovsky DB, Hedley BA, Kalna G, Watson DG, Gottlieb E (2011) Metabolic profiling of hypoxic cells revealed a catabolic signature required for cell survival. PLoS ONE 6:e24411.
52. Fuller KK, Rhodes JC (2012) Protein kinase A and fungal virulence: a sinister side to a conserved nutrient sensing pathway. Virulence 3:109-121.
53. Furuya H, Ikeda R (2009) Interaction of triosephosphate isomerase from the cell surface of Staphylococcus aureus and alpha-(1->3)-mannooligosaccharides derived from glucuronoxylomannan of *Cryptococcus neoformans*. Microbiology 155:2707–2713.
54. Gillespie MN, Pastukh V, Ruchko MV (2009) Oxidative DNA modifications in hypoxic signaling. Ann. N Y Acad. Sci. 1177:140-150.

55. Gillespie MN, Pastukh VM, Ruchko MV (2010) Controlled DNA "damage" and repair in hypoxic signaling. Respir. Physiol. Neurobiol. 174:244-251.
56. Gleason JE, Corrigan DJ, Cox JE, Reddi AR, McGinnis LA, Culotta VC (2011) Analysis of hypoxia and hypoxia-like states through metabolite profiling. PLoS ONE 6:e24741.
57. Gancedo C, Flores CL (2008) Moonlighting proteins in yeasts. Microbiol. Mol. Biol. Rev. 72:197-210.
58. Gao X, Wang H, Yang JJ, Liu X, Liu ZR (2012) Pyruvate kinase M2 regulates gene transcription by acting as a protein kinase. Mol. Cell 45:598-609.
59. Glass JI, Assad-Garcia N, Alperovich N, Yooseph S, Lewis MR, Maruf M, Hutchison CA 3rd, Smith HO, Venter JC (2006) Essential genes of a minimal bacterium. Proc. Natl. Acad. Sci. USA. 10:425-430.
60. Gomes A, Fernandes E, Lima JL (2005) Fluorescence probes used for detection of reactive oxygen species. J. Biochem. Biophys. Methods 65:45-80.
61. Grahl N, Cramer RA Jr. (2010) Regulation of hypoxia adaptation: an overlooked virulence attribute of pathogenic fungi? Med. Mycol. 48:1-15.
62. Grahl N, Puttikamonkul S, Macdonald JM, Gamcsik MP, Ngo LY, Hohl TM, Cramer RA (2011) In vivo hypoxia and a fungal alcohol dehydrogenase influence the pathogenesis of invasive pulmonary aspergillosis. PLoS Pathog. 7:e1002145.
63. Graw J (2009) Genetics of crystallins: cataract and beyond. Exp. Eye Res. 88:173-189.
64. Gurney ME, Heinrich SP, Lee MR, Yin HS (1986) Molecular cloning and expression of neuroleukin, a neurotrophic factor for spinal and sensory neurons. Science 234:566–574.
65. Guzy RD, Hoyos B, Robin E, Chen H, Liu L, Mansfield KD, Simon MC, Hammerling U, Schumacker PT (2005) Mitochondrial complex III is required for hypoxia-induced ROS production and cellular oxygen sensing. Cell Metab.1:401-408.
66. Guzy RD, Schumacker PT (2006) Oxygen sensing by mitochondria at complex III: the paradox of increased reactive oxygen species during hypoxia. Exp. Physiol. 91:807-819.
67. Hagen T, Taylor CT, Lam F, Moncada S (2003) Redistribution of intracellular oxygen in hypoxia by nitric oxide: effect on HIF1alpha. Science 302:1975-1978.
68. Hannaert V, Michels PA (1994) Structure, function, and biogenesis of glycosomes in kinetoplastida. J. Bioenerg. Biomembr. 26:205-212.
69. Hernández S, Amela I, Cedano J, Piñol J, Perez-Pons J, Mozo-Villarias AM, Querol E (2012) Do moonlighting proteins belong to the intrinsically disordered protein class? J. Proteomics Bioinform. 5:11.
70. Hickman MJ, Spatt D, Winston F (2011) The Hog1 mitogen-activated protein kinase mediates a hypoxic response in *Saccharomyces cerevisiae*. Genetics 188:325-338.
71. Huberts DHEW, van der Klei IJ (2010) Moonlighting proteins: An intriguing mode of

multitasking. Biochim. Biophys. Acta. 1803:520-525.

72. Huh WK, Falvo JV, Gerke LC, Carroll AS, Howson RW, Weissman JS, O'Shea EK (2003) Global analysis of protein localization in budding yeast. Nature 425:686-691.

73. Iida H, Yahara I (1985) Yeast heat-shock protein of Mr 48,000 is an isoprotein of enolase. Nature 315:688-690.

74. Iyer NV, Kotch LE, Agani F, Leung SW, Laughner E, Wenger RH, Gassmann M, Gearhart JD, Lawler AM, Yu AY, Semenza GL (1998) Cellular and developmental control of O2 homeostasis by hypoxia-inducible factor 1 alpha. Genes Dev. 12:149-162.

75. Jahn R, Scheller RH (2006) SNAREs-engines for membrane fusion. Nat. Rev. Mol. Cell Biol. 7:631-663.

76. Jeffery CJ (1999) Moonlighting proteins. Trends Biochem. Sci. 24:8-11.

77. Jeganathan S, von Bergen M, Mandelkow EM, Mandelkow E (2008) The natively unfolded character of tau and its aggregation to Alzheimer-like paired helical filaments. Biochemistry 47:10526-10539.

78. Jensen RA (1976) Enzyme recruitment in evolution of new function. Annu. Rev. Microbiol. 30:409-425.

79. Jewett TJ, Sibley LD (2003) Aldolase forms a bridge between cell surface adhesins and the actin cytoskeleton in apicomplexan parasites. Mol. Cell 11:885-894.

80. Jung SN, Yang WK, Kim J, Kim HS, Kim EJ, Yun H, Park H, Kim SS, Choe W, Kang I, Ha J (2008) Reactive oxygen species stabilize hypoxia-inducible factor-1 alpha protein and stimulate transcriptional activity via AMP-activated protein kinase in DU145 human prostate cancer cells. Carcinogenesis 29:713-721.

81. Kanda T, Sullivan KF, Wahl GM (1998) Histone-GFP fusion protein enables sensitive analysis of chromosome dynamics in living mammalian cells. Curr. Biol. 8:377-385.

82. Katakura Y, Sano R, Hashimoto T, Ninomiya K, Shioya S (2010) Lactic acid bacteria display on the cell surface cytosolic proteins that recognize yeast mannan. Appl. Microbiol. Biotechnol. 86:319-326.

83. Kato H, Fukuda T, Parkison C, McPhie P, Cheng SY (1989) Cytosolic thyroid hormone-binding protein is a monomer of pyruvate kinase. Proc. Natl. Acad. Sci. USA 86:7861-7865.

84. Kim IS, Sohn HY, Jin I (2011) Adaptive stress response to menadione-induced oxidative stress in *Saccharomyces cerevisiae* KNU5377. J. Microbiol. 49:816-823.

85. Kolarova M, García-Sierra F, Bartos A, Ricny J, Ripova D (2012) Structure and pathology of tau protein in Alzheimer disease. Int. J. Alzheimers Dis. 2012:731526.

86. Kumagai H, Sakai H (1983) A porcine brain protein (35 K protein) which bundles microtubules and its identification as glyceraldehyde 3-phosphate dehydrogenase. J. Biochem.

93:1259–1269.

87. Kwast KE, Lai LC, Menda N, James DT 3rd, Aref S, Burke PV (2002) Genomic analyses of anaerobically induced genes in *Saccharomyces cerevisiae*: functional roles of Rox1 and other factors in mediating the anoxic response. J. Bacteriol. 184:250-265.
88. Lai LC, Kissinger MT, Burke PV, Kwast KE (2008) Comparison of the transcriptomic "stress response" evoked by antimycin A and oxygen deprivation in *Saccharomyces cerevisiae*. BMC Genomics 9:627.
89. Lay AJ, Jiang XM, Kisker O, Flynn E, Underwood A, Condron R, Hogg PJ (2000) Phosphoglycerate kinase acts in tumour angiogenesis as a disulphide reductase. Nature 408:869-873.
90. Lee H, Guo Y, Ohta M, Xiong L, Stevenson B, Zhu JK (2002) LOS2, a genetic locus required for cold-responsive gene transcription encodes a bi-functional enolase. EMBO J. 21:2692-2702.
91. Linden M, Gellerfors P, Nelson BD (1982) Pore protein and the hexokinase-binding protein from the outer membrane of rat liver mitochondria are identical. FEBS Lett. 141:189–192.
92. Liu W, Shen SM, Zhao XY, Chen GQ (2012) Targeted genes and interacting proteins of hypoxia inducible factor-1. Int. J. Biochem. Mol. Biol. 3:165-178.
93. López-Villar E, Monteoliva L, Larsen MR, Sachon E, Shabaz M, Pardo M, Pla J, Gil C, Roepstorff P, Nombela C (2006) Genetic and proteomic evidences support the localization of yeast enolase in the cell surface. Proteomics 6:S107-S118.
94. Lu M, Holliday LS, Zhang L, Dunn WA Jr, Gluck SL (2001) Interaction between aldolase and vacuolar H+-ATPase: evidence for direct coupling of glycolysis to the ATP-hydrolyzing proton pump. J. Biol. Chem. 276:30407–30413.
95. Lu M, Sautin YY, Holliday LS, Gluck SL (2004) The glycolytic enzyme aldolase mediates assembly, expression, and activity of vacuolar H+-ATPase. J. Biol. Chem. 279:8732–8739.
96. Luo W, Hu H, Chang R, Zhong J, Knabel M, O'Meally R, Cole RN, Pandey A, Semenza GL (2011) Pyruvate kinase M2 is a PHD3-stimulated coactivator for hypoxia-inducible factor 1. Cell 145:732-744.
97. Majewski N, Nogueira V, Bhaskar P, Coy PE, Skeen JE, Gottlob K, Chandel NS, Thompson CB, Robey RB, Hay N (2004) Hexokinase-mitochondria interaction mediated by Akt is required to inhibit apoptosis in the presence or absence of Bax and Bak. Mol. Cell. 16:819-830.
98. Margittai M, Langen R (2006) Side chain-dependent stacking modulates tau filament structure. J. Biol. Chem. 281:37820-37827.
99. Masters C (1984) Interactions between glycolytic enzymes and components of the cytomatrix. J. Cell. Biol. 99:222s-225s.

100. Matsumoto T, Fukuda H, Ueda M, Tanaka A, Kondo A (2002) Construction of yeast strains with high cell surface lipase activity by using novel display systems based on the Flo1p flocculation functional domain. Appl. Environ. Microbiol. 68:4517-4522.
101. Mazzola JL, Sirover MA (2003) Subcellular localization of human glyceraldehyde-3-phosphate dehydrogenase is independent of its glycolytic function. Biochim. Biophys. Acta. 1622:50-56.
102. Meyer-Siegler K, Mauro DJ, Seal G, Wurzer J, deRiel JK, Sirover MA (1991) A human nuclear uracil DNA glycosylase is the 37-kDa subunit of glyceraldehyde-3-phosphate dehydrogenase. Proc. Natl. Acad. Sci. USA 88:8460–8464.
103. Miki K, Qu W, Goulding EH, Willis WD, Bunch DO, Strader LF, Perreault SD, Eddy EM, O'Brien DA (2004) Glyceraldehyde 3-phosphate dehydrogenase-S, a sperm-specific glycolytic enzyme, is required for sperm motility and male fertility. Proc. Natl. Acad. Sci. USA 101:16501–16506.
104. Miles LA, Dahlberg CM, Plescia J, Felez J, Kato K, Plow EF (1991) Role of cell-surface lysines in plasminogen binding to cells: identification of alpha-enolase as a candidate plasminogen receptor. Biochemistry 30:1682-1691.
105. Mizushima N, Yoshimori T, Ohsumi Y (2011) The role of Atg proteins in autophagosome formation. Annu. Rev. Cell Dev. Biol. 27:107-132.
106. Mowbray J, Moses V (1976) The tentative identification in *Escherichia coli* of a multienzyme complex with glycolytic activity. Eur. J. Biochem. 66:25-36.
107. Mungai PT, Waypa GB, Jairaman A, Prakriya M, Dokic D, Ball MK, Schumacker PT (2011) Hypoxia triggers AMPK activation through reactive oxygen species-mediated activation of calcium release-activated calcium channels. Mol. Cell Biol. 31:3531-3545.
108. Murphy MP (2009) How mitochondria produce reactive oxygen species. Biochem. J. 417:1-13.
109. Murphy MP (2012) Modulating mitochondrial intracellular location as a redox signal. Sci. Signal. 5:pe39.
110. Nagy E, Rigby WF (1995) Glyceraldehyde-3-phosphate dehydrogenase selectively binds AU-rich RNA in the NAD(+)-binding region (Rossmann fold). J. Biol. Chem. 270:2755-2763.
111. Nakatogawa H, Suzuki K, Kamada Y, Ohsumi Y (2009) Dynamics and diversity in autophagy mechanisms: lessons from yeast. Nat. Rev. Mol. Cell Biol. 10:458-467.
112. Narayanaswamy R, Levy M, Tsechansky M, Stovall GM, O'Connell JD, Mirrielees J, Ellington AD, Marcotte EM (2009) Widespread reorganization of metabolic enzymes into reversible assemblies upon nutrient starvation. Proc. Natl. Acad. Sci. USA. 106:10147-10152.

113. Netzer NC, Breitenbach M (2010) Metabolic changes through hypoxia in humans and in yeast as a comparable cell model. Sleep Breath 14:221-225.
114. Noree C, Sato BK, Broyer RM, Wilhelm JE (2010) Identification of novel filament-forming proteins in *Saccharomyces cerevisiae* and *Drosophila melanogaster*. J. Cell Biol. 190:541-551.
115. Novick P, Schekman R (1979) Secretion and cell-surface growth are blocked in a temperature-sensitive mutant of *Saccharomyces cerevisiae*. Proc. Natl. Acad. Sci. USA. 76:1858-1862.
116. Novick P, Field C, Schekman R (1980) Identification of 23 complementation groups required for post-translational events in the yeast secretory pathway. Cell 21:205-215.
117. Ogino T, Yamadera T, Nonaka T, Imajoh-Ohmi S, Mizumoto K (2001) Enolase, a cellular glycolytic enzyme, is required for efficient transcription of Sendai virus genome. Biochem. Biophys. Res. Commun. 285:447- 455.
118. Oliveira DL, Freire-de-Lima CG, Nosanchuk JD, Casadevall A, Rodrigues ML, Nimrichter L (2010) Extracellular vesicles from *Cryptococcus neoformans* modulate macrophage functions. Infect. Immun. 78:1601-1609.
119. Oliveira DL, Nakayasu ES, Joffe LS, Guimarães AJ, Sobreira TJ, Nosanchuk JD, Cordero RJ, Frases S, Casadevall A, Almeida IC, Nimrichter L, Rodrigues ML (2010) Characterization of yeast extracellular vesicles: evidence for the participation of different pathways of cellular traffic in vesicle biogenesis. PLoS ONE 6:e11113.
120. Ortiz-Barahona A, Villar D, Pescador N, Amigo J, del Peso L (2010) Genome-wide identification of hypoxia-inducible factor binding sites and target genes by a probabilistic model integrating transcription-profiling data and in silico binding site prediction. Nucleic Acids Res. 238:2332-2345.
121. Pancholi V (2001) Multifunctional α-enolase: its role in diseases. Cell. Mol. Life Sci. 58:902-920.
122. Parsot C, Saint-Girons I, Cohen GN (1987) Enzyme specialization during the evolution of amino acid biosynthetic pathways. Microbiol. Sci. 4: 260-262.
123. Phillips GJ (2001) Green fluorescent protein--a bright idea for the study of bacterial protein localization. FEMS Microbiol. Lett. 204:9-18.
124. Piatigorsky J, Wistow GJ (1989) Enzyme/crystallins: gene sharing as an evolutionary strategy. Cell 57:197-199.
125. Piatigorsky J (1998) Gene sharing in lens and cornea: facts and implications. Prog. Retin. Eye Res. 17:145-74.
126. Piatigorsky (2003) Crystallin genes: specialization by changes in gene regulation may precede gene duplication. J. Struct. Funct. Genomics 3:131-137.

127. Poltermann S, Kunert A, von der Heide M, Eck R, Hartmann A, Zipfel PF (2007) Gpm1p is a factor H-, FHL-1-, and plasminogen-binding surface protein of Candida albicans. J. Biol. Chem. 282:37537-37544.
128. Poyton RO, Ball KA, Castello PR (2009) Mitochondrial generation of free radicals and hypoxic signaling. Trends. Endocrinol. Metab. 20:332-340.
129. Quaranta D, Krans T, Espírito Santo C, Elowsky CG, Domaille DW, Chang CJ, Grass G (2011) Mechanisms of contact-mediated killing of yeast cells on dry metallic copper surfaces. Appl. Environ. Microbiol. 77:416-426.
130. Rintala E, Wiebe MG, Tamminen A, Ruohonen L, Penttilä M (2008) Transcription of hexose transporters of *Saccharomyces cerevisiae* is affected by change in oxygen provision. BMC Microbiol. 8:53.
131. Robbins AR, Ward RD, Oliver C (1995) A mutation in glyceraldehyde 3-phosphate dehydrogenase alters endocytosis in CHO cells. J. Cell Biol. 130:1093–1104.
132. Rocha M, Licausi F, Araújo WL, Nunes-Nesi A, Sodek L, Fernie AR, van Dongen JT (2010) Glycolysis and the tricarboxylic acid cycle are linked by alanine aminotransferase during hypoxia induced by waterlogging of *Lotus japonicus*. Plant Physiol. 152:1501-1513.
133. Rodríguez Plaza JG, Villalón Rojas A, Herrera S, Garza-Ramos G, Torres Larios A, Amero C, Zarraga Granados G, Gutiérrez Aguilar M, Lara Ortiz MT, Polanco Gonzalez C, Uribe Carvajal S, Coria R, Peña Díaz A, Bredesen DE, Castro-Obregon S, Del Rio G (2012) Moonlighting peptides with emerging function. PLoS ONE 7: e40125.
134. Rosenfeld E, Beauvoit B, Blondin B, Salmon JM (2003) Oxygen consumption by anaerobic *Saccharomyces cerevisiae* under enological conditions: effect on fermentation kinetics. Appl. Environ. Microbiol. 69:113-121.
135. Roux CM, DeMuth JP, Dunman PM (2011) Characterization of components of the Staphylococcus aureus mRNA degradosome holoenzyme-like complex. J. Bacteriol. 193:5520-5526.
136. Rudner DZ, Losick R (2010) Protein Subcellular Localization in Bacteria. Cold Spring Harb. Perspect. Biol. 2010. 2:a000307.
137. Ruchko MV, Gorodnya OM, Pastukh VM, Swiger BM, Middleton NS, Wilson GL, Gillespie MN (2009) Hypoxia-induced oxidative base modifications in the VEGF hypoxia-response element are associated with transcriptionally active nucleosomes. Free Radic. Biol. Med. 46:352-359.
138. Rumsey WL, Abbott B, Bertelsen D, Mallamaci M, Hagan K, Nelson D, Erecinska M (1999) Adaptation to hypoxia alters energy metabolism in rat heart. Am. J. Physiol. 276:H71-80.
139. Rytkönen KT, Storz JF (2011) Evolutionary origins of oxygen sensing in animals. EMBO Rep. 12:3-4.

140. Sakai N, Sasaki K, Ikegaki N, Shirai Y, Ono Y, Saito N (1997) Direct visualization of the translocation of the gamma-subspecies of protein kinase C in living cells using fusion proteins with green fluorescent protein. J. Cell Biol. 139:1465-1476.
141. Schekman R (2010) Charting the secretory pathway in a simple eukaryote. Mol. Biol. Cell 21:3781-3784.
142. Schödel J, Oikonomopoulos S, Ragoussis J, Pugh CW, Ratcliffe PJ, Mole DR (2011) High-resolution genome-wide mapping of HIF-binding sites by ChIP-seq. Blood 117:e207-217.
143. Seibel NM, Eljouni J, Nalaskowski MM, Hampe W (2007) Nuclear localization of enhanced green fluorescent protein homomultimers. Anal. Biochem. 368:95-99.
144. Semenza GL, Jiang BH, Leung SW, Passantino R, Concordet JP, Maire P, Giallongo A (1996) Hypoxia response elements in the aldolase A, enolase 1, and lactate dehydrogenase A gene promoters contain essential binding sites for hypoxia-inducible factor 1. J. Biol. Chem. 271:32529-32537.
145. Shaw ML, Stone KL, Colangelo CM, Gulcicek EE, Palese P (2008) Cellular proteins in influenza virus particles. PLoS Pathog. 6:e1000085.
146. Simeonidis E, Murabito E, Smallbone K, Westerhoff HV (2010) Why does yeast ferment? A flux balance analysis study. Biochem. Soc. Trans. 38:1225-1229.
147. Sinthuvanich C, Veiga AS, Gupta K, Gaspar D, Blumenthal R, Schneider JP (2012) Anticancer β-hairpin peptides: membrane-induced folding triggers activity. J. Am. Chem. Soc. 134:6210-6217.
148. Sriram G, Martinez JA, McCabe ER, Liao JC, Dipple KM (2005) Single-gene disorders: what role could moonlighting enzymes play? Am. J. Hum. Genet. 76:911-924.
149. Stannard C, Brown LR, Godovac-Zimmermann J (2004) New Paradigms in Cellular Function and the Need for Top-Down Proteomics. Curr. Proteomics 1:13-25.
150. Stephan P, Clarke F, Morton D (1986) The indirect binding of triose-phosphate isomerase to myofibrils to form a glycolytic enzyme mini-complex. Biochim. Biophys. Acta. 873:127-135.
151. Sugase K, Dyson HJ, Wright PE (2007) Mechanism of coupled folding and binding of an intrinsically disordered protein. Nature 447:1021-1025.
152. Swenerton RK, Zhang S, Sajid M, Medzihradszky KF, Craik CS, Kelly BL, McKerrow JH (2011) The oligopeptidase B of Leishmania regulates parasite enolase and immune evasion. J. Biol. Chem. 286:429–440.
153. Takahashi E, Takano T, Nomura Y, Okano S, Nakajima O, Sato M (2006) In vivo oxygen imaging using green fluorescent protein. Am. J. Physiol. Cell Physiol. 291:C781-787.
154. Tanimoto K, Tsuchihara K, Kanai A, Arauchi T, Esumi H, Suzuki Y, Sugano S (2010) Genome-wide identification and annotation of HIF-1α binding sites in two cell lines using

massively parallel sequencing. Hugo J. 4:35-48.

155. Tatton WG, Chalmers-Redman RM, Elstner M, Leesch W, Jagodzinski FB, Stupak DP, Sugrue MM, Tatton NA (2000) Glyceraldehyde-3-phosphate dehydrogenase in neurodegeneration and apoptosis signaling. J. Neural Transm. Suppl:77–100.
156. Teicher BA (1994) Hypoxia and drug resistance. Cancer Metastasis Rev. 13:139-168.
157. Thiele I, Jamshidi N, Fleming RM, Palsson BØ (2009) Genome-scale reconstruction of *Escherichia coli*'s transcriptional and translational machinery: a knowledge base, its mathematical formulation, and its functional characterization. PLoS Comput. Biol. 5:e1000312.
158. Tilsner J, Oparka KJ (2010) Tracking the green invaders: advances in imaging virus infection in plants. Biochem. J. 430:21-37.
159. Tompa P, Szasz C, Buday L (2005) Structural disorder throws new light on moonlighting. Trends Biochem. Sci. 30:484-489.
160. Torimura T, Ueno T, Kin M, Harada R, Nakamura T, Kawaguchi T, Harada M, Kumashiro R, Watanabe H, Avraham R, Sata M (2001) Autocrine motility factor enhances hepatoma cell invasion across the basement membrane through activation of beta1 integrins. Hepatology 34:62-71.
161. True JR, Carroll SB (2002) Gene co-option in physiological and morphological evolution. Annu. Rev. Cell Dev. Biol. 18:53-80.
162. Tsutsumi S, Gupta SK, Hogan V, Tanaka N, Nakamura KT, Nabi IR, Raz A (2003) The enzymatic activity of phosphoglucose isomerase is not required for its cytokine function. FEBS Lett. 534:49 -53.
163. Ungar D, Hughson FM (2003) SNARE protein structure and function. Annu. Rev. Cell Dev. Biol. 19:493-517.
164. Walsh JL, Keith TJ, Knull HR (1989) Glycolytic enzyme interactions with tubulin and microtubules. Biochim. Biophys. Acta. 999:64-70.
165. Wang J, Morris AJ, Tolan DR, Pagliaro L (1996) The molecular nature of the F-actin binding activity of aldolase revealed with site-directed mutants. J. Biol. Chem. 271:6861-6865.
166. Watanabe H, Takehana K, Date M, Shinozaki T, Raz A (1996) Tumor cell autocrine motility factor is the neuroleukin/phosphohexose isomerase polypeptide. Cancer Res. 56:2960–2963.
167. Weinberg JM, Venkatachalam MA, Garzo-Quintero R, Roeser NF, Davis JA (1990) Structural requirements for protection by small amino acids against hypoxic injury in kidney proximal tubules. FASEB J. 4:3347-3354.
168. Whyte JR, Munro S (2002) Vesicle tethering complexes in membrane traffic. J. Cell Sci. 115:2627-2637.
169. Wistow G, Piatigorsky J (1987) Recruitment of enzymes as lens structural proteins. Science

236:1554-1556.

170. Wistow GJ, Lietman T, Williams LA, Stapel SO, de Jong WW, Horwitz J, Piatigorsky J (1988) Tau-crystallin/alpha-enolase: one gene encodes both an enzyme and a lens structural protein. J. Cell Biol. 107:2729-36.

171. Woods A, Munday MR, Scott J, Yang X, Carlson M, Carling D (1994) Yeast SNF1 is functionally related to mammalian AMP-activated protein kinase and regulates acetyl-CoA carboxylase in vivo. J. Biol. Chem. 269:19509-19515.

172. Xu W, Seiter K, Feldman E, Ahmed T, Chiao JW (1996) The differentiation and maturation mediator for human myeloid leukemia cells shares homology with neuroleukin or phosphoglucose isomerase. Blood 87:4502–4506.

173. Yang CK, Ewis HE, Zhang X, Lu CD, Hu HJ, Pan Y, Abdelal AT, Tai PC (2011) Nonclassical protein secretion by *Bacillus subtilis* in the stationary phase is not due to cell lysis. J. Bacteriol. 193:5607-5615.

174. Yang F, Moss LG, Phillips GN Jr (1996) The molecular structure of green fluorescent protein. Nat. Biotechnol. 14:1246-1251.

175. Zheng L, Roeder RG, Luo Y (2003) S phase activation of the histone H2B promoter by OCA-S, a coactivator complex that contains GAPDH as a key component. Cell 114:255-266.

176. Zhong H, De Marzo AM, Laughner E, Lim M, Hilton DA, Zagzag D, Buechler P, Isaacs WB, Semenza GL, Simons JW (1999) Overexpression of hypoxia-inducible factor 1alpha in common human cancers and their metastases. Cancer Res. 59:5830-5835.

CHAPTER I

Searching for secretory pathway of enolase and discovery of enolase foci-forming region

Introduction

Glycolytic enzymes play various roles inside and outside the cell (Tristan et al. 2011). Although they are cytosolic proteins, numerous large-scale analyses have revealed their extracellular existence, in both unicellular and multicellular organisms (Lamonica et al. 2005, Nombela et al. 2006, Chiellini et al. 2008, Oliveira et al. 2010, Oliveira et al. 2010, Shinya et al. 2010). Many glycolytic enzymes have been reported to play roles in important cellular processes such as signal transduction and surface binding (Sriram et al. 2005, Makhina et al. 2009, Ghosh and Jacobs-Lorena 2011, Renigunta et al. 2011). For example, extracellular enolase, which is a glycolytic enzyme, is a virulence factor in *Candida albicans* and other parasites (Jong et al. 2003, Avilan et al. 2011). Enolase has been found in small vesicles outside the cell (Oliveira et al. 2010, Oliveira et al. 2010) and in the cell wall (Edwards et al. 1999). In addition, enolase is secreted in a sequence-dependent manner (Lopez-Villar et al. 2006, Yang et al. 2011), and presents in the cell wall with no enzymatic activity, but binds to plasminogen and helps the pathogen invade (Swenerton et al. 2011). Enolase is also found in viral particles (Bechtel et al. 2005, Chertova et al. 2006, Shaw et al. 2008), and is required for transcription of the Sendai virus (Ogino et al. 2001). Therefore, enolase is a therapeutic target for many diseases, including candidiasis (van Deventer et al. 1996, Capello et al. 2011). Another extracellular glycolytic enzyme, phosphoglucose isomerase, enhances the motility of tumor cells (Dobashi et al. 2006) and performs like a cytokine (Torimura et al. 2001), although it possesses no enzymatic activity outside the cell (Tsutsumi et al. 2003). However, the secretory pathway of glycolytic enzymes such as enolase and phosphoglucose isomerase remains to be revealed. This pathway appears to be unconventional because glycolytic enzymes have no known secretion signals. Therefore, in this study, I analyzed the secretory pathway of glycolytic enzymes.

A number of secreted proteins without known secretion signals have been found (Kinseth et al. 2007), and several unconventional secretory pathways have been discovered and suggested (Duran et al. 2010, Manjithaya et al. 2010, Nickel and Rabouille 2009). Recently, Duran and coworkers identified the novel unconventional secretory pathway of the Acb1 protein (Duran et al. 2010). The budding yeast *Saccharomyces cerevisiae* is a useful organism to identify previously unknown secretory pathways, because it is a commonly used and well-understood model for studying cellular processes (Schekman 2010).

Two popular methods can be used to detect cellular secretion, namely, secretome analysis and glucoamylase assay (Innis et al. 1985). Although these methods are highly informative and convenient, three major problems arise when using them to detect unknown secretory pathways. First, because proteome analysis targets naturally produced proteins, the proportion of each protein

varies. Therefore, the secretory abilities of different proteins are incommensurable, and detecting leakage is inevitable. Second, the glucoamylase assay cannot detect changes in the size of proteins. Therefore, this method can miss the processing of proteins during secretion, which is important for the prediction of the secretory pathway. Third, neither method can visually trace the intracellular secretory pathway. Therefore, it is important to be cautious with the information obtained by these methods and investigate all the possible pathways.

Previously, Morisaka and colleagues have developed a novel two-dimensional high-performance liquid chromatography (2D-HPLC)-based method that detects proteins on the living cell surface (Morisaka et al. 2012). Using this method, an overview of the proteins on the outside of the cell can be gained. In addition, glycolytic enzymes suitable for secretion analyses can be selected. In this study, I utilized enhanced green fluorescence protein conjugated with FLAG-tag (EGFP-FLAG)-tagged glycolytic enzymes to analyze the secretory pathway of glycolytic enzymes. Western blot analysis enabled detection of the secreted proteins in the culture media. Moreover, the use of plasmid-based protein expression facilitated uniform protein levels and analysis of the secreted proteins. Moreover, the secretory pathway was visualized and assessed with the aid of the conjugated fluorescent proteins (Hirschberg and Lippincott-Schwartz 1999, Huang and Shusta 2005).

Materials and methods

Strains and media

Escherichia coli DH5α (F^-, Φ80d*lac*ZΔM15, Δ(*lac*ZYA-*arg*F)U169, *deo*R, *rec*A1, *end*A1, *hsd*R17(r_K^-, m_K^+), *pho*A, *sup*E44, λ^-, *thi*-1, *gyr*A96, *rel*A1) strain was used for host cells in the cloning experiments. The temperature-sensitive *sec23-1* strain RSY282 (*MAT*a, *leu*2Δ, *ura*3Δ, *sec23-1*) was kindly provided by Dr. Randy Schekman (Department of Molecular and Cell Biology and Howard Hughes Medical Institute, University of California at Berkeley). The yeast strain BY4741 (*MAT*a, *his*3Δ1, *leu*2Δ, *met*15Δ, *ura*3Δ), and the derived deletion strains of *SED1* (sed1Δ), *SSO1* (sso1Δ), *SSO2* (sso2Δ), *SEC22* (sec22Δ), *SNC2* (snc2Δ), *TLG2* (tlg2Δ), *BTN2* (btn2Δ), *PEP12* (pep12Δ), *VPS51* (vps51Δ), *GOS1* (gos1Δ), *ATG1* (atg1Δ), *ATG8* (atg8Δ), *ATG11* (atg11Δ), *ATG17* (atg17Δ), *ATG20* (atg20Δ), *VAM3* (vam3Δ), and *GRH1* (grh1Δ) were purchased from EUROSCARF (Frankfurt, Germany). The yeast GFP clones (Invitrogen, Carlsbad, CA, USA) with GFP-tagged endogenous proteins (Pma1p, Nup84p, Mae1p, Chs5p, Snf7p, Vrg4p, Pex11p, and Sec13p) and *HIS3* marker in the parent BY4741 strain were used to determine the localization of proteins. *E. coli* was grown in lysogeny broth (LB) (1% (w/v) tryptone, 0.5% (w/v) yeast extract, 0.5% (w/v) sodium chloride, and 100 ng/mL ampicillin). The yeast cells were grown in yeast extract peptone dextrose (YPD) medium (1% (w/v) yeast extract, 2% (w/v) polypeptone, and 2% (w/v) glucose), SD+HM medium (0.67% (w/v) yeast nitrogen base without amino acids, 2% (w/v) glucose, 0.002%

$_L$-histidine-HCl, and 0.003% $_L$-methionine), SDC+HM medium (0.67% (w/v) yeast nitrogen base without amino acids, 2% (w/v) glucose, 0.002% $_L$-histidine-HCl,0.003% $_L$-methionine, 2% casamino acids (BD, Franklin Lakes, NJ), and 2% (w/v) agar), SC+ML medium (0.67% (w/v) yeast nitrogen base without amino acids, 2% (w/v) glucose, 0.003% $_L$-methionine,0.003% $_L$-leucine, 0.13% SD Multiple drop Out (-Ade, -His, -Leu, -Lys, -Trp, -Ura, Funakoshi Co., Ltd., Tokyo, Japan), 2% (w/v) agar), SD+ML medium (0.67% (w/v) yeast nitrogen base without amino acids, 2% (w/v) glucose, 0.003% $_L$-methionine,0.003% $_L$-leucine), or SDC+ML medium (SD+ML supplemented with 2% casamino acids).

Construction of *S. cerevisiae* expression plasmids

The plasmids were constructed using a conventional PCR-based method and our novel PCR-free method (one-step construction method for plasmids (OSCoM-P); Fig. 1). In addition, iProof DNA polymerase (Bio-Rad, Richmond, CA, USA), KOD-plus-DNA polymerase (Toyobo, Osaka, Japan), KOD-plus-Neo-DNA polymerase (Toyobo), Ligation High (Toyobo), and synthetic oligonucleotides (Japan Bio Services, Saitama, Japan) were used. All primers used in this study are shown in Table 1. The plasmids for the internal production of the recombinant proteins were constructed from pULSG1 (Matsui et al. 2009). The primers coding the ATG codon were mixed with the pULSG1 digest and inserted using the *EcoR* I and *Xho* I sites by OSCoM-P (Fig. 1); the resulting plasmid was named pUL-ATG-EGFP. The section of pUL-ATG-EGFP including the *GAPDH* promoter, the terminator, the FLAG-tag (DYKDDDDK; 21), and the EGFP sequence was amplified and added to the *BamH* I and *Not* I sites by PCR using the primers *GAPDH* promoter-F and *GAPDH* terminator-R, and inserted into the *BamH* I–*Not* I section of pRS423 (47, from ATCC); the resulting plasmid was named pRS423-ATG-EGFP. For constructing the plasmid pULGI2, OSCoM-P was also performed. Oligonucleotide fragments with several restriction sites were inserted into pULSG1 by using the *EcoR* I and *Xho* I sites. The plasmids for the internal expression of the glycolytic enzymes conjugated with EGFP-FLAG were constructed as follows. The yeast genomic DNA was extracted and purified from the *S. cerevisiae* BY4741 strain, and each gene coding a glycolytic enzyme was cloned using the appropriate primer set (Table 1). The fragments were digested and inserted into pULGI2 by using the *BamH* I and *Xho* I sites or the *BamH* I and *Sac* I sites. The internal expression vector without EGFP was constructed from pULSG1C (Matsui et al. 2009) and pWGP3 (Takahashi et al. 2001). The multi-cloning site followed by the *GAPDH* terminator sequence was amplified from pWGP3 and inserted into pULSG1C by using the *Sac* I and *Kpn* I sites; the resulting plasmid was named pULI1. For the construction of the plasmid for the intercellular production of enolase-EGFP-FLAG with the N-terminal peptide sequence (HA-tag), the HA-tag sequence was inserted into pULGI2 by using OSCoM; the resultant plasmid was named pULGI2-HA. The *ENO2* coding sequence from pULGI2-ENO2 was inserted into pULGI2-HA, and the resultant plasmid was

named pULGI2-HA-ENO2. For the construction of plasmids to produce the red-fluorescent proteins, the *Discosoma* red fluorescent protein (DsRED) monomer with *EcoR* I and *Xho* I sites at the N-terminus and *Sal* I at the C-terminus was cloned from pKRD4 (Kuroda et al. 2009). The amplified fragments were digested with *EcoR* I and *Sal* I, and then inserted into the same site of pULSG1; the resultant plasmid was named pUL-ATG-DsRED. For production of the enolase fragments fused with EGFP or DsRED, amplified fragments were digested and inserted into pULSG1 or pUL-ATG-DsRED by using the *EcoR* I and *Xho* I sites (see Table 1). Plasmids for production of Tlg2p (p413-ADH-TLG2) were constructed as follows: *TLG2*-coding sequence was cloned from the genomic DNA extracted from *S.cerevisiae* BY4741 and inserted into MCS of p413-ADH (ATCC 87370) using *EcoR* I and *Xho* I sites. The plasmid construction was confirmed by DNA sequencing performed using a BigDye Terminator v3.1 cycle sequencing kit and an ABI PRISM 3100 Genetic Analyzer (Applied Biosystems, Foster City, CA, USA).

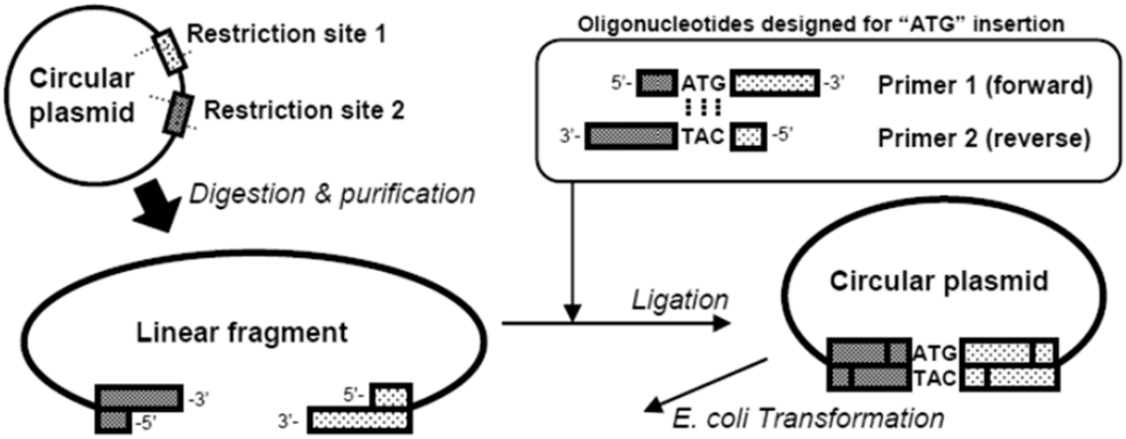

Fig. 1 Schematic illustration of the one-step construction method for plasmids (OSCoM-P) The digested linear fragments of the plasmids were ligated with the designed primers at a dry weight ratio of 1:1–1:10 (linear plasmid:each primer). The reaction solution was directly transformed into *E. coli* DH5α competent cells (Toyobo). The purchased oligonucleotides were dissolved in dH_2O at 10 ng/mL before use. TE buffer was not used because OSCoM-P was severely inhibited by the presence of TE buffer (data not shown). Maximum length of fragments to be inserted into plasmids using OSCoM-P is 45 bp (data not shown).

Production of recombinant proteins in yeast cells

The yeast cells were transformed with plasmids by using a Frozen-EZ Yeast Transformation II™ kit (Zymo Research, Orange, CA, USA) and grown on SDC+HM agar plates. The transformants were

selected as single colonies and inoculated into 10 mL of SD+HM medium for pre-cultivation at 25°C with shaking. At the late-log phase, the pre-culture was subcultured into 10 mL (for secretion analysis of the *sec23-1* strains) or 25 mL of the same medium to obtain an optical density at 600 nm (OD_{600}) of 0.01 (for secretion analysis of the glycolytic enzymes) or 0.3. The cells were cultivated at 25°C for 26 h (for secretion analysis of the glycolytic enzymes) or 4 h with shaking until they reached an OD_{600} of 0.9–1.1 or 0.5. Genotypes of knockout strains were checked by colony PCR. For secretion analysis of plasmid co-transformed strains, plasmids for internal overexpression of EGFP-FLAG-conjugated proteins (pUL-X) were co-transformed with p413-plasmids into BY4741wt and Δ*TLG2* strains. Transformants were grown on SC+ML agar medium. Single colonies were picked up and re-cultivated on the same medium, and then used for secretion analysis. Transformants were pre-cultivated in 10 mL of SDC+ML media at 25°C for 26 h with shaking. Cells were washed with fresh media SD+ML and inoculated into 25 mL of SD+ML media. The cells were cultivated at 25°C for 4 h with shaking until they reached an OD_{600} of 0.5.

Identification of noncovalently bound cell surface proteins of living cells

The budding yeast BY4741 sed1Δ strain transformed with the plasmids pRS423-ATG-EGFP and pKRD4 (Kuroda et al. 2009) was grown in SDC+HM media. The noncovalently bound cell surface proteins extracted from living yeast cells by using CHAPS were separated by a 2D-HPLC system optimized for protein separation (34). The fractionated proteins were lyophilized using a Labconco vacuum centrifuge (Labconco, MO, USA) and solubilized in 50 mM ammonium hydrogencarbonate. The collected proteins were reduced with 50 mM DTT for 30 min at 60°C and alkylated with 500 mM iodoacetamide for 45 min at room temperature. The alkylated proteins were digested by trypsin (sequencing grade modified trypsin; Promega Corp., WI, USA) for 12 h at 37°C for protein identification by mass spectrometry using a Prominence nanoflow system (Shimadzu, Kyoto, Japan) and an LTQ Velos linear ion trap mass spectrometer (Thermo Scientific Inc., Bremen, Germany). The proteolytic digests were separated by reversed-phase chromatography using a packed tip column (NTCC-360, 150 mm × 100 μm I.D.; Nikyo Technos, Tokyo, Japan) at a flow rate of 500 nL/min. The gradient was provided by changing the mixing ratio of the 2 eluents (A, 0.1% (v/v) formic acid and B, acetonitrile containing 0.1% (v/v) formic acid). The gradient was started with 5% B, increased to 45% B for 60 min, further increased to 95% B to wash the column, and then returned to the initial condition and held for re-equilibration. For data-dependent acquisition of mass spectrometry detection, the method was set to automatically analyze the top 3 most intense ions observed in the mass spectrometry scan. An ESI voltage of 1.9 kV was directly applied to the flow using a microtee. The ion transfer tube temperature on the LTQ Velos ion trap was set to 300°C. The experiments were independently repeated twice. Protein identification was performed using the combined tandem mass spectrometry data and the Protein Discoverer software (Thermo Scientific).

The results were compared to the *Saccharomyces* Genome Database (SGD; http://www.yeastgenome.org) and filtered at a q-value of ≤0.05 corresponding to 5% false discovery rate (FDR) on a spectral level, and the identified proteins contained >2 peptide fragments.

Preparation of extracellular and intracellular proteins

The detection was performed as follows. The culture media (25 mL) was centrifuged at 900 *g* for 10 min at 4°C to remove cells. Following this, the culture media were filtered through a 0.2-μm Acrodisc syringe filter (PALL Corporation, MI, USA) and concentrated by ultrafiltration (YM-10 filter for pULI1, pULSG1C, pUL-ATG-EGFP, pUL-eno(1–17), pUL-eno(1–28), and pUL-eno(1–30), and a YM-30 filter for the others; Amicon, Millipore, Millford, MA, USA). After washing thrice with 4 volumes of 20 mM Tris-HCl (pH 7.8), the concentrated proteins were frozen and lyophilized. The proteins were then suspended with 15 μL (for secretion analysis of the glycolytic enzymes) or 30 μL of loading buffer and analyzed by SDS-PAGE. The cells were suspended with 500 μL of 20 mM Tris-HCl (pH 7.8) containing 0.1% SDS. After homogenization at 4,000 rpm for 20 sec using glass beads (GB-05, diameter 0.5 mm; TOMY, Tokyo, Japan) and Bead Smash 12 (Wakenyaku, Kyoto, Japan), the sample solutions were centrifuged at 9,700 *g* for 5 min. Aliquots (5 μL) of the supernatants were suspended with 5 μL of 2× loading buffer and analyzed by SDS-PAGE.

Inhibition of conventional secretion by using the *sec23-1* strain

After pre-culture in SD+HM medium, the cells were washed with fresh media and inoculated into fresh 10 mL of the same media to obtain an OD_{600} of 0.3, and incubated at 25 or 37°C with shaking. After 4 h, the culture media was filtered and concentrated. Following measurement of the protein concentration, the solution was lyophilized and suspended in 10 μL of loading buffer.

SDS-PAGE

SDS-PAGE was conducted according to the previously described method (Laemmli, 1970) by using a continuous polyacrylamide gel (5%–20%, 120 × 100 mm, e-PAGEL; Atto, Tokyo, Japan). The samples were heated in the loading buffer at 100°C for 3 min, centrifuged at 21,900 *g* at 4°C for 5 min to remove the debris, and loaded. As an external standard, the FLAG-protein (48-kDa cleavage control protein; Novagen, Inc., WI, USA) was used.

Western blotting

After transfer to a nitrocellulose membrane (0.45 μm, pore size) by using trans-blot transfer medium (Bio-Rad), western blot analysis was performed using an anti-FLAG M2 antibody conjugated with HRP (Sigma). The loading control Pgi1p was detected using the rabbit anti-baker's yeast Pgi1p (Acris Antibodies GmbH, Hiddenhausen, Germany) and an anti-rabbit antibody conjugated to HRP

(GE Healthcare, UK, Ltd., Buckinghamshire, UK). The detection was enhanced by using the Can Get Signal Immunoreaction Enhancer solution (Toyobo). After detection, the antibodies were removed using a stripping agent (WB Stripping solution; Nacalai), and the membranes were blocked and reprobed using an anti-FLAG M2 antibody conjugated to HRP (Sigma). The chemiluminescence was detected using ECL Plus™ western blotting detection reagents (GE Healthcare). The membranes treated with the detection reagent were exposed to Amersham Hyperfilm ECL (GE Healthcare) and developed using Rendol and Renfix (Fujifilm, Kanagawa, Japan) to detect the secreted glycolytic enzymes and enolase fragments. Other data were taken by using the ImageQuant LAS 4000 mini system (GE Healthcare). Gained signals from extracellular Pgi1p and Eno2p conjugated with EGFP-FLAG-tag using anti-Pgi1p and anti-FLAG were processed by setting signals obtained from 0.4 ng/ lane of FLAG-protein as 1. Relative amounts of Eno2p-EGFP-FLAG-tag were calculated as: [signal intensities of anti-FLAG treatment/ that of anti-Pgi1p treatment]. One-tailed t-tests were performed to detect significant differences.

Fluorescence microscopy

For confocal microscopy, the cells were grown to the mid-log phase and fixed with PBS (pH 7.4) containing 3.7% paraformaldehyde. The cells were then fixed to the bottom of a 35-mm glass-base dish (Synapse Fine View Dish SF-G-D27; FPI Inc., Kyoto, Japan) by using the same buffer. The fluorescence images were obtained at room temperature with a 60× objective (oil immersion NA, 1.35) by using a laser-scanning confocal microscope (FluoView FV1000; Olympus) and FV10-ASW software (Olympus). The efficiency of colocalization was analyzed using ImageJ software (http://rsb.info.nih.gov/ij/). To observe the cells producing recombinant proteins and perform time-course observations, an epifluorescence microscope IX71 (Olympus) with a 100× objective (oil immersion NA, 1.40) and Aquacosmos software (Hamamatsu Photonics, Hamamatsu, Japan) were used.

Time-course observation of the living cells on agarose pad

To observe the time-dependent localization changes of the foci, the agarose pad was prepared using a slightly modified method (Tanaka et al. 2010). Briefly, 2% agarose was added to the SD+HM media, heated, and dissolved. The solution at 60°C was spotted onto the slide glass with vinyl tape wrapped on each side. Immediately following this, the cover glass was overlaid and left at room temperature. Before observation, the yeast culture in the mid-log phase with an OD_{600} of 0.4 was spotted onto the agarose pad and covered with the cover glass. Time-lapse observations were conducted by fitting a small incubator (MI-IBC-IF; Olympus) onto the microscopy system and by manually photographing at every 5 min for 30 min. The incubator was pre-warmed to 30°C, and the excitation light source was turned on only during image recording.

Table 1 Primers used in CHAPTER I

Plasmid	Oligo name	Description	Sequence (5'-3')
pULI1	GAP-Pro-F	Primer for amplification of MCS-t*GAPDH* (forward)	CTTAAACTTCTTAAATTCTACTTTTATAGTTAGTC
	*Kpn*I-TGAP-R	Primer for amplification of MCS-t*GAPDH* (reverse)	ATGCTGGTACCTCAATCAATGAATCGAAAATGTCATTAAAATAG
pUL-ATG-EGFP	*Ec*ATG*Xh*OSCoM_F	Oligonucleotide for OSCoM (forward)	AATTCATGC
	*Ec*ATG*Xh*OSCoM_R	Oligonucleotide for OSCoM (reverse)	TCGAGCATG
pRS423-ATG-EGF	*GAPDH* promoter -F	Primer for amplification of p*GAPDH*-*EGFP*-FLAGtag-t*GAPDH* (forward)	GGTACGGGATTCACCAGTTCTCACACGGAACACCAC
	GAPDH terminator -R	Primer for amplification of p*GAPDH*-*EGFP*-FLAGtag-t*GAPDH* (forward)	ATAAGAATGCGGCCGCTCAATCAATGAATCGAAAATGTCAT
pUL-ATG-DsRED	*DsRed-EcoR1*ATG*Xho1* F	Primer for amplification of *DsRED* from pKRD4 (forward)	TAAACAGAATTCATGCTCGAGGGTGGATCTGGTGGCGACAACACCGA
	DsRed-Sal1 R	Primer for amplification of *DsRED* from pKRD4 (reverse)	GTTCAACCAAGTCGACTTACTGGGAGCCGGAGTGGCGGGCCTCG
	seq*DsRED* (27-34)	Primer for sequencing *DsRED*	CGAGTTCATGCGCTTCAAGG
pULGI2	pULSG1mcskaiF	Oligonucleotide for OSCoM (forward)	AATTCGGATCCCGGCTCGAGCGGAGATCTCGGGAGCTCCCGG
	pULSG2mcskaiR	Oligonucleotide for OSCoM (reverse)	TCGACCGGGAGCTCCCGAGATCTCCGCTCGAGCCGGGATCCG
pULGI2-ATG-HA	ATG-HAtagF (pULIG2)	Oligonucleotide for OSCoM (forward)	AATTCATGTACCCATACGATGTTCCAGATTACGCTG
	ATG-HAtagR (pULIG2)	Oligonucleotide for OSCoM (reverse)	GATCCAGCGTAATCTGGAACATCGTATGGGTACATG
pULGI2-ENO2/ pULGI2-HA-ENO2	pULIG-eno2 F (*BamH1*)	Primer for amplification of *ENO2* (forward)	GAATTCGGATCCATGGCTGTCTCTAAAGTTTACGCT
	pULIG-eno2all R (*Sac1*)	Primer for amplification of *ENO2* (reverse)	CGACCGGGAGCTCCAACTTGTCACCGTGGTGGAAGT
	eno2-1 F	Primers for cloning *ENO2* from genome and for sequencing	ATACCAAGTCAGCATACACC
	eno2-2 F		TTATCTTCCTACCAGAGTTG
	eno2-3 F		AAGTCGAATTAACCACCGAA
	eno2-4 F		TCTTGTTGTCTTTGGATGGT
	eno2-5 F		GTTCCGAAGTTTACCACAAC
	eno2-6 F		TTCAAGGACGGTAAGTACGA
	eno2-7 F		ACTGGGAAGCTTGGTCTCAC
	eno2-8 F		CTGGTGAAACTGAAGACACT
	eno2-9 F		TTTTCAAAGACTCGTGCTGT
	eno2-10 R		ACACGTATTCTTGTATGACC
pULGI2-CDC19	*CDC19-BamH1* F	Primer for amplification of *CDC19* (forward)	AACAGAATTCGGATCCATGTCTAGATTAGAAAGATTGACCTCATTA
	CDC19-Xho1 R	Primer for amplification of *CDC19* (reverse)	GAGATCTCCGCTCGAGAACGGTAGAGACTTGCAAAGTGTTGGAGTG
	CDC19 (291-310) seqF	Primers for sequencing *CDC19*	CGATGTTGACTACCCAATCC
	CDC19 (681-700) seqF		CTTGGGTGAACAAGGTAAGG
	CDC19 (1078-1097) seqF		GCTTACTTGCCAAACTACGA
	CDC19 (1306-1325) seqF		TACAGAGGTGTCTTCCCATT
pULGI2-PYK2	*PYK2-BamH1* F	Primer for amplification of *PYK2* (forward)	AACAGAATTCGGATCCATGCCAGAGTCCAGATTGCAGAGACTAGCT
	PYK2-Xho1 R	Primer for amplification of *PYK2* (reverse)	GAGATCTCCGCTCGAGGAATTCTTGACCAACAGTAGAAATGCGTAA

Table 1 Primers used in CHAPTER I (continued)

pULGI2-PYK2	*PYK2* (211-230) seqF	Primers for sequencing *PYK2*	AAATCGGAACAGCAATTCCC
	PYK2 (592-611) seqF		ATGAAGGACTTGCAATTCGG
	PYK2 (993-1012) seqF		TATGCTTTCTGGAGAAACGG
	PYK2 (1336-1355) seqF		TATGAACCGAAACGCCTAGA
pULGI2-GPM1	*GPM1-BamH1* F	Primer for amplification of *GPM1* (forward)	AACAGAATTCGGATCCATGCCAAAGTTAGTTTTAGTTA GACACGGT
	GPM1-Xho1 R	Primer for amplification of *GPM1* (reverse)	GAGATCTCCGCTCGAGTTTCTTACCTTGGTTGGCAACA GCAGCGGC
	GPM1 (281-300) seqF	Primer for sequencing *GPM1*	AAGGTAAGGACAAGGCTGAA
pULGI2-TPI1	*TPI1-BamH1* F	Primer for amplification of *TPI1* (forward)	AACAGAATTCGGATCCATGGCTAGAACTTTCTTTGTCG GTGGTAAC
	TPI1-Xho1 R	Primer for amplification of *TPI1* (reverse)	GAGATCTCCGCTCGAGGTTTCTAGAGTTGATGATATCA ACAAATTC
	TPI1 (243-262) seqF	Primer for sequencing *TPI1*	CCAAATCAAGGATGTTGGTG
pULGI2-PGI1	*PGI1-BamH1* F	Primer for amplification of *PGI1* (forward)	AACAGAATTCGGATCCATGTCCAATAACTCATTCACTA ACTTCAAA
	PGI1-Xho1 R	Primer for amplification of *PGI1* (reverse)	AACAGAATTCGGATCCATGACTGTTACTACTCCTTTTG TGAATGGT
	PGI1 (252-271) seqF	Primers for sequencing *PGI1*	TAACGTCACCGGTTTGAGAG
	PGI1 (697-716) seqF		GCCAAGAACTGGTTCTTGTC
	PGI1 (1178-1197) seqF		CTACCAACGCTCAACACTCT
pULGI2-PGK1	*PGK1-BamH1* F	Primer for amplification of *PGK1* (forward)	AACAGAATTCGGATCCATGTCTTTATCTTCAAAGTTGT CTGTCCAA
	PGK1-Xho1 R	Primer for amplification of *PGK1* (reverse)	GAGATCTCCGCTCGAGTTTCTTTTCGGATAAGAAAGCA ACACCTGG
	PGK1 (221-240) seqF	Primers for sequencing *PGK1*	AATACTCTTTGGCTCCAGTT
	PGK1 (510-529) seqF		TCACTCTTCTATGGTCGGTT
	PGK1 (848-867) seqF		ACTTCATCATTGCTGATGCT
pULGI2-FBA1	*FBA1-BamH1* F	Primer for amplification of *FBA1* (forward)	AACAGAATTCGGATCCATGGGTGTTGAACAAATCTTAA AGAGAAAG
	FBA1-Xho1 R	Primer for amplification of *FBA1* (reverse)	GAGATCTCCGCTCGAGTAAAGTGTTAGTGGTACGGAA AGTTTCCAA
	FBA1 (296-315) seqF	Primers for sequencing *FBA1*	CAGCTTACGGTATCCCAGTT
	FBA1 (627-646) seqF		TTTGCACCCAATCTCTCCAA
pUL-eno(1-10)	*Eno2*(-10)_*Xho1*R	Primers for cloning *ENO2* fragments	CACCAGATCCACCCTCGAGGGATCTAGCGTAAACTTT AGAGACAGCCAT
pUL-eno(1-28)/ pULR-eno(1-28)	*Eno2*(-28)_*Xho1*R		CAGATCCACCCTCGAGCTTTTCGGTGGTTAATTCGACT T
pUL-eno(1-30)	*Eno2*(-30)_*Xho1*R		CACCAGATCCACCCTCGAGAACACCCTTTTCGGTGGT TAATTCGACTTC
pUL-eno(1-50)	*Eno2*(-50)_*Xho1*R		CACCAGATCCACCCTCGAGTCTCATTTCCAAAGCTTCG T
pUL-eno(1-110)	*Eno2*(-110)_*Xho1*R		CACCAGATCCACCCTCGAGAGCGTTAGCACCCAACTT GG
pUL-eno(1-169)	*Eno2*(-169)_*Xho1*R		AGATCCACCCTCGAGTTCTTGCAAAGCCAAAGCACC
GAPDH promotor	pGAP_F	Primer for sequencing	AGACGGTAGGTATTGATTGTAATTCTG
p413-ADH-TLG2	*BamH1-TLG2* F	Primer for amplification of *TLG2* (forward)	AGAACTAGTGAATTCATGTTTAGAGATAGAACTAATTTAT
	Xho1-TLG2 R	Primer for amplification of *TLG2* (reverse)	ACATGACTCGAGTCAAAGTAGGTCATCCAAAGCATCATTC
	ADH pro F	Primer for sequencing p413-ADH plasmid	ATGAGCAACGGTATACGG
	TLG2 (140-164) seqF	Primers for sequencing *TLG2*	ACGATATATCGGCCAGATTGACAGA
	TLG2 (444-466) seqF		GCAATTAAGTCGAGAAGAGCTGA
	TLG2 (786-807) seqF		AGAAGTGAGCACTATTTTCAGG

Table 1 Primers used in CHAPTER I (continued)

Δ*TLG2* (genome)	*TLG2* (coloP) F	Primers for checking the sizes of cording regions	GCAAGACAGGAAAGTCTCCAA
	TLG2 (coloP) R		GCAACAGGTCATATGAACGCT
KanMX4 (gene)	*KanB*-R	Primers for checking genotypes	CTGCAGCGAGGAGCCGTAAT
Δ*SEC22* (genome	*SEC22* (coloP) F		AATTTTCAACCAAACGTGTTGTACT
Δ*GOS1* (genome)	*GOS1* (coloP) F		AAAGATGCTTATGAAAAATCTCACG
Δ*PEP12* (genome	*PEP12* (coloP) F		TGCCTTAGCTGGAAAATTGTATTTA
Δ*VPS51* (genome	*VPS51* (coloP) F		AATCTACCCAGGCCTTAAAAGTATG
Δ*BTN2* (genome)	*BTN2* (coloP) F		CGAGAGTTGTATCCAGTTTTCTTGT
Δ*SNC2* (genome)	*SNC2* (coloP) F		AGTGATCTTGGTCACATGATATACG
Δ*SNX4* (genome)	*SNX4* (coloP) F		AATAACAGTTCAAAAATCTATGCCG
Δ*SSO1* (genome)	*SSO1* (coloP) F		CACACTAACGACAAAAGACGATATG
Δ*SSO2* (genome)	*SSO2* (coloP) F		TACCCATAAGAGAGCTGGAATAGTG
Δ*ATG1* (genome)	*ATG1* (coloP) F		AAGTTAAGTACCAAGGCCATCTTTT
Δ*ATG20* (genome	*ATG20* (coloP) F		ATAAGGCTTGGCTTATTTGCTTACT
Δ*ATG17* (genome	*ATG17* (coloP) F		CTTGAATTATTATCTTCCTCATCGC

Table 2 List of genes and proteins used in Chapter 1

Category	Accession	Name	Description
Organelle marker proteins	YGL008C	PMA1	Plasma membrane H+-ATPase, pumps protons out of the cell
	TDL116W	NUP84	Subunit of the nuclear pore complex (NPC)
	YKL029C	MAE1	Mitochondrial malic enzyme
	YLR330W	CHS5	Component of the exomer complex
	YLR025W	SNF7	One of four subunits of the endosomal sorting complex required for transport III (ESCRT-III)
	YGL225W	VRG4	Golgi GDP-mannose transporter; regulates Golgi function and glycosylation in Golgi
	YOL147C	PEX11	Peroxisomal membrane protein required for medium-chain fatty acid oxidation and peroxisome proliferation
	YLR208W	SEC13	Component of the Nup84 nuclear pore sub-complex, the Sec13p-Sec31p complex of the COPII vesicle coat, and the SEA (Seh1-associated) complex; required for vesicle formation in ER to Golgi transport and nuclear pore complex organization
SNAREs	YPL232W	SSO1	Plasma membrane t-SNARE involved in fusion of secretory vesicles at the plasma membrane and in vesicle fusion during sporulation
	YMR183C	SSO2	Plasma membrane t-SNARE involved in fusion of secretory vesicles at the plasma membrane
	YLR268W	SEC22	R-SNARE protein; assembles into SNARE complex with Bet1p, Bos1p and Sed5p; cycles between the ER and Golgi complex; involved in anterograde and retrograde transport between the ER and Golgi
	YOR327C	SNC2	Vesicle membrane receptor protein (v-SNARE) involved in the fusion between Golgi-derived secretory vesicles with the plasma membrane
	YOL018C	TLG2	Syntaxin-like t-SNARE that forms a complex with Tlg1p and Vti1p and mediates fusion of endosome-derived vesicles with the late Golgi
	YGR142W	BTN2	v-SNARE binding protein that facilitates specific protein retrieval from a late endosome to the Golgi
	YOR036W	PEP12	Target membrane receptor (t-SNARE) for vesicular intermediates traveling between the Golgi apparatus and the vacuole
	YKR020W	VPS51	Component of the GARP (Golgi-associated retrograde protein) complex,which is required for the recycling of proteins from endosomes to the late Golgi
	YHL031C	GOS1	v-SNARE protein involved in Golgi transport, homolog of the mammalian protein GOS-28/GS28
	YOR106W	VAM3	Syntaxin-like vacuolar t-SNARE that functions with Vam7p in vacuolar protein trafficking; mediates docking/fusion of late transport intermediates with the vacuole
Transport	YDR517W	GRH1	Acetylated, cis-golgi localized protein involved in ER to Golgi transport; homolog of human GRASP65; forms a complex with the coiled-coil protein Bug1p; mutants are compromised for the fusion of ER-derived vesicles with Golgi membranes
Autohagy-related proteins	YGL180W	ATG1	Protein ser/thr kinase required for vesicle formation in autophagy and the cytoplasm-to-vacuole targeting (Cvt) pathway
	YBL078C	ATG8	Component of autophagosomes and Cvt vesicles; undergoes conjugation to phosphatidylethanolamine (PE)
	YPR049C	ATG11	Adapter protein for pexophagy and the cytoplasm-to-vacuole targeting (Cvt) pathway
	YLR423C	ATG17	Scaffold protein responsible for phagophore assembly site organization; regulatory subunit of an autophagy-specific complex that includes Atg1p and Atg13p
	YDL113C	ATG20	Sorting nexin family member required for the cytoplasm-to-vacuole targeting (Cvt) pathway and for endosomal sorting
Cell wall protein	YDR077W	SED1	Major stress-induced structural GPI-cell wall glycoprotein in stationary-phase cells

Table 3. List of identified noncovalently-bound cell surface proteins

Cellular process			Accession	SGDID	Name	Description	# AAs	MW [kDa]	calc. pI	Σ Coverag	Σ# PSM	Σ# Peptide
Metabolism	Glycolysis		YHR174W	S000001217	ENO2	Enolase II, a phosphopyruvate hydratase	437	46.9	6	31	41	9
			YGR192C	S000003424	TDH3	Glyceraldehyde-3-phosphate dehydrogenase,	332	35.7	7	40	53	8
			YCR012W	S000000605	PGK1	3-phosphoglycerate	416	44.7	7.6	32	28	8
			YJL052W	S000003588	TDH1	Glyceraldehyde-3-phosphate dehydrogenase,	332	35.7	8.3	32	32	7
			YDR050C	S000002457	TPI1	Triose phosphate isomerase	248	26.8	6	35	38	6
			YJR009C	S000003769	TDH2	Glyceraldehyde-3-phosphate dehydrogenase,	332	35.8	7	26	33	6
			YGR254W	S000003486	ENO1	Enolase I, a phosphopyruvate hydratase	437	46.8	6.6	20	32	6
			YKL152C	S000001635	GPM1	Tetrameric phosphoglycerate	247	27.6	8.8	26	21	5
			YAL038W	S000000036	CDC19	Pyruvate kinase	500	54.5	7.7	13	10	5
			YBR196C	S000000400	PGI1	Phosphoglucose isomerase	554	61.3	6.5	10	6	4
			YKL060C	S000001543	FBA1	Fructose 1,6-bisphosphate aldolase	359	39.6	5.8	13	5	3
	Amino acid biosynthesis	Methionine biosynthesis	YER091C	S000000893	MET6	Cobalamin-independent methionine synthase	767	85.8	6.5	17	21	10
		Isoleucine biosynthesis	YIL051C	S000001313	MMF1	Mitochondrial protein required for transamination of	145	15.9	9.3	49	15	5
		Methionine and threonine	YDR158W	S000002565	HOM2	Aspartic beta semi-aldehyde	365	39.5	6.7	19	13	5
		Glycine catabolic process	YAL044C	S000000042	GCV3	H subunit of the mitochondrial glycine decarboxylase complex	170	18.8	4.7	30	12	4
		Lysine biosynthesis	YIL094C	S000001356	LYS12	Homo-isocitrate dehydrogenase	371	40	8	15	7	4
		Histidine biosynthesis	YOR202W	S000005728	HIS3	Imidazoleglycerol-phosphate dehydratase	220	23.8	6.4	15	5	2
	TCA cycle		YKL085W	S000001568	MDH1	Mitochondrial malate dehydrogenase	334	35.6	8.5	10	3	2
	Pentose phosphate pathway		YPR074C	S000006278	TKL1	Transketolase	680	73.8	7	4	3	2
	Alcoholic fermentation		YLR044C	S000004034	PDC1	Pyruvate decarboxylase	563	61.5	6.2	33	36	13
	Fatty acid metabolism		YGR037C	S000003269	ACB1	Acyl-CoA-binding	87	10.1	4.9	59	7	3

Table 3. List of identified noncovalently-bound cell surface proteins (continued)

Protein binding		YAL005C	S000000004	SSA1	protein folding and nuclear localization signal (NLS)-directed nuclear transport	642	69.6	5.1	5	5	3
		YMR186W	S000004798	HSC82	Cytoplasmic chaperone of the Hsp90 family	705	80.8	4.8	4	8	2
		YDR155C	S000002562	CPR1	Cytoplasmic peptidyl-prolyl cis-trans	162	17.4	7.4	17	6	2
		YLL050C	S000003973	COF1	Cofilin (Actin binfing)	143	15.9	5.2	22	4	2
		YBR109C	S000000313	CMD1	Calmodulin	147	16.1	4.3	21	3	2
		YJL034W	S000003571	KAR2	ATPase involved in protein import into the	682	74.4	4.9	3	2	2
Homeostasis		YML028W	S000004490	TSA1	Thioredoxin peroxidase	196	21.6	5.1	31	10	4
		YLR043C	S000004033	TRX1	Cytoplasmic thioredoxin isoenzyme	103	11.2	4.9	49	8	4
		YGR209C	S000003441	TRX2	Cytoplasmic thioredoxin isoenzyme	104	11.2	4.9	49	8	4
		YFL014W	S000001880	HSP12	Heat Shock Protein	109	11.7	5.4	23	4	3
		YHR008C	S000001050	SOD2	Mitochondrial manganese superoxide	233	25.8	8.5	17	2	2
Translation		YJL138C	S000003674	TIF2	Translation initiation factor eIF4A	395	44.7	5.1	10	8	3
		YEL034W	S000000760	HYP2	Translation elongation factor eIF-5A	157	17.1	5	19	12	2
		YDR385W	S000002793	EFT2	Elongation factor 2	842	93.2	6.3	3	2	2
		YDR382W	S000002790	RPP2B	Ribosomal protein P2	110	11	4.1	24	2	2
Folding		YCL043C	S000000548	PDI1	Protein disulfide	522	58.2	4.5	27	28	10
Signaling		YMR116C	S000004722	ASC1	G-protein beta subunit and guanine nucleotide dissociation inhibitor for Gpa2p	319	34.8	6.2	34	28	8
Traffic	Endocytosis	YIL041W	S000001303	GVP36	BAR domain-containing protein	326	36.6	5	20	6	4
Unknown		YOL154W	S000005514	ZPS1	Zinc- and pH-regulated surface protein	249	27.5	5	27	17	5
		YDR519W	S000002927	FPR2	Membrane-bound peptidyl-prolyl cis-trans isomerase (PPIase),	135	14.5	5.5	34	8	3
		YPL225W	S0000061	YPL225	Unknown	146	17.4	5.3	16	4	2

Results

Detection of unconventional secretion of glycolytic enzymes

2D-HPLC-based cell surface proteome analysis was done to detect the extracellular presence of 11 glycolytic enzymes, namely, enolases (Eno1p and Eno2p), glyceraldehyde-3-phosphate dehydrogenases (Tdh1p, Tdh2p, and Tdh3p), 3-phosphoglycerate kinase (Pgk1p), fructose 1,6-bisphosphate aldolase (Fba1p), phosphoglucose isomerase (Pgi1p), triose phosphate isomerase (Tpi1p), phosphoglycerate mutase (Gpm1p), and pyruvate kinase (Cdc19p; Table 3 and 4). To shortlist the candidate proteins for analysis of the secretory pathway, the detected glycolytic enzymes were produced as recombinant proteins fused to EGFP-FLAG. Although all the glycolytic enzymes were successfully produced in the cell, only 4 (Eno2p, Pgi1p, Tpi1p, and Fba1p) were reproducibly detected in the culture media (Fig. 2A left). Among these, Eno2p and Pgi1p were both thought to be important molecules when secreted, and thus, were used for further investigation. To examine whether Eno2p and Pgi1p were secreted via the conventional pathway, a *sec23-1* temperature-sensitive mutant strain was used. The secretion of EGFP fused with the conventional glucoamylase secretion signal sequence was successfully inhibited at 37°C. Comparatively, under the same conditions, by using the same strain, both Eno2p and Pgi1p were detected in the culture media (Fig. 2B). To examine whether a cleavable peptide sequence existed at the N-terminus of Eno2p, which is typical for conventionally secreted proteins, an extra N-terminal peptide sequence (in this case, HA-tag) was added to Eno2p. In the wild-type cells, Eno2p with the extra N-terminal peptide sequence was detected in the culture media as well as Eno2p without the extra sequence (Fig. 2C). These results suggest that glycolytic enzymes, at least Eno2p, can be secreted via an unconventional pathway in *S. cerevisiae*. Among the glycolytic enzymes detected in the culture media, Pgi1p-EGFP-FLAG gave the clearest bands. Moreover, the secretion of endogenous Pgi1p has been detected in the previous study (Oliveira et al. 2010). Therefore, I used endogenous Pgi1p as a control in the following experiments.

Table 4 List of identified noncovalently-bound cell surface proteins

Cellular process		Number of identified proteins
Metabolism	Glycolysis	11
	Amino acid biosynthesis	6
	TCA cycle	1
	Pentose phosphate pathway	1
	Alcoholic fermentation	1
	Fatty acid metabolism	1
Protein binding		6
Homeostasis		5
Translation		4
Signaling		1
Folding		1
Traffic		1
Unknown		3
	Total	42

Searching for the enolase sequence responsible for secretion

N-terminal fragments of Eno2p containing 169 amino acids (1–169) were prepared in reference with the previous report (29). In addition, N-terminal fragments of Eno2p containing 17, 28, 30, 50, and 110 amino acids ((1–17), (1–28), (1–30), (1–50), and (1–110)) were prepared. Subsequently, the (1–28), (1–50), and (1–169) fragments were reproducibly detected in the culture media (Fig.3A). In addition, secretion of the (1–28) Eno2p fragment (eno(1–28)) conjugated to EGFP and FLAG in the *sec23-1* strain was not inhibited at 37°C (Fig. 3B). These results suggest that eno(1–28), as well as Eno2p, is secreted via an unconventional pathway.

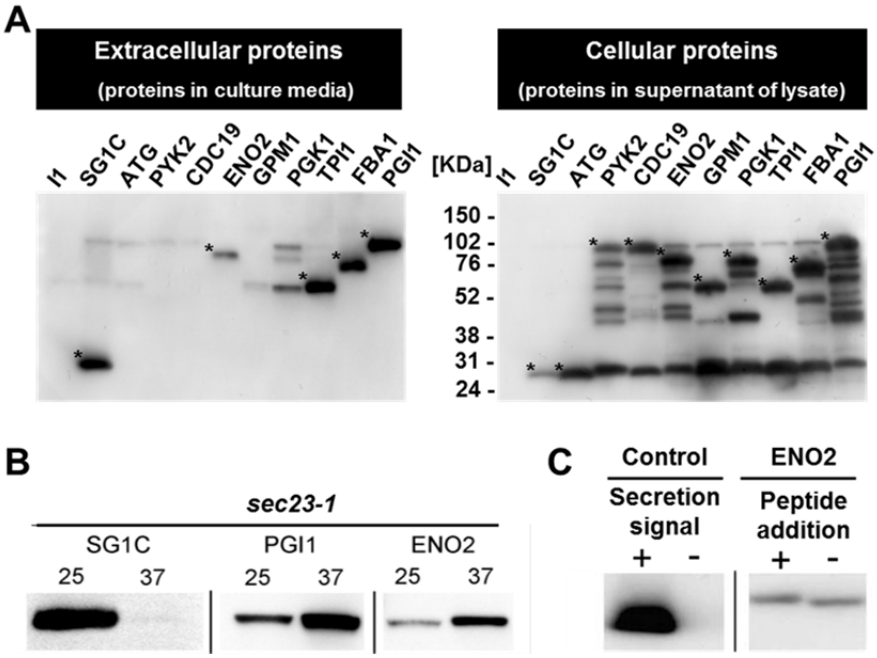

Fig. 2 Detection of unconventional secretion of glycolytic enzymes Anti-FLAG antibody was used for detection. A: Secretion of glycolytic enzymes. (Left) secreted proteins. (Right) cellular proteins. I1, pULI1; SG1C, pULSG1C; ATG, pUL-ATG-EGFP; PYK2, pULGI2-PYK2; CDC19, pULGI2-CDC19; ENO2, pULGI2-ENO2; GPM1, pULGI2-GPM1; PGK1, pULGI2-PGK1; TPI1, pULGI2-TPI1; FBA1, pULGI2-FBA1; PGI1, pULGI2-PGI1. B: The effect of inhibition of the conventional pathway on the secretion of the glycolytic enzymes. Secretion of recombinant proteins in *sec23-1* strains under 25°C or 37°C is shown. C: The effect of the N-terminal peptide (HA-tag) on the secretion of enolase. Control (secretion signal +, secretion of EGFP-FLAG protein with conventional secretion signal sequence), pULSG1C; control (secretion signal -, secretion of EGFP-FLAG protein without secretion signal sequence), pUL-ATG-EGFP; ENO2 (peptide addition +, secretion of N-terminal HA peptide-tagged Eno2p-EGFP-FLAG), pULGI2-ATG-HA-ENO2; ENO2 (peptide addition -, secretion of Eno2p-EGFP-FLAG without peptide addition),

pULGI2-ENO2. Similar results were obtained from 3 independent experiments. *Glycolytic enzymes conjugated to EGFP and FLAG. Additional bands are either nonspecific binding of antibody or degradation products of target proteins.

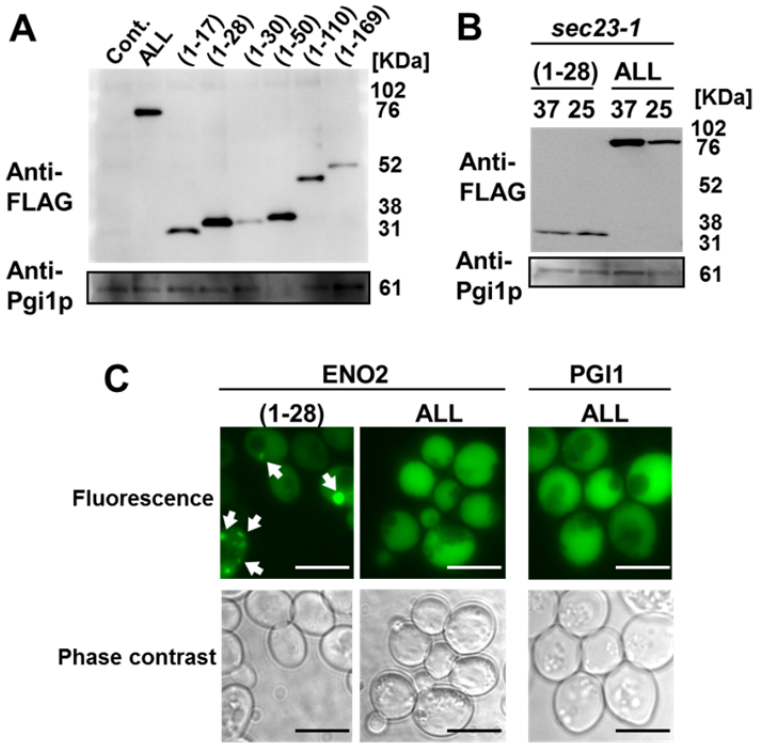

Fig. 3 Detection and monitoring of the secretion of the N-terminal fragment of enolase conjugated to EGFP and FLAG A: Detection of secreted enolase fragments. Cont., pUL-ATG-EGFP; ALL, pULGI2-ENO2; (1–17), pUL-eno(1–17); (1–28), pUL-eno(1–28); (1–30), pUL-eno(1–30); (1–50), pUL-eno(1–50); (1–110), pUL-eno(1–110); (1–169), pUL-eno(1–169). B: *SEC23*-independent secretion of the enolase fragment. Secretion of recombinant proteins in *sec23-1* strains under 25°C or 37°C is shown. (1–28), pUL-eno(1–28); ALL, pULGI2-ENO2; 37, cultivated at 37°C; 25: cultivated at 25°C. C: Fluorescence microscopy of cells transformed with pUL-eno(1–28), pULGI2-ENO2, and pULGI2-PGI1. Scale bar: 10 μm. Similar results were obtained from 3 independent experiments.

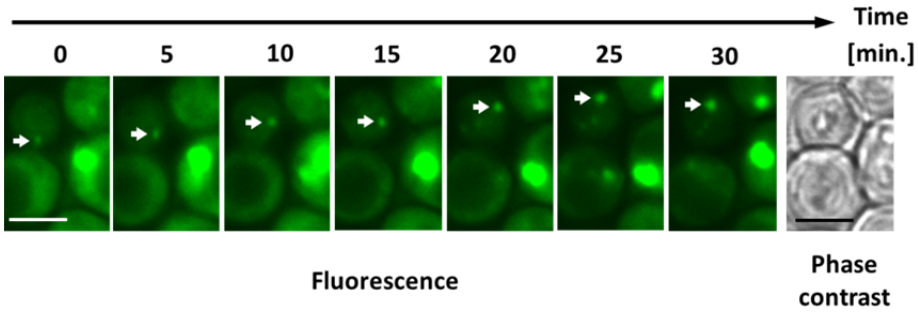

Fig. 4 Time-dependent localization change of the eno(1–28) fragment fused to EGFP Scale bar: 5 μm.

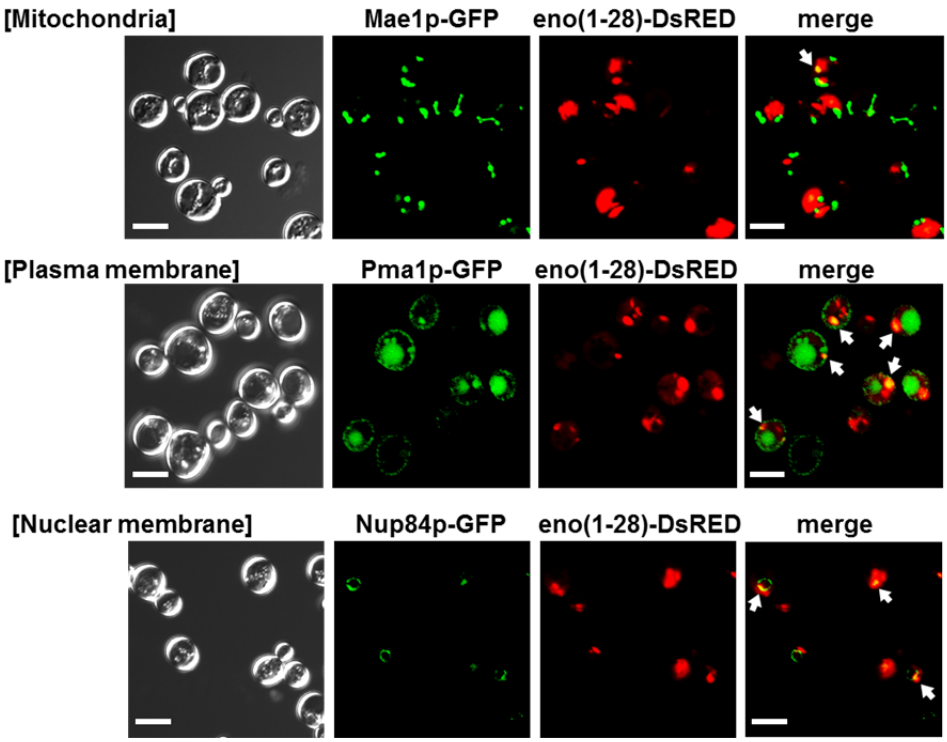

Fig. 5 Colocalization of the enolase fragment conjugated to DsRED and the GFP-tagged organelle markers The fixed cells were observed at room temperature. The numbers of cells forming foci are shown in Table 5. White arrow, foci colocalized with organelle markers. Scale bar: 5 μm.

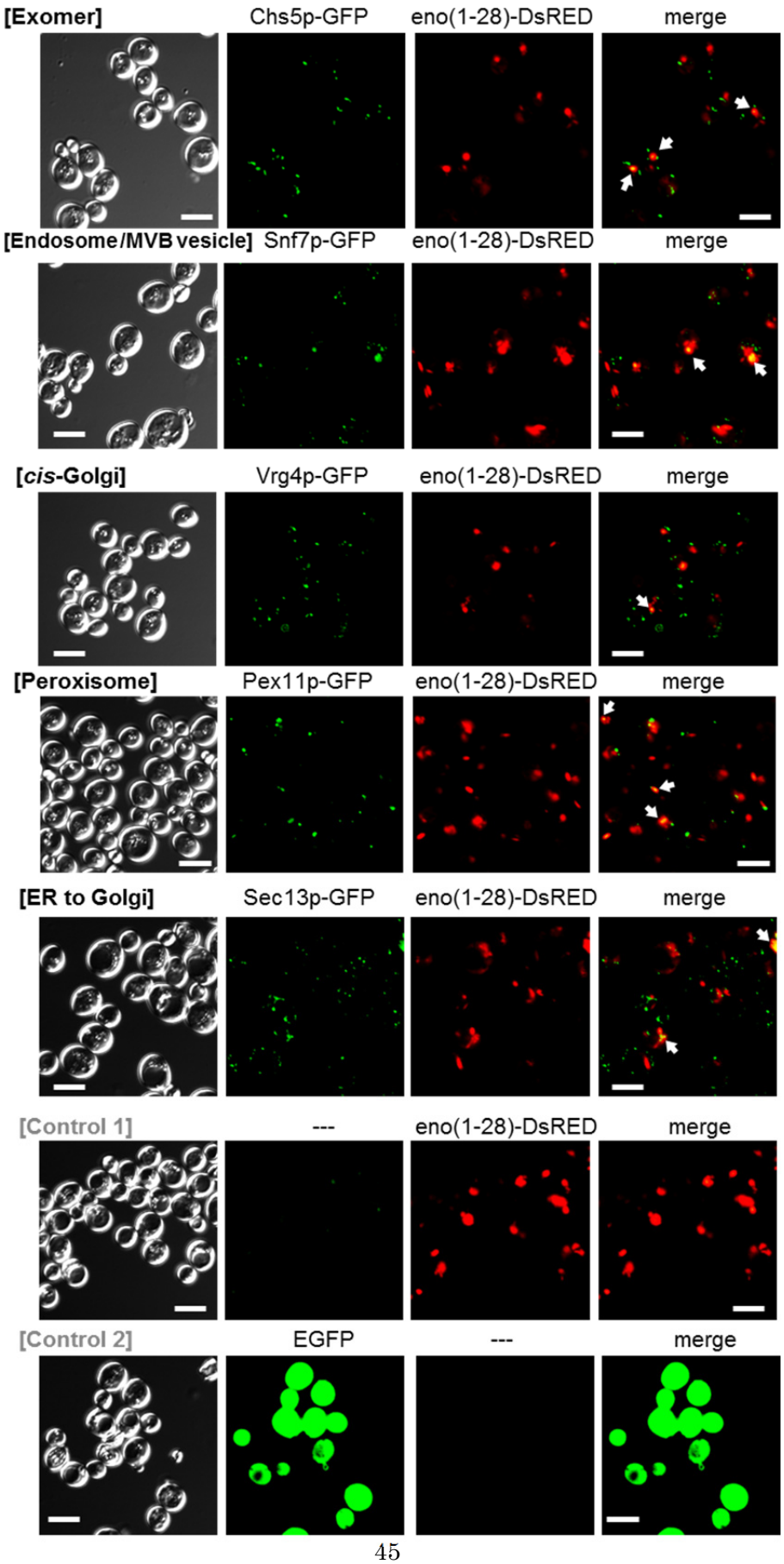

Fig. 6 Co-localization of the enolase fragment conjugated to DsRED and the organelle markers conjugated to GFP (continued from Fig. 5)

Control 1, wild-type cells transformed with pULR-eno(1–28); control 2, wild-type cells transformed with pUL-ATG-EGFP. Scale bar: 5 μm.

Table 5 Calculation of Figure 5 and 6

Organelle marker	a. Number of cells forming DsRED foci	b. Number of cells with GFP fluorescence	c. Number of cells with colocalized foci	c/a [%]
Nup84p	28	72	19	68
Pma1p	21	224	14	67
Snf7p	28	77	15	54
Chs5p	20	80	9	45
Sec13p	20	159	8	40
Pex11p	48	40	16	33
Vrg4p	41	198	15	27
Mae1p	72	27	1	3.7

Foci formation and intracellular translocation of eno(1–28)

To monitor the secretion of the eno(1–28) fragment, the cells producing eno(1–28) conjugated with EGFP and FLAG were observed by fluorescence microscopy (Fig. 3C). The green fluorescence from EGFP was detected as a dot, suggesting that eno(1–28) formed foci. In addition, some of the foci changed location when observed at 30°C on the agarose pad (Fig. 4).

Colocalization of eno(1–28) with organelle marker proteins

To examine the localization of the foci formed by eno(1–28) in the cells, eno(1–28) conjugated with the DsRED monomer was produced in the GFP clones carrying the organelle-marker protein-coding genes (Table 2; *PMA1* (plasma membrane), *NUP84* (nuclear membrane), *MAE1* (mitochondria), *CHS5* (exomer), *SNF7* (endosome and multivesicular body (MVB) vesicle), *VRG4* (*cis*-Golgi), *PEX11* (peroxisome), and *SEC13* (ER to Golgi transport vesicle)), fused with the GFP-coding sequence at the 3′-end. Our results showed that eno(1–28)-DsRED colocalized with the plasma membrane, nuclear membrane, exomer, endosome/MVB vesicle, Golgi, and peroxisome, but not with the mitochondria (Fig. 5, 6, and Table 5).

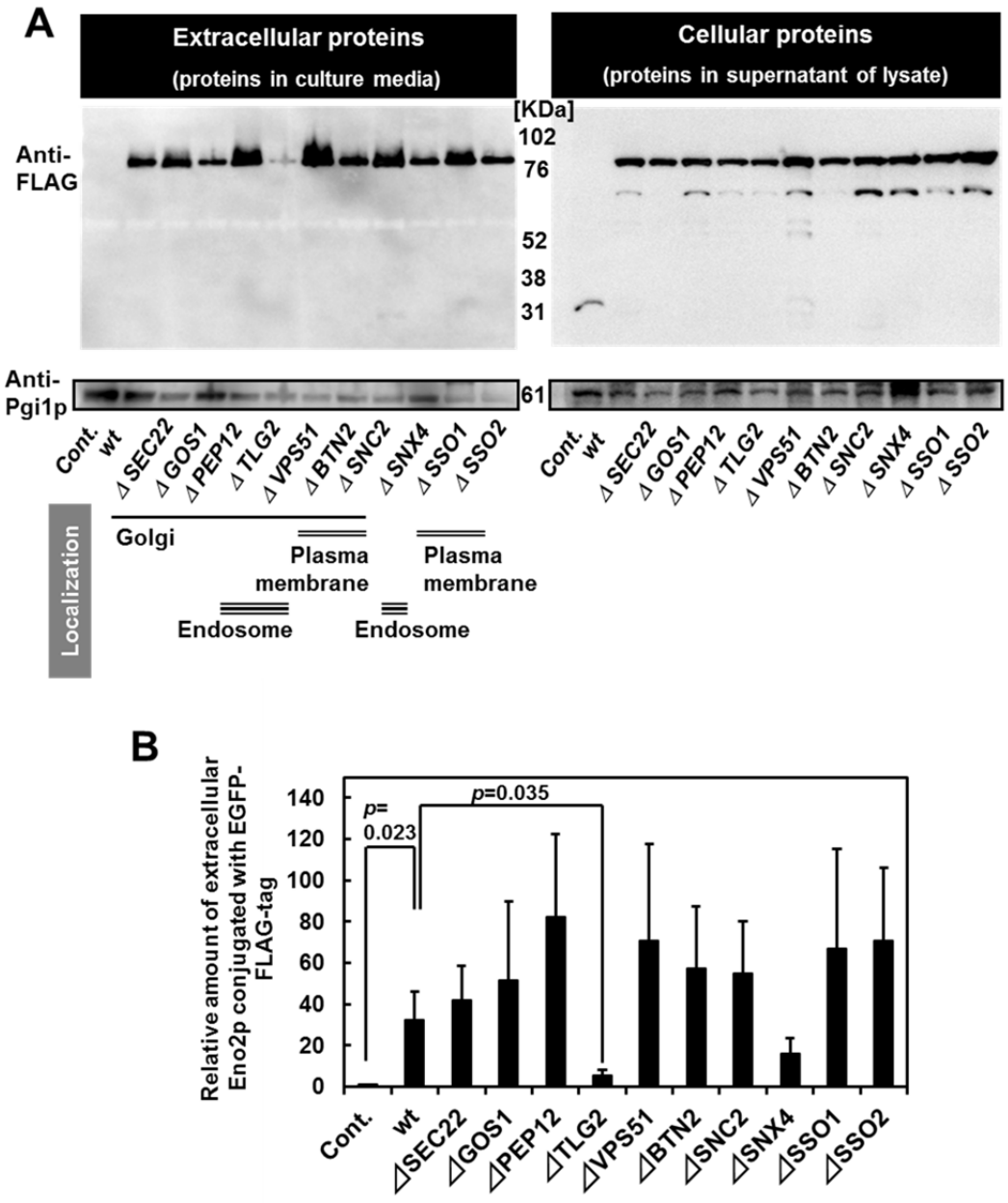

Fig. 7 Intracellular SNARE dependence of Eno2p and Pgi1p secretion A: Secretion in strains transformed with Eno2-expressing plasmids. Cont., wild-type BY4741 cells transformed with pUL-ATG-EGFP; wt, wild-type BY4741 cells transformed with pULGI2-ENO2; Δ, knockout strains transformed with pULGI2-ENO2. B: Calculated amounts of secreted Eno2p by comparison to the levels of Pgi1p secreted. Values are the mean ± SEM of ≥3 independent experiments.

Inhibition of enolase secretion by knockout strains

Knockout strains of SNAREs (see Table 2; *SEC22*, *GOS1*, *PEP12*, *TLG2*, *VPS51*, *BTN2*, *SNC2*, *SNX4*, *SSO1*, and *SSO2*), which play a major role in intracellular protein transportation were utilized to examine their effects on the secretion of Eno2p conjugated with EGFP and endogenous Pgi1p (Fig. 7A). Pgi1p was detected in the culture media of all strains, while the levels of Eno2p-EGFP-FLAG were lower in the culture media of the *TLG2* knockout strain. Inhibition of the translocation of Eno2p-EGFP-FLAG to the cell surface was also tested using immunostaining (Fig. 7B). The *ATG1*, *ATG8*, *ATG11*, *ATG17*, *ATG20*, *VAM3*, and *GRH1* knockout strains (see Table 2) as well as wild-type BY4741 were further tested to investigate the role of autophagy-related genes in secretion (Fig. 9). The secretion of Eno2p was not inhibited in the knockout strains of the autophagy-related genes, demonstrating that of all the SNARE and autophagy-related genes analyzed, only the *TLG2* knockout strain inhibited the secretion of Eno2p (Fig. 7A). *TLG2*-dependency of Eno2p-EGFP-FLAG secretion was further confirmed by complementation of the mutation with a wild-type plasmid (Fig.8). Therefore, I concluded that Eno2p is secreted by an unknown *TLG2*-dependent pathway.

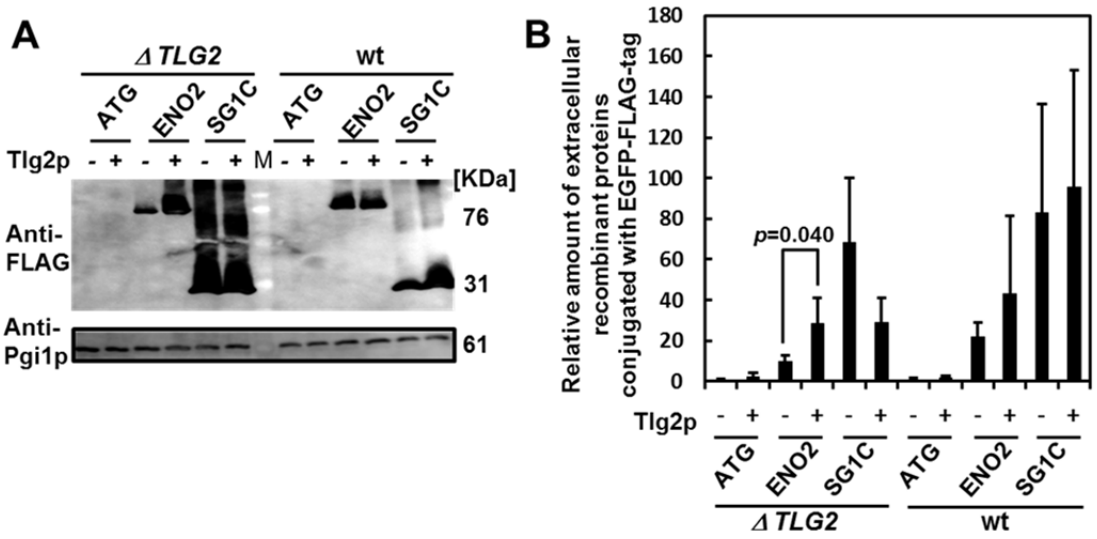

Fig. 8 *TLG2*-dependency of Eno2p secretion A: Secretion in strains transformed with Eno2-expressing plasmids. B: Calculated amounts of secreted proteins by comparison to the levels of Pgi1p secreted. ATG, cells transformed with pUL-ATG-EGFP; ENO2, cells transformed with pULGI2-ENO2; SG1C, cells transformed with pULSG1C, Δ*TLG2*, *TLG2* knockout strains; wt, wild type BY4741 strains; M, marker; Tlg2p -, cells transformed with p413-ADH (control vector); Tlg2p +, cells transformed with p413-ADH-TLG2 (plasmid for producing Tlgp2). Values are the mean ± SEM of ≥3 independent experiments.

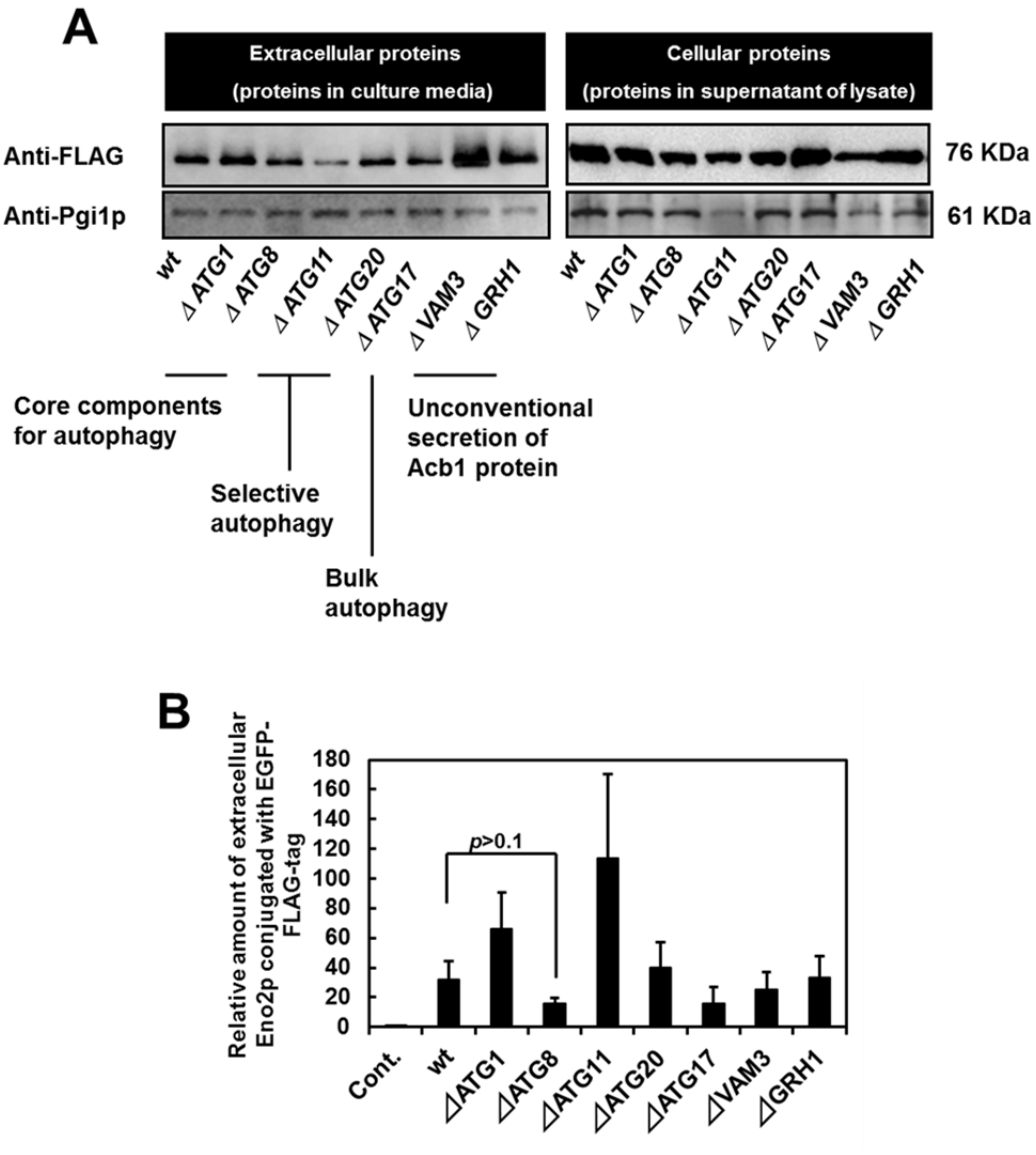

Fig. 9 Autophagy independency of Eno2p and Pgi1p secretion A: Western blots. B: Calculated amounts of secreted Eno2p by comparison to the Pgi1p secreted. Values are the mean ± SEM of 3 independent experiments.

Discussion

The 11 glycolytic enzymes detected by the cell surface proteome analysis, including the 4 detected in the secretion analysis, were all previously reported to be secreted or present in the cell wall in *S. cerevisiae* (Nombela et al. 2006, Oliveira et al 2010). These results demonstrate both the different detection capacities of proteome analysis and western blotting, and the efficacy of our detection method (Table 3). The lower number of glycolytic enzymes detected in the secretion analysis compared to those detected by proteome analysis suggests that the secretion of some of the proteins was undetectable, because the tendency to secrete was too low. However, it is also possible that the conjugated extra amino acid sequence inhibited the secretion of the glycolytic enzymes. I utilized Eno2p to analyze the secretory pathway because enolase secretion is thought to be important for many diseases, and the secretory pathway has not yet been investigated. I utilized Pgi1p as a control because it was detected in high amounts in the culture media. Conjugation of an extra peptide sequence to the N-terminus of Eno2p slightly increased its molecular weight (Fig. 2C), suggesting that Eno2p does not possess a conventional secretion signal sequence that is cleaved during secretion. In addition, Eno2p and Pgi1p were secreted in the *sec23-1* mutant at 37°C. These results provide persuasive evidence that the secretion of glycolytic enzymes, at least Eno2p and Pgi1p, is not dependent on the conventional secretory pathway.

Although full-length Eno2p conjugated with EGFP had a broad subcellular localization, the Eno2p fragment formed foci in the cell, and some of the foci changed location from the center of the cell to the cell periphery (Fig. 3C and 4). Therefore, I assumed that the short amino acid sequence of enolase that can be secreted from the cell exemplifies the secretory pathway of enolase. In the previous report, Lopez-Villar and colleagues demonstrated that eno(1–46) and (1–101) did not exist in the cell wall, whereas the eno(1-169) fragment conjugated with glucoamylase did (Lopez-Villar et al. 2006). Recently, Yang et al. identified the hydrophobic domain required for enolase secretion (Yang et al. 2011). The domain includes the 96–132-aa-long region of *S. cerevisiae* enolase that is a conserved membrane-embedded (EM) domain (Yang et al.), and the domain is not identical to 1-28-aa-long region of enolase. Although EM domain is a bacterial domain, eukaryotic *S.cerevisiae* may have similar mechanisms for secretion of enolase. Because the eno(1–28) region has similarity with the 96–132-aa-long region and EM domain of yeast enolase to some extent, respectively, the secretion of eno(1–28) may depend on the same secretion mechanism as that of the 96–132-aa-long region. There may be a sequence in the N-terminal (29–96) region that inhibits secretion, because in contrast to eno(1–28), eno(1–30) was hardly detected in the culture media. It will be important to complete further investigations and to determine the precise signal sequence required for enolase secretion.

Eno(1–28) conjugated with EGFP and FLAG formed foci in the cell, and changed location over time (Fig. 4). The fragment localized to various cellular membranes, but not to the mitochondria (Fig.

5, 6, and Table 5). It has been previously reported that glycolytic enzymes, including enolase, associate with the post-Golgi vesicles (Forsmark et al. 2011), and that yeast enolase takes part in a macromolecular complex associated with the mitochondria (Brandina et al. 2006), and assists in the transport of tRNA (Entelis et al. 2006). However, the localization of enolase to the mitochondria seems to be regulated by a different region of enolase.

It is reasonable that not all DsRED were colocalized with a particular marker, regarding that enolase colocalized with several markers (Fig. 5, 6, and Table 5). The difference in the number of DsRED and GFP cells reflects the difference in the producing way of each fluorescent protein in the cell; the GFP encoding gene is integrated in the genome of yeast cells, after the each ORF which codes organelle marker protein, whilst DsRED is produced by plasmids. The numbers of GFP-conjugated organelle marker proteins in the cell are dependent on endogenous promoter for each organelle marker protein. Although GFP should be produced in all the cells, some organelle marker proteins are weekly translated and therefore in some case the fluorescence is undetectable. The number of eno(1-28)-DsRED molecules seem to be dependent on transfection efficiency of plasmids, regarding that the plasmid uses the strong *GAPDH* promoter.

I assumed that the major elements that participate in intracellular trafficking also play a role in the secretion of Eno2p. SNAREs govern the translocation of proteins, and although many SNARE-coding genes are lethal when deleted, some non-lethal deletion mutants are available. I used the SNAREs from the *S. cerevisiae* genome database (SGD; http://www.yeastgenome.org/) that participate in the translocation of proteins between the Golgi, endosome, and plasma membrane (Table 2). Analyses of the deletion mutants revealed that knocking out *TLG2* inhibits enolase secretion. However, I propose other proteins may be involved because the inhibition was not complete. In contrast to the previously reported unconventional secretion of the Acb1 protein (Duran et al. 2010, Manjithaya et al. 2010), secretions of Eno2p and Pgi1p were not inhibited in the *GRH1*, *SSO1*, and *BTN2* knockout strains (Fig. 7). Therefore, it is probable that regulation of the secretion of these glycolytic enzymes differs from that of the Acb1 protein. There was also no incorporation of the GRASP protein Vps51p; this is surprising as GRASP proteins have been reported to participate in several unconventional secretory pathways (Kinseth et al. 2007, Manjithaya et al. 2010, Giuliani et al. 2011, Schotman et al. 2008). Therefore, the secretion of glycolytic enzymes in *S. cerevisiae* seems to be independent of the GRASP-regulated pathway. Moreover, Gos1p, which has a role in the cytoplasm-to-vacuole (Cvt) pathway (Bensen et al. 2001), had no influence on the secretion of Eno2p. In addition to its involvement in the Cvt pathway, Tlg2p is a syntaxin-like t-SNARE that participates in vesicle fusion, endocytosis, Golgi-to-vacuole transport, endosomal protein sorting, and protein release from the endoplasmic reticulum (Abeliovich et al. 1999, Coe et a. 1999, Holthuis et al. 1998, Paumet et al. 2001, Gurunathan et al 2002, Mousley et al. 2008). Mousley and colleagues have previously shown that Tlg2p has a role in protein secretion in combination with Sec14p

(Mousley et al. 2008), and our results suggest that the participation of Tlg2p in the secretion of Eno2p is plausible. Therefore, I conclude that the secretory pathway of glycolytic enzymes is regulated in a different manner compared with the Cvt pathway. *S. cerevisiae* is reported to have autophagosome-mediated membrane compartments for the unconventional secretion of proteins (Bruns et al. 2011), and it is, therefore, possible that the secretion of Eno2p is related to an autophagy-related pathway. However, our results using the knockout strains of autophagy-related proteins (Fig. 9) suggest that the absence of active participation of autophagy-related genes in Eno2p secretion.

Foci formation of N-terminal region of Eno2p conjugated with EGFP has not been reported before. Because plasmids for overexpression were used in this study, the observed foci can be aggregates of proteins. However, for the following three reasons, the foci can be a signature of unknown property of the amino acid sequence of Eno2p. First, although full length of Eno2p was overexpressed in the cell in the same way as N-terminal region, full length Eno2p conjugated with EGFP didn't form foci. If the N-terminal foci formation was aggregation of proteins, there should be inhibitory sequences of aggregation inside the sequence of Eno2p. Second, the foci were moving in the cell, and colocalized with various membranes of intracellular organelles. Foci forming region was secreted from the cell without degradation. These observations make it plausible that N-terminal region may be the "carrier" region of Eno2p. Since regulation of intracellular and intercellular localization of moonlighting proteins, including enolase, is highly important for their function, N-terminal region of Eno2p can have unknown roles for moonlighting function of Eno2p.

Summary

Glycolytic enzymes are cytosolic proteins, while they play important extracellular roles in cell-cell communication and infection. I used *S. cerevisiae* to analyze the secretory pathway of some of these enzymes, including enolase, phosphoglucose isomerase, triose phosphate isomerase, and fructose 1,6-bisphosphate aldolase. Enolase, phosphoglucose isomerase, and an N-terminal 28-aa-long fragment of enolase were secreted in a *sec23*-independent manner. The EGFP-conjugated enolase fragment formed cellular foci, some of which were found at the cell periphery. Therefore, we speculated that an overview of the secretory pathway can be gained by investigating the colocalization of the enolase fragment with intracellular proteins. The DsRED-conjugated enolase fragment colocalized with membrane proteins at the *cis*-Golgi, nucleus, endosome, and plasma membrane, but not the mitochondria. In addition, the secretion of full-length enolase was inhibited in a knockout mutant of the intracellular SNARE protein-coding gene *TLG2*. The results suggest that enolase is secreted *via* a SNARE-dependent secretory pathway in *S. cerevisiae*.

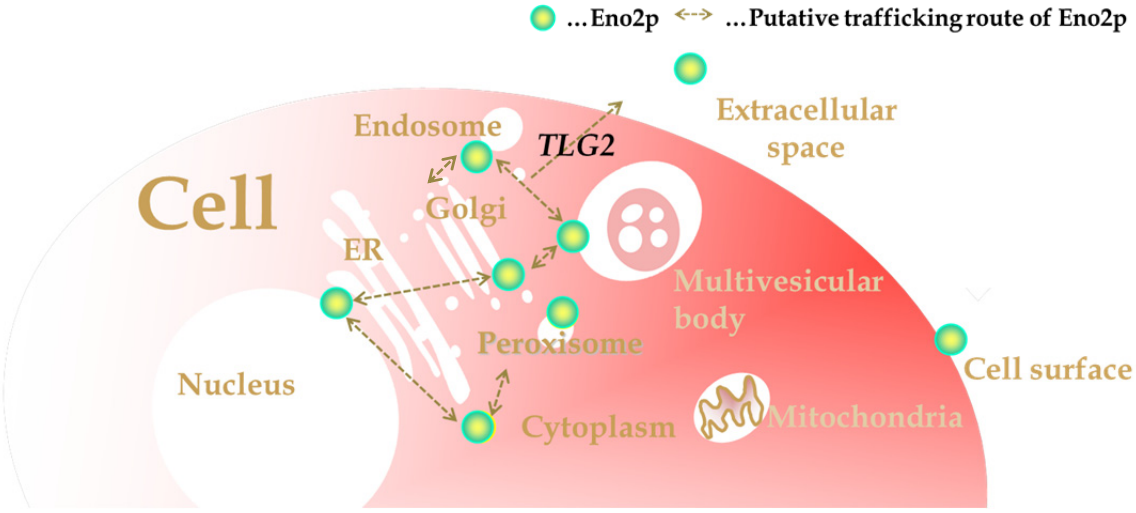

Fig. 10 Putative trafficking pathway of Eno2p

References

1. Abeliovich H, Darsow T, Emr SD (1999) Cytoplasm to vacuole trafficking of aminopeptidase I requires a t-SNARE-Sec1p complex composed of Tlg2p and Vps45p. EMBO J. 21: 6005-6016.
2. Avilan L, Gualdron-Lopez M, Quinones W, Gonzalez-Gonzalez L, Hannaert V, Michels PA, Concepcion JL (2011) Enolase: a key player in the metabolism and a probable virulence factor of trypanosomatid parasites-perspectives for its use as a therapeutic target. Enzyme Res. 2011: 932549.
3. Bechtel JT, Winant RC, Ganem D (2005) Host and viral proteins in the virion of Kaposi's sarcoma-associated herpesvirus. J. Virol. 8: 4952-4964.
4. Bensen ES, Yeung BG, Payne GS (2001) Ric1p and the Ypt6p GTPase function in a common pathway required for localization of trans-Golgi network membrane proteins. Mol. Biol. Cell. 1: 13-26.
5. Brandina I, Graham J, Lemaitre-Guillier C, Entelis N, Krasheninnikov I, Sweetlove L, Tarassov I, Martin RP (2006) Enolase takes part in a macromolecular complex associated to mitochondria in yeast. Biochim. Biophys. Acta. 9-10: 1217-1228.
6. Bruns C, McCaffery JM, Curwin AJ, Duran JM, Malhotra V (2011) Biogenesis of a novel compartment for autophagosome-mediated unconventional protein secretion. J. Cell. Biol. 6: 979-992.
7. Capello M, Ferri-Borgogno S, Cappello P, Novelli F (2011) Alpha-Enolase: a promising therapeutic and diagnostic tumor target. FEBS J. 7: 1064-1074.
8. Chertova E, Chertov O, Coren LV, Roser JD, Trubey CM, Bess JW, Sowder RC, Barsov E,

Hood BL, Fisher RJ, Nagashima K, Conrads TP, Veenstra TD, Lifson JD, Ott DE (2006) Proteomic and biochemical analysis of purified human immunodeficiency virus type 1 produced from infected monocyte-derived macrophages. J. Virol. 18: 9039-9052. doi:10.1128/JVI.01013-06.

9. Chiellini C, Cochet O, Negroni L, Samson M, Poggi M, Ailhaud G, Alessi MC, Dani C, Amri EZ (2008) Characterization of human mesenchymal stem cell secretome at early steps of adipocyte and osteoblast differentiation. BMC Mol. Biol. 9: 26.
10. Coe JG, Lim AC, Xu J, Hong W (1999) A role for Tlg1p in the transport of proteins within the Golgi apparatus of Saccharomyces cerevisiae. Mol. Biol. Cell. 7: 2407-2423.
11. Dobashi Y, Watanabe H, Matsubara M, Yanagawa T, Raz A, Shimamiya T, Ooi A (2006) Autocrine motility factor/glucose-6-phosphate isomerase is a possible predictor of metastasis in bone and soft tissue tumours. J. Pathol. 1: 44-53.
12. Duran JM, Anjard C, Stefan C, Loomis WF, Malhotra V (2010) Unconventional secretion of Acb1 is mediated by autophagosomes. J. Cell. Biol. 4: 527-536.
13. Edwards SR, Braley R, Chaffin WL (1999) Enolase is present in the cell wall of *Saccharomyces cerevisiae*. FEMS Microbiol. Lett. 2: 211-216.
14. Entelis N, Brandina I, Kamenski P, Krasheninnikov IA, Martin RP, Tarassov I (2006) A glycolytic enzyme, enolase, is recruited as a cofactor of tRNA targeting toward mitochondria in *Saccharomyces cerevisiae*. Genes Dev. 12: 1609-1620.
15. Forsmark A, Rossi G, Wadskog I, Brennwald P, Warringer J, Adler L (2011) Quantitative proteomics of yeast post-Golgi vesicles reveals a discriminating role for Sro7p in protein secretion. Traffic. 6: 740-753.
16. Ghosh AK, Jacobs-Lorena M (2011) Surface-expressed enolases of *Plasmodium* and other pathogens. Mem. Inst. Oswaldo Cruz. 106: 85-90.
17. Giuliani F, Grieve A, Rabouille C (2011) Unconventional secretion: a stress on GRASP. Curr. Opin. Cell Biol. 4: 498-504.
18. Gurunathan S, Marash M, Weinberger A, Gerst JE (2002) t-SNARE phosphorylation regulates endocytosis in yeast. Mol. Biol. Cell. 5: 1594-1607.
19. Hirschberg K, Lippincott-Schwartz J (1999) Secretory pathway kinetics and in vivo analysis of protein traffic from the Golgi complex to the cell surface. FASEB J. 13: S251-256.
20. Holthuis JC, Nichols BJ, Dhruvakumar S, Pelham HR (1998) Two syntaxin homologues in the TGN/endosomal system of yeast. EMBO J. 1: 113-126.
21. Hopp TP, Prickett KS, Price VL, Libby RT, March CJ, Pat Cerretti D, Urdal DL, Conlon PJ (1988) A short polypeptide marker sequence useful for recombinant protein identification and purification. Nat. Biotech. 10: 1204-1210.
22. Huang D, Shusta EV (2005) Secretion and surface display of green fluorescent protein using the

yeast *Saccharomyces cerevisiae*. Biotechnol. Prog. 2: 349-357.

23. Innis MA, Holland MJ, McCabe PC, Cole GE, Wittman VP, Tal R, Watt KW, Gelfand DH, Holland JP, Meade JH (1985) Expression, glycosylation, and secretion of an *Aspergillus* glucoamylase by *Saccharomyces cerevisiae*. Science. 4695: 21-26.
24. Jong AY, Chen SH, Stins MF, Kim KS, Tuan TL, Huang SH (2003) Binding of *Candida albicans* enolase to plasmin(ogen) results in enhanced invasion of human brain microvascular endothelial cells. J. Med. Microbiol. Pt 8: 615-622.
25. Kinseth MA, Anjard C, Fuller D, Guizzunti G, Loomis WF, Malhotra V (2007) The Golgi-associated protein GRASP is required for unconventional protein secretion during development. Cell. 3: 524-534.
26. Kuroda K, Matsui K, Higuchi S, Kotaka A, Sahara H, Hata Y, Ueda M (2009) Enhancement of display efficiency in yeast display system by vector engineering and gene disruption. Appl. Microbiol. Biotechnol. 4: 713-719.
27. Laemmli UK (1970) Cleavage of structural proteins during the assembly of the head of bacteriophage T4. Nature. 5259: 680-685.
28. Lamonica JM, Wagner M, Eschenbrenner M, Williams LE, Miller TL, Patra G, DelVecchio VG (2005) Comparative secretome analyses of three *Bacillus anthracis* strains with variant plasmid contents. Infect. Immun. 6: 3646-3658.
29. Lopez-Villar E, Monteoliva L, Larsen MR, Sachon E, Shabaz M, Pardo M, Pla J, Gil C, Roepstorff P, Nombela C (2006) Genetic and proteomic evidences support the localization of yeast enolase in the cell surface. Proteomics. 6: S107-118.
30. Makhina T, Loers G, Schulze C, Ueberle B, Schachner M, Kleene R (2009) Extracellular GAPDH binds to L1 and enhances neurite outgrowth. Mol. Cell Neurosci. 2: 206-218..
31. Manjithaya R, Anjard C, Loomis WF, Subramani S (2010) Unconventional secretion of *Pichia pastoris* Acb1 is dependent on GRASP protein, peroxisomal functions, and autophagosome formation. J. Cell Biol. 4: 537-546.
32. Matsui K, Kuroda K, Ueda M (2009) Creation of a novel peptide endowing yeasts with acid tolerance using yeast cell-surface engineering. Appl. Microbiol. Biotechnol. 1: 105-113.
33. Morisaka H, Kirino A, Kobayashi K, Ueda M (2012) Two dimensional protein separation by HPLC system with monolithic column. Biosci. Biotech. Biochem. 76:110770-1-4.
34. Mousley CJ, Tyeryar K, Ile KE, Schaaf G, Brost RL, Boone C, Guan X, Wenk MR, Bankaitis VA (2008) Trans-Golgi network and endosome dynamics connect ceramide homeostasis with regulation of the unfolded protein response and TOR signaling in yeast. Mol. Biol. Cell. 11: 4785-4803.
35. Nickel W, Rabouille C (2009) Mechanisms of regulated unconventional protein secretion. Nat. Rev. Mol. Cell Biol. 2: 148-155.

36. Nombela C, Gil C, Chaffin WL (2006) Non-conventional protein secretion in yeast. Trends Microbiol. 1: 15-21.
37. Ogino T, Yamadera T, Nonaka T, Imajoh-Ohmi S, Mizumoto K (2001) Enolase, a cellular glycolytic enzyme, is required for efficient transcription of Sendai virus genome. Biochem. Biophys. Res. Commun. 2: 447-455.
38. Oliveira DL, Freire-de-Lima CG, Nosanchuk JD, Casadevall A, Rodrigues ML, Nimrichter L (2010) Extracellular vesicles from *Cryptococcus neoformans* modulate macrophage functions. Infect. Immun. 4: 1601-1609.
39. Oliveira DL, Nakayasu ES, Joffe LS, Guimaraes AJ, Sobreira TJ, Nosanchuk JD, Cordero RJ, Frases S, Casadevall A, Almeida IC, Nimrichter L, Rodrigues ML (2010) Characterization of yeast extracellular vesicles: evidence for the participation of different pathways of cellular traffic in vesicle biogenesis. PLoS One. 6: e11113.
40. Paumet F, Brugger B, Parlati F, McNew JA, Sollner TH, Rothman JE (2001) A t-SNARE of the endocytic pathway must be activated for fusion. J. Cell. Biol. 6: 961-968.
41. Renigunta A, Mutig K, Rottermann K, Schlichthorl G, Preisig-Muller R, Daut Waldegger JS, Renigunta V (2011) The Glycolytic Enzymes Glyceraldehyde 3-Phosphate Dehydrogenase and Enolase Interact with the Renal Epithelial K Channel ROMK2 and Regulate its Function. Cell Physiol. Biochem. 4: 663-672.
42. Schekman R (2010) Charting the secretory pathway in a simple eukaryote. Mol. Biol. Cell. 22: 3781-3784.
43. Schotman H, Karhinen L, Rabouille C (2008) dGRASP-mediated noncanonical integrin secretion is required for *Drosophila* epithelial remodeling. Dev. Cell. 2: 171-182.
44. Shaw ML, Stone KL, Colangelo CM, Gulcicek EE, Palese P (2008) Cellular proteins in influenza virus particles. PLoS Pathog. 6: e1000085..
45. Shinya R, Morisaka H, Takeuchi Y, Ueda M, Futai K (2010) Comparison of the surface coat proteins of the pine wood nematode appeared during host pine infection and in vitro culture by a proteomic approach. Phytopathology. 12: 1289-1297.
46. Sikorski RS, Hieter P (1989) A system of shuttle vectors and yeast host strains designed for efficient manipulation of DNA in Saccharomyces cerevisiae. Genetics. 1: 19-27.
47. Sriram G, Martinez JA, McCabe ER, Liao JC, Dipple KM (2005) Single-gene disorders: what role could moonlighting enzymes play? Am. J. Hum. Genet. 6: 911-924.
48. Swenerton RK, Zhang S, Sajid M, Medzihradszky KF, Craik CS, Kelly BL, McKerrow JH (2011) The oligopeptidase B of *Leishmania* regulates parasite enolase and immune evasion. J. Biol. Chem. 1: 429-440.
49. Takahashi S, Ueda M, Tanaka A (2001) Function of the prosequence for in vivo folding and secretion of active *Rhizopus oryzae* lipase in *Saccharomyces cerevisiae*. Appl. Microbiol.

Biotechnol. 4: 454-462.

50. Tanaka K, Kitamura E, Tanaka TU (2010) Live-cell analysis of kinetochore-microtubule interaction in budding yeast. Methods. 2: 206-213.
51. Torimura T, Ueno T, Kin M, Harada R, Nakamura T, Kawaguchi T, Harada M, Kumashiro R, Watanabe H, Avraham R, Sata M (2001) Autocrine motility factor enhances hepatoma cell invasion across the basement membrane through activation of beta1 integrins. Hepatology. 1: 62-71.
52. Tristan C, Shahani N, Sedlak TW, Sawa A (2011) The diverse functions of GAPDH: views from different subcellular compartments. Cell Signal. 2: 317-323.
53. Tsutsumi S, Gupta SK, Hogan V, Tanaka N, Nakamura KT, Nabi IR, Raz A (2003) The enzymatic activity of phosphoglucose isomerase is not required for its cytokine function. FEBS Lett. 1-3: 49-53.
54. van Deventer HJ, Goessens WH, van Vliet AJ, Verbrugh HA (1996) Anti-enolase antibodies partially protective against systemic candidiasis in mice. Clin. Microbiol. Infect. 1: 36-43.
55. Yang CK, Ewis HE, Zhang X, Lu CD, Hu HJ, Pan Y, Abdelal AT, Tai PC (2011) Nonclassical protein secretion by *Bacillus subtilis* in the stationary phase is not due to cell lysis. J. Bacteriol. 20: 5607-5615.

CHAPTER II

Foci-formation of enolase under hypoxia

Introduction

Spatial rearrangements of proteins and organelles are often a sign of unexpected phenomena in the cell. Some researchers have found novel phenomena by tracking the fluorescence of protein-conjugated GFP (Huh et al. 2003). For example, in several organisms, purine and CTP synthesis is promoted by the formation of protein complexes (An et al. 2008, Noree et al. 2010, An et al. 2010, Ingerson-Mahar et al. 2010). I have found that recombinant EGFP conjugated with N-terminal (1–28) amino acid residues of enolase (Eno2p) can form fluorescent foci in the cell. In addition to its function as a glycolytic enzyme, Eno2p is known as one of the moonlighting proteins (Jeffery 1999). Moonlighting proteins, which have more than one function, often localize to different sites of the cell in association with particular proteins and cellular components to perform their functions (Jeffery 1999). I speculated that the N-terminal (1–28) amino acid sequence might be the region regulating the intercellular localization of Eno2p. Full-length Eno2p conjugated with EGFP localizes uniformly in the cell in shake culture. If the N-terminal region of Eno2p participates in Eno2p localization, full-length Eno2p conjugated with fluorescent proteins would be expected to form foci under unknown environmental stimuli or in a specific phase of cell life. Moreover, amino acid substitution that inhibits foci formation by the N-terminal region should inhibit foci formation by full-length Eno2p. Comparison of foci-forming and -non-forming cells in conjunction with the inhibition of foci formation by reagents that inhibit specific cellular processes may reveal the mechanisms of the regulation and the biological functions of foci formation.

Ununiformed intracellular localization of glycolytic enzymes has been reported in some organisms and cells. An intracellular assembly of glycolytic enzymes was recently reported in mammalian cells; one of the glycolytic enzymes, GAPDH, conjugated with GFP was found to form fluorescent foci under hypoxia (Agbor et al. 2011). Regulation of metabolic pathways by spatial rearrangement of glycolytic enzymes is plausible, given that changes in carbon metabolism under hypoxia have been reported (Feala et al. 2009, Frezza et al. 2011, Postmus et al. 2012). If foci formation by Eno2p could be triggered by hypoxia, the regulatory pathways and biological effects of foci formation might be the same with hypoxic responses. If this hypothesis were borne out, it would be the first case in which spatial rearrangement of glycolytic enzymes under hypoxia was found to regulate a carbon metabolic pathway.

Materials and methods

Strains and media

The *Escherichia coli* DH5α (F^-, Φ80d*lac*ZΔM15, Δ(*lac*ZYA-*arg*F)U169, *deo*R, *rec*A1, *end*A1, *hsd*R17(r_K^-, m_K^+), *pho*A, *sup*E44, λ^-, *thi*-1, *gyr*A96, *rel*A1) strain was used as host cells in the cloning experiments. The yeast strain BY4741 (*MAT*a, *his*3Δ1, *leu*2Δ, *met*15Δ, *ura*3Δ) and the derived deletion strains of *HOG1* (hog1Δ), *SCH9* (sch9Δ), *SNF1* (snf1Δ), and *UPC2* (upc2Δ) were purchased from EUROSCARF (Frankfurt, Germany). The yeast GFP clones (Invitrogen, Carlsbad, CA, USA) with GFP-tagged endogenous proteins (Eno2p, Eno1p, Hxk1p, Pgi1p, Pfk1p, Fba1p, Tpi1p, Gpd1p, Gpp1p, Znf1p, Sol1p, Gnd1p, Tal1p, Tkl1p, Tlk1p, Tdh3p, Pgk1p, Gpm1p, Cdc19p, Pyc1p, Pyc2p, and Pdc1p) and the *HIS3* marker in the parent BY4741 strain were used to determine localization changes in proteins. *E. coli* was grown in lysogeny broth (1% (w/v) tryptone, 0.5% (w/v) yeast extract, 0.5% (w/v) sodium chloride, and 100 ng/mL ampicillin). The yeast cells were grown in yeast extract peptone dextrose (YPD) medium [1% (w/v) yeast extract, 2% (w/v) polypeptone, and 2% (w/v) glucose], YPD+G418 medium [YPD medium supplemented with 0.2 mg/mL G418], SDC+HM agar medium [0.67% (w/v) yeast nitrogen base without amino acids, 2% (w/v) glucose, 0.002% $_L$-histidine-HCl, 0.003% $_L$-methionine, 2% casamino acids (BD, Franklin Lakes, NJ, USA), and 2% (w/v) agar], SDC+HM medium [0.67% (w/v) yeast nitrogen base without amino acids, 2% (w/v) glucose, 0.002% $_L$-histidine-HCl, 0.003% $_L$-methionine, 2% casamino acids (BD), 50 mM MES, pH 6.0], or SC+ML medium [0.67% (w/v) yeast nitrogen base without amino acids, 2% (w/v) glucose, 0.003% $_L$-methionine, 0.003% $_L$-leucine, 0.13% SD Multiple drop out (-Ade, -His, -Leu, -Lys, -Trp, -Ura, Funakoshi Co., Ltd., Tokyo, Japan), and 2% (w/v) agar].

Construction of plasmids

All primers and plasmids used are described in Table 1. Plasmids pULI1 and pUL-ATG-EGFP were used both to adjust growth conditions of different cell types and as controls. To determine the amino acid residue important for foci formation by enolase (Eno2p), plasmids encoding Eno2p fragments and fragments carrying alanine substitutions (Table 1) were constructed. iProof DNA polymerase (Bio-Rad, Richmond, CA, USA), Ligation High (Toyobo, Tokyo, Japan), and synthetic oligonucleotides (Japan Bio Services, Saitama, Japan) were used for plasmid construction. DNA sequencing was performed using BigDye Terminator v3.1 Cycle Sequencing Kit and ABI PRISM 3100 Genetic Analyzer (Applied Biosystems, Foster City, CA, USA). All other chemicals were of analytical grade. The primers and restriction enzymes used are listed in Table 1. In brief, nucleotide sequences were amplified or mixed (for pUL-ATG-EGFP construction) and ligated with restriction fragments of plasmids [pULSG1 (Matsui et al. 2009) and pRS423 (ATCC), respectively].

Plasmid transformation

Yeast cells were transformed with plasmids using Frozen-EZ Yeast Transformation II™ kit (Zymo Research, Orange, CA, USA) and grown on SDC+HLM agar plates. Transformants were selected as single colonies and inoculated into 10 mL of SDC+HM medium with 50 mM MES (pH 6.0) for preculture at 25°C with shaking. At the late log phase, the preculture was subcultured in 100 mL of SD+HM medium at A600 = 0.01 and incubated at 25°C with shaking for 24 h. The culture was subcultured in 100 mL of SDC+HM medium with 50 mM MES (pH 6.0) at A600 = 0.1 for aerobic or semi-anaerobic (CO_2 bubbled) culture at the indicated temperatures.

Preparation of genomes

Gentoru-kun High Recovery kit (Takara, Otsu, Shiga, Japan) was used to extract genomic DNA of GFP clones and yeast knockout mutants. The resulting genomes were used as templates for preparing nucleotide fragments to be transformed into cells.

Construction of GFP-encoding yeast cells

To construct a GFP clone of *ENO2* containing the V22A substitution, an *ENO2* knockout strain was constructed (Table 1). Oligonucleotide fragments containing *ENO2-GFP-HIS3* and *ENO2*V22A-*GFP-HIS3* were prepared (Fig. 1) and then inserted into the genome of the Δ*ENO2* strain at the position of *ENO2*. Yeast cells were transformed with nucleotide fragments and grown on SC+MLU agar plates. Single colonies were picked and again cultured on SC+ML or SC+MLU agar plates. The resulting cells were inoculated into SDC+HM media with 50 mM MES (pH 6.0) and cultured. Construction was confirmed by microscopic observation of fluorescence.

Preparation of knock-out mutants of GFP clones

Primers used are listed in Table 1. In this case, two methods were adopted. For the first, *KanMX4*-containing gene fragments were amplified from genomic DNA of yeast knockout mutant strains and transformed into yeast GFP clones. Transformants were cultivated on YPD+G418 agar plates, and resulting single colonies were again plated on SC+MLU+G418 agar media. For the second method, target gene fragments conjugated with *GFP-HIS3* were amplified and transformed into knockout strains. Transformants were cultured on SC+MLU agar plates, and resulting single colonies were again plated on the same media. Constructed yeast strains were cultured in YPD+G418 liquid media and transformed with plasmid pULI1. Transformants were cultured on SDC+HM agar plates and the resulting colonies were used.

Culture conditions

For aerobic cultivation, a 500-mL Erlenmeyer flask with 100 mL of media was used. For

semi-anaerobic cultivation, a modified method of Katahira et al. (2006) was used. In brief, a culture vial with 100 mL media and stir bar was used. For introduction of CO_2 before cultivation, CO_2 was bubbled for 2 min into the media of the culture vial to remove DO. To provide air in the culture vial, a small air pump (Ei-bukubuku set; Kotobuki-kogei, Matsubara, Osaka, Japan) equipped with a needle-connected tube was used. For static culture, a test tube with 10 mL media was used. Yeast cells were cultivated at the indicated temperatures.

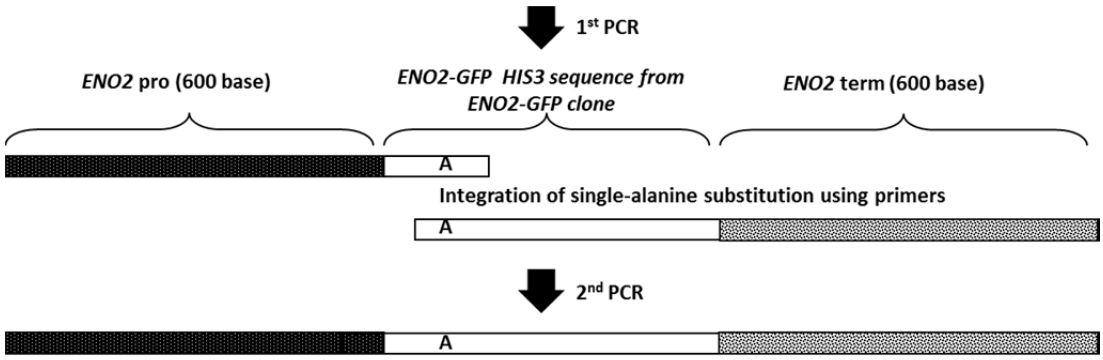

Fig. 1 Preparation of fragments for integration of *ENO2*V22A-GFP pro, promoter, term, terminator

Treatments of cells with reagents

Stock solutions of 100 mM farnesol and 1 mg/mL rapamycin (Santa Cruz Biotechnology, Santa Cruz, CA, USA) in ethanol and 1 mM oligomycin A (Sigma, St. Louis, MO, USA) and 10 mM rotenone (Sigma) in DMSO were prepared. To determine whether mitochondria participate in foci formation, CCCP (a mitochondria depolarizing agent) was used. A stock solution of 5 mM CCCP (Sigma) was prepared in ethanol and added to the media. Antioxidant NAC was directly added to the media.

Fluorescence microscopy

For confocal microscopy, cells were immediately fixed with 4% paraformaldehyde-containing PBS buffer for 1 h and observed. For observation of foci, the cells were immediately fixed or without fixation, immediately mounted on a glass slide and observed. For confocal microscopy, a Carl Zeiss LSM 700 laser scanning microscope (Carl Zeiss, Oberkochen, Germany) with a 60× objective (oil immersion NA, 1.35) and ZEN software were used. Otherwise, an epifluorescence microscope IX71 (Olympus, Lake Success, NY, USA) with a 100× objective (oil immersion NA, 1.40) and Aquacosmos software (Hamamatsu Photonics, Hamamatsu, Shizuoka, Japan) were used.

Table 1 Primers used in CHAPTER II

Plasmid or genotype	Oligo name	Description	Sequence (5'-3')
pUL-eno(30)	eno(1-8) -*EcoR* 1_F	Primers for cloning ENO2 fragments	ACATAAACAGAATTCATGGCTGTCTCTAAAGTTTACGCT
	eno(19-30)_*Xho* 1_R		CAGATCCACCCTCGAGAACACCCTTTTCGGTGGTTAATTCGACTTCGACGGT
pUL-eno(30)V6A	eno(1-8)V6A_*EcoR* 1_F	Primers for introducing amino acid substitution	ATAAACAGAATTCATGGCTGTCTCTAAAGCTTACGCTAGA
pUL-eno(30)Y7A	eno(1-8)Y7A_*EcoR* 1_F		ATAAACAGAATTCATGGCTGTCTCTAAAGTTGCTGCTAGA
pUL-eno(30)R9A	eno(30)R9A_F		TAAACAGAATTCATGGCTGTCTCTAAAGTTTACGCTGCTTCCGTC
pUL-eno(30)S10A	eno(30)S10A_F		TAAACAGAATTCATGGCTGTCTCTAAAGTTTACGCTAGAGCTGTCTAC
pUL-eno(30)V11A	eno(6-21)V11A		GTTTACGCTAGATCCGCTTACGACTCCCGTGGTAACCCAACCGTCGAA
	V11A R		GGAGTCGTAAGCGGATCTAGC
pUL-eno(30)Y12A	eno(30)Y12A_F		TAAACAGAATTCATGGCTGTCTCTAAAGTTTACGCTAGATCCGTCGCTGACTCC
pUL-eno(30)D13A	eno(30)D13A_F		TAAACAGAATTCATGGCTGTCTCTAAAGTTTACGCTAGATCCGTCTACGCTTCCCGT
pUL-eno(30)S14A	eno(6-21)S14A		GTTTACGCTAGATCCGTCTACGACGCTCGTGGTAACCCAACCGTCGAA
pUL-eno(30)R15A	eno(6-21)R15A		GTTTACGCTAGATCCGTCTACGACTCCGCTGGTAACCCAACCGTCGAA
pUL-eno(30)G16A	eno(6-21)G16A		GTTTACGCTAGATCCGTCTACGACTCCCGTGCTAACCCAACCGTCGAA
pUL-eno(30)N17A	eno(6-21)N17A		GTTTACGCTAGATCCGTCTACGACTCCCGTGGTGCTCCAACCGTCGAA
pUL-eno(30)P18A	eno(6-21)P18A		GTTTACGCTAGATCCGTCTACGACTCCCGTGGTAACGCTACCGTCGAA
pUL-eno(30)T19A	Eno(30)T19A -*Xho* 1 R		AGATCCACCCTCGAGAACACCCTTTTCGGTGGTTAATTCGACTTCGACAGCTGG
pUL-eno(30)V20A	Eno(30)V20A -*Xho* 1 R		AGATCCACCCTCGAGAACACCCTTTTCGGTGGTTAATTCGACTTCAGCGGT
pUL-eno(30)E21A	Eno(30)E21A -*Xho* 1 R		AGATCCACCCTCGAGAACACCCTTTTCGGTGGTTAATTCGACAGCGAC
pUL-eno(30)V22A	Eno(30)V22A -*Xho* 1 R		AGATCCACCCTCGAGAACACCCTTTTCGGTGGTTAATTCAGCTTC
pUL-eno(30)E23A	Eno(30)E23A -*Xho* 1 R		AGATCCACCCTCGAGAACACCCTTTTCGGTGGTTAAAGCGAC
pUL-eno(30)E21AE23A	Eno(30)E21E23A -*Xho* 1 R		AGATCCACCCTCGAGAACACCCTTTTCGGTGGTTAAAGCGACAGCGACGGTTGG
pUL-eno(30)V22L pUL-eno(30)V22I pUL-eno(30)V22W pUL-eno(30)V22P pUL-eno(30)V22E pUL-eno(30)V22D pUL-eno(30)V22Y pUL-eno(30)V22S pUL-eno(30)V22T pUL-eno(30)V22R pUL-eno(30)V22H pUL-eno(30)V22K pUL-eno(30)V22N	eno(-25)V22X+GGS *Xho* 1-R		AGATCCACCCTCGAGGGAGCCACCGGTTAATTCMNNTTCGACGGTTGGGTTACC
pUL-eno(1-28)	eno12 (28) R	Primers for cloning ENO2 fragments	CAGATCCACCCTCGAGCTTTTCGGTGGTTAATTCGACTT
pUL-eno(5-28)	eno12 (5-28) F		ACATAAACAGAATTCATGAAAGTTTACGCTAGATCCGTCTACGAC
pUL-eno(6-28)	eno12 (6-28) F		TTCTGCCGAATTCATGGTTTACGCTAGATCCGTCTACGACTCC
pUL-eno(7-28)	eno12 (7-28) F		TTCTGCCGAATTCATGTACGCTAGATCCGTCTACGACTCCCGT
pUL-eno(1-23)	eno(-23) *Xho* 1-R		AGATCCACCCTCGAGTTCGACTTCGACGGTTGGGTTACC
pUL-eno(1-24)	eno(-24) *Xho* 1-R		TCTAGGTGGGAGCTCTAATTCGACTTCGACGGTTGGGTTA
pUL-eno(1-25)	eno(-25) *Xho* 1-R		AGATCCACCCTCGAGGGTTAATTCGACTTCGACGGTTGG
pUL-eno(5-25)			
pUL-eno(5-25)+GGS	eno(-25)+GGS *Xho* 1-R		AGATCCACCCTCGAGGGAGCCACCGGTTAATTCGACTTCGACGGTTGGGTTACC
pUL-eno(5-25)V22A+GGS	eno(-25)V22A+GGS *Xho* 1-R		AGATCCACCCTCGAGGGAGCCACCGGTTAATTCAGCTTCGACGGTTGGGTTACC
pYEX-BX	pYEX-BX (4921-4937)seqF	primer for sequencing pYEX-plasmids	CATATAGAAGTCATCGA
pYEX-BX2	pYEX-BX OSCoMF(in*EcoR* 1/*Kpn* 1)	primers for introducing new restriction sites by OSCoM	GATCAGAATTCGGCGAAGGTAC
	pYEX-BX OSCoMR(in*EcoR* 1/*Kpn* 1)		CTTCGCCGAATTCT
pYEXGI2	-	Produced from pYEX-BX and pULGI2	-
pYEXGI2-eno(30)	-	Produced from pYEX-BX2 and pUL-eno(30)	-
pULGI2-ENO2	-	-	-
pULGI2-ENO2V22A	QuickEno2V22A_F	Primers for introducing V22A substitution	GTGGTAACCCAACCGTCGAAGCTGAATTAACCACCGAAAAGGGT
	QuickEno2V22A_R		ACCCTTTTCGGTGGTTAATTCAGCTTCGACGGTTGGGTTACCAC
pYEX-ENO2G	-	Produced from pYEX-BX and pULGI2-ENO2	-
pYEX-ENO2V22AG	-	Produced from pYEX-BX and pULGI2-ENO2V22A	-

Table 1 Primers used in CHAPTER II (continued)

pUL-E.coliENO(1-31)	E.coli ENO *EcoR* 1-F	Primers for clonig N-terminal domains of various enolase	CATAAATAGAATTCATGTCCAAAATCGTAAAAATCATCG
	E.coli ENO(-31) *Xho* 1-R		AGATCTCCGCTCGAGGAAACCACCCTCCAGATGTACTTCG
pUL-C.albiENO(1-31)	C.albi ENO *EcoR* 1-F		CATAAATAGAATTCATGTCTTACGCCACTAAAATCCACG
	C.albi ENO(-31) *Xho* 1-R		AGATCTCCGCTCGAGTAAACCTTTGTCGGTGGTGAAATCA
pUL-MusENOalpha(1-30)	mouseAlphaEno *EcoR* 1-F		ACATAAACAGAATTCATGTCTATTCTCAGGATCCACGCCA
	mouseAlphaEno(-30) *Xho* 1-R		AGATCCACCCTCGAGGAGACCTTTTGCGGTGTACAGATCG
pUL-MusENObeta(1-30)	mouseBetaEno *EcoR* 1-F		ACATAAACAGAATTCATGGCCATGCAAAAAATCTTCGCCC
	mouseBetaEno(-30) *Xho* 1-R		AGATCCACCCTCGAGTCGACCCTTGGCTGTGTGCAGGTCC
pUL-MusENOgamma(1-30)	mouseGammaEno *EcoR* 1-F		CATAAATAGAATTCATGTCTATAGAGAAGATTTGGGCCC
	mouseGammaEno(-30) *Xho* 1-R		AGATCTCCGCTCGAGAAGACCTTTGGCAGTATAGAGATCC
pULR-eno(1-28)	p*GAP* _F	Primer for sequencing	AGACGGTAGGTATTGATTGTAATTCTG
p416-ADH	*ADH* pro F	primer for sequencing p413pADH and p416-ADH plasmids	ATGAGCAACGGTATACGG
p416-ADH-ATG-FLAG	-	Produced from p416-ADH and pULI-ATG-FLAG	-
p416-ADH-SNF1-FLAG	*SNF1 BamH* 1-F	Primer for amplification of *SNF1* (forward)	ACTAGTGGATCCATGAGCAGTAACAACAACACAAACA
	SNF1 Xho 1-R	Primer for amplification of *SNF1* (reverse)	TCCACCCTCGAGATTGCTTTGACTGTTAACGGCTAAT
	SNF1 seq(147-167) F	Primers for sequencing *SNF1*	TGCACATATCGGGAACTACC
	SNF1 seq(394-413) F		ATAGAGTACGCCGGGAACGA
	SNF1 seq(680-699) F		TGTACGCAGGCCCAGAAGTG
	SNF1 seq(1053-1072) F		TTTATCATCGACCATGGGTT
	SNF1 seq(1302-1321) F		CAAGCAACACGCAAGAAGGA
	SNF1 seq(1605-1629) F		GCCATCTGAAGAGGATTTATGGACT
pULI1	-	-	-
pUL-ATG-EGFP	-	-	-
pULI-ATG-FLAG	*Xho* 1-FLAG-*Sal* 1 OSCoM-F	Primers for forming FLAG sequence by OSCoM	TCGAGGGTGGATCTGATTACAAGGATGACGATGACAAGTAAG
	Xho 1-FLAG-*Sal* 1 OSCoM-R		TCGACTTACTTGTCATCGTCATCCTTGTAATCAGATCCACCC
△*ENO2::URA3*	del*ENO2*-Oligo1	Primers for introducing *URA3* instead of *ENO2*	CATAACACCAAGCAACTAATACTATAACATACAATAATAATGGCT GTCTCCATGGAAAAGAGAAG
	del*ENO2*-Oligo2		TTGATACTACTTTTTTATTCGTCTTTTCTGATTATTAAGAATCAATT TTACGACTCACTATAGGG
	pBS1539URA3coloP-F	Primers for checking *URA3*	GACCCAATGCATCGCCTTTG
	pBS1539URA3coloP-R		TGGGCCATTTTGTGAAAGCC
△*ENO2::KanMX4*	*ENO2*::*KanMX4* [1-F]	Primers for introducing *KanMX4* instead of *ENO2*	TAACATACAATAATAATGGATGTCCACGAGGTCTCTAGCA
	ENO2::*KanMX4* [1-R]		TTAGTTAAAAGCACTTTACGGTGTCGGTCTCGTAGGATTA
	ENO2::*KanMX4* [2-F]		AGACCGACACCGTAAAGTGCTTTTAACTAAGAATTATTAG
	ENO2::*KanMX4* [2-R]		CTCGTGGACATCCATTATTATTGTATGTTATAGTATTAGT
△*ENO2::ENO2G*	*ENO2-GFP-HIS3* F	Primers for introducing *ENO2-GFP* instead of *ENO2*	AAAGCATTATCTTCCTACCAGAGTTGATTGTTAAAAACGTATTTAT AGCAAACGCAATTG
	ENO2-GFP-HIS3 R		AATAAGCAGAAAAGACTAATAATTCTTAGTTAAAAGCACTTCGAT GAATTCGAGCTCGTT
	eno2-1 F	Primers for cloning *ENO2* from genome and for sequencing	ATACCAAGTCAGCATACACC
	eno2-2 F		TTATCTTCCTACCAGAGTTG
	eno2-3 F (eno1-3 F)		AAGTCGAATTAACCACCGAA
	eno2-4 F		TCTTGTTGTCTTTGGATGGT
	eno2-5 F (eno1-5 F)		GTTCCGAAGTTTACCACAAC
	eno2-6 F (eno1-6 F)		TTCAAGGACGGTAAGTACGA
	eno2-7 F (eno1-7 F)		ACTGGGAAGCTTGGTCTCAC
	eno2-8 F		CTGGTGAAACTGAAGACACT
	eno2-9 F		TTTTCAAAGACTCGTGCTGT
	eno2-10 R		ACACGTATTCTTGTATGACC
△*ENO2::ENO2V22AG*	QuickEno2V22A_F	Primers for introducing V22A substitution	GTGGTAACCCAACCGTCGAAGCTGAATTAACCACCGAAAAGGGT
	QuickEno2V22A_R		ACCCTTTTCGGTGGTTAATTCAGCTTCGACGGTTGGGTTACCAC
ENO2-GFP, △*HOG1*	*HOG1* (up) F	Primers for checking genotype	ACAAAGGGAAAACAGGGAAAACTACAACTATCGTATATAA
	HOG1 (down) R		AAGAAGTAAGAATGAGTGGTTAGGGACATTAAAAAAACAC
	KANB_R		CTGCAGCGAGGAGCCGTAAT
ENO2-GFP, △*UPC2*	*UPC2* (up) F		GAATCAAAAAAAGTTAAGTACAAATATTTACAGTTCAGCA
	UPC2 (down) R		TTGGGAATCTATTTCGAATATTCTGCACTTTTAAATTTTC
ENO2-GFP, △*SNF1*	*SNF1* (up) F		CTGCGCATTCGTGTCCAAAC
	SNF1 (down) R		TTTTGTCGCAGACTCCGTTCT
ENO2-GFP, △*SCH9*	*SCH9* (up) F		CATAATCACCTAAGGGCATCT
	SCH9 (down) R		TCGGATGATATAACCGACCT

pH and DO measurement

pH measurement of culture media was performed using a F-52 pH meter (Horiba, Kyoto, Japan). Time course measurement of DO (mg/L) was performed using a luminescent DO (LDO) meter (HQ30d; Hach Co., CO, USA). Measurements were recorded automatically every 15 min for 8 h. As an indicator of anoxia, 1 mg/mL stock solution of resazurin (Sigma) was added to the media to a final concentration of 1 μg/mL to make a blue-colored solution. Under anoxia, the resazurin-containing media has no color, while under hypoxia, it turns red.

FACS analysis

Cells were suspended in PBS and assayed immediately using a cell sorter (JSAN, Bay Bioscience, Kobe, Hyogo, Japan) using the detection channel FLT1 (535DF45). In each case, the fluorescence of 10,000 cells was acquired.

Sample preparation of yeast proteins for proteomic analysis

S. cerevisiae BY4741 strains transformed with pYEX-ENO2G or pYEX-ENO2V22AG were cultivated aerobically or semi-anaerobically at 30°C. The cells were lysed as described above, and proteins were extracted. Protein purification was performed as follows:

250 μL of 25 mM Tris-HCl buffer (pH 7.8) was added to frozen cells. After homogenization for 3 times at 4,000 rpm for 60 sec using glass beads (GB-05, diameter 0.5 mm; TOMY, Tokyo, Japan) and Bead Smash 12 (Wakenyaku, Kyoto, Japan), the sample solutions were centrifuged at 9,700 g for 5 min at 4°C. Aliquots (500 μL) of the supernatants were filtrated using 0.45 μm spin column filter membrane (Durapore PVDF membrane; Millipore, Eschborn, Germany) and set still on ice. Purification of proteins was carried out immediately after extraction of proteins using ANTI-FLAG M2 affinity gel (Sigma) and column (Poly-Prep Chromatography Columns; Bio-Rad) following the manufacturer's protocol. After purification, samples were washed with 20 mM triethylammonium bicarbonate using Microcon YM-3 concentrator (Millipore).

The collected proteins were reduced with 10 mM tris(2-carboxyethyl)phosphine (Thermo Scientific) for 30 min and alkylated with 20 mM iodoacetamide (Thermo Scientific) for 60 min in the dark at room temperature. After acetone precipitation, the proteins were solubilized in 200 mM triethylammonium bicarbonate (Sigma). Protein digestion (trypsin:protein = 1:50) was performed overnight at 37°C. Tryptic digests were applied to a proteome analysis system.

Liquid chromatography–tandem mass spectrometry (LC-MS/MS) analysis and MS data analysis

rotein identification was performed with a liquid chromatography/mass spectrometry system as described in (Aoki et al. 2012). Proteolytic digests were separated by reversed-phase

chromatography using a UltiMate3000 nano LC system (Dionex). A monolithic silica capillary column (200 cm long, 0.1 mm i.d.) prepared with a mixture of tetramethoxysilane and methyltrimethoxysilane was used at a flow rate of 500 nL/min. The gradient was provided by changing the mixing ratio of the 2 eluents: A, 0.1% (v/v) formic acid and B, 80% acetonitrile containing 0.1% (v/v) formic acid. The gradient was started with 5% B and increased to 50% B for 600 min. The separated analytes were detected on an LTQ Velos linear ion trap mass spectrometer (Thermo Scientific). An ESI voltage of 2.4 kV was applied directly to the LC buffer distal to the chromatography column using a microtee. The ion transfer tube temperature on the LTQ Velos ion trap was set to 300°C. For data-dependent acquisition, the method was set to automatically analyze the five most intense ions observed in the MS scan. The mass spectrometry data were used for protein identification by the Mascot search engine on Protein Discoverer software (Thermo Scientific) against the information in the Saccharomyces Genome Database (SGD; http://www.yeastgenome.org). Search parameters for peptide identification included a precursor mass tolerance of 2.2 Da, a fragment mass tolerance of 0.8 Da, a minimum of one tryptic terminus, and a maximum of one internal trypsin cleavage site. Cysteine carbamidomethylation (+57.021 Da) and methionine oxidation (+15.995 Da) were set as a differential amino acid modification. The data were then filtered at a q value ≤ 0.01 corresponding to 1% FDR at the spectral level, and identified proteins coimmunoprecipitated with Eno2p-EGFP-FLAG-tag contained $\geq$4 peptide fragments.

Extraction of cellular metabolites

Cellular metabolites were extracted by modified methods of Mashego et al. (2003). Cells incubated at 30°C in 500 μL media containing [U-^{13}C]-glucose for 0, 2, 5, and 10 min were immediately injected into 5 mL of 60% methanol at −40°C. After centrifugation at 5,000 ×*g* at −9°C for 5 min, the supernatants were discarded and 3 mL of 75% ethanol was added. After heating at 100°C for 30 min and cooling on ice and then at −40°C, the cells were lyophilized and stored at −80°C. For sample preparation, 1 mL of MilliQ and 60 μL of 0.2 mg/mL ribitol were added to lyophilized cells and heated at 37°C for 30 min in a 1.5 mL test tube. The samples were then centrifuged at 16,000 ×*g* for 5 min at 4°C, 900 μL of supernatant was transferred to a new tube, 400 μL of MilliQ was added to each sample followed by centrifugation at the same rate, and 400 μL of supernatant was transferred to a new tube, lyophilized, and used for metabolite analysis.

Extracted metabolites were derivatized as described (Tsugawa et al. 2011). For oximation, 100 μL of methoxyamine hydrochloride in pyridine (20 mg/mL) was added and incubated at 30°C for 90 min. For trimethylsilylation, 50 μL of *N*-methyl-*N*-(trimethylsilyl) trifluoroacetamide was added, followed by incubation at 37°C for 30 min. Insoluble residue was removed by centrifugation at, 10,000 ×*g* for 10 min at 4°C, and the supernatant was transferred to a clean vial.

GC/MS analysis

Derivatized metabolites were analyzed using GCMS-QP2010 Ultra (Shimadzu, Kyoto, Japan) equipped with a 30 m × 0.25 μm i.d. fused silica capillary column coated with 0.25-μm CP-SIL 8 CB low bleed (Agilent Technologies, Palo Alto, CA, USA). Aliquots of 1 μL were injected in split mode (25/1, split mode) at 230°C using helium as carrier gas at a flow rate of 1.12 mL/min. The column temperature was held at 80°C for 2 min isothermally, then raised at 4°C/min to 130°C, and then raised at 25°C/min to 330°C and held for 6 min isothermally. Interface and MS source temperatures were 250°C and 200°C, respectively, and ion voltage was 1 kV. Data were collected by GC-MS solution software (Shimadzu), and identified metabolites are shown in Table 2. Mass isotopomer distributions were corrected for natural isotope abundance as described (Nanchen et al. 2007).

Table 2 Target metabolites in GC/MS analysis

Name	Retention time (min)	Formula	m/z range
Pyruvate & Oxaloacetate	4.63	$C_6H_{12}NO_3Si$	174-177
Alanine	7.57	$C_8H_{20}NO_2Si_2$	218-221
Glycerol	13.20	$C_{12}H_{32}O_3Si_3$	218-221
Malate	17.29	$C_{12}H_{27}O_5Si_3$	335-339
Aspartate	17.60	$C_9H_{22}NO_2Si_2$	232-235
PEP	18.27	$C_{11}H_{26}O_6PSi_3$	369-372

Section 1 Determination of foci-forming region of enolase

Determination of the region of Eno2p that is sufficient for foci formation

To determine the key residue for foci formation by Eno2p, the N-terminal foci-forming Eno2p region was investigated. The shortest foci-forming region of N-terminal Eno2p fused with EGFP was amino acid residues 5–24 (Fig. 2). Foci-forming cells increased when the amount of proteins increased, while still there were foci-forming cells with few proteins (Fig. 3).

Determination of important amino acid residues for foci formation by single alanine substitution

In amino acid residues 6–23, alanine substitution of V22 inhibited foci formation (Fig. 4).

Amino acid substitution of V22 residue to gain information on the role of V22

Substitution of V22 with A, P, E, D, S, T, R, H, K, and N also inhibited foci formation by the N-terminal region, while substitution with L, I,Y, and W conserved foci (Fig.5).

Effects of foci-inhibiting V22A substitution on secretion of Eno2p

To test whether the foci forming property of Eno2p correlates secretion, secretion of V22A substituted proteins of both N-terminal region and full length Eno2p were investigated. As the result, substitution of V22 to alanine didn't inhibit secretion of both N-terminal region of and full length Eno2p (Fig. 6).

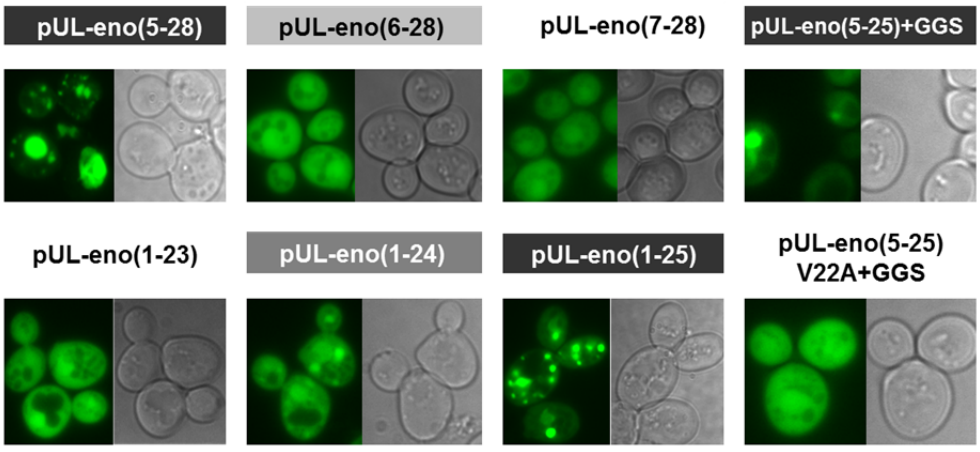

Fig.2 Determination of the foci-forming region of N-terminal Eno2p conjugated with EGFP and a FLAG tag. pUL-eno(X-Y): cells transformed with plasmids pUL-eno(X-Y). pUL-eno(5–25)+GGS: cells transformed with plasmid pUL-eno(5–25)+GGS. Cells were aerobically cultivated and observed.

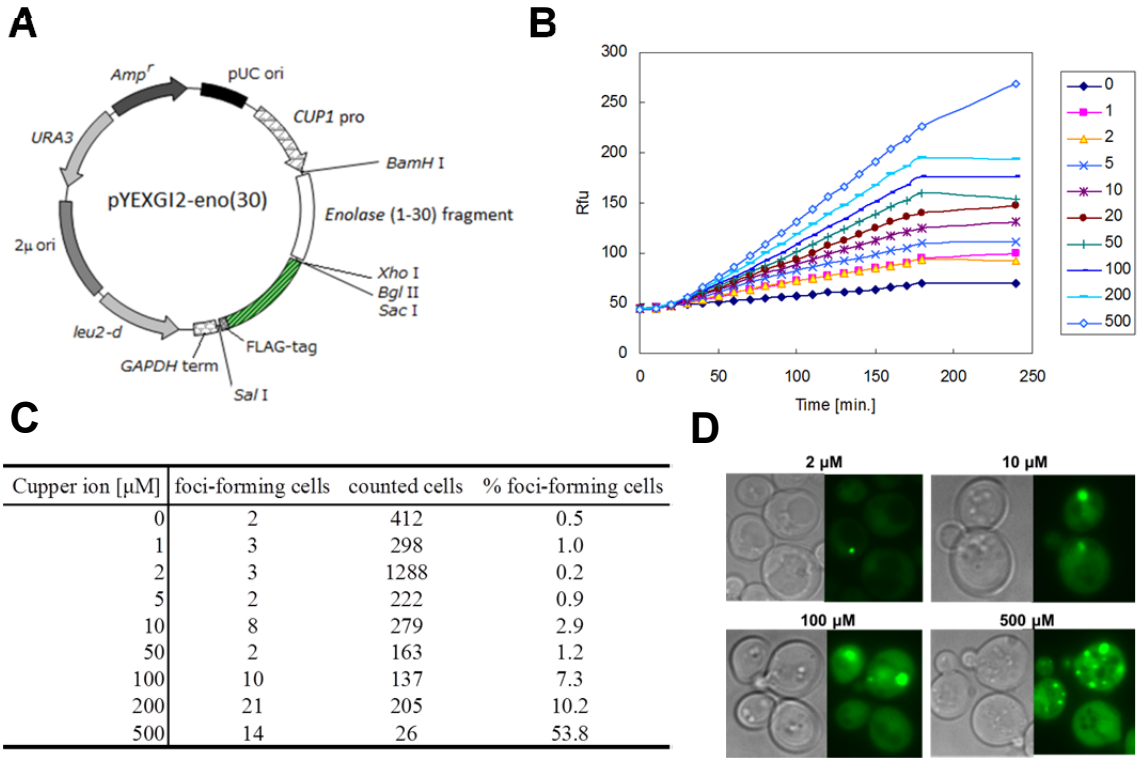

Cupper ion [μM]	foci-forming cells	counted cells	% foci-forming cells
0	2	412	0.5
1	3	298	1.0
2	3	1288	0.2
5	2	222	0.9
10	8	279	2.9
50	2	163	1.2
100	10	137	7.3
200	21	205	10.2
500	14	26	53.8

Fig. 3 Protein amount-dependent changes in the proportion of foci-forming cells. A: Illustration of the plasmid used. B: Time- and Cu^{2+}-dependent fluorescence induction. The number off the line indicate the concentration of $CuSO_4$ [μM] in the reaction solution. C: Percentage of foci-forming cells. D: Images of foci forming cells.

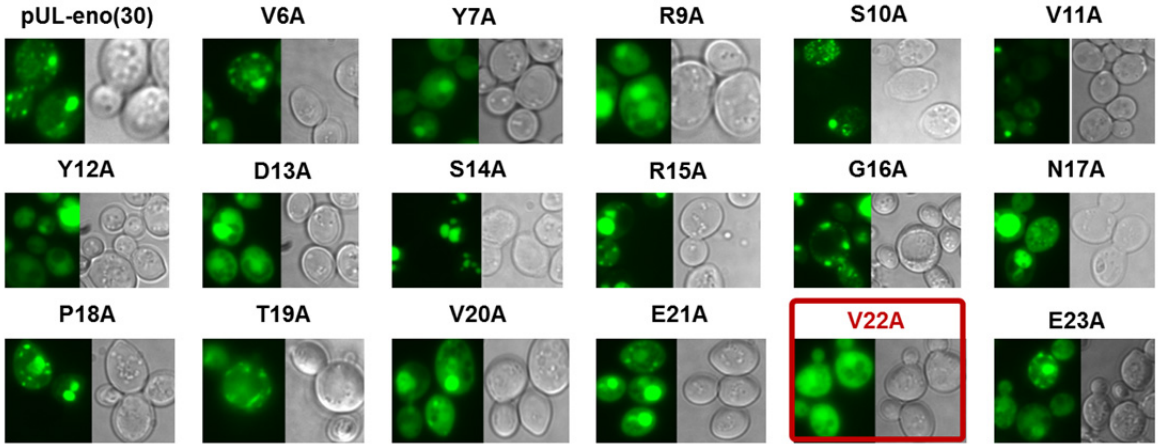

Fig. 4 Single alanine substitution of N-terminal amino acids of Eno2p conjugated with EGFP and FLAG. pUL-eno(30): cells transformed with plasmid pUL-eno(30). XxA: cells transformed with plasmids pUL-eno(30)XxA.

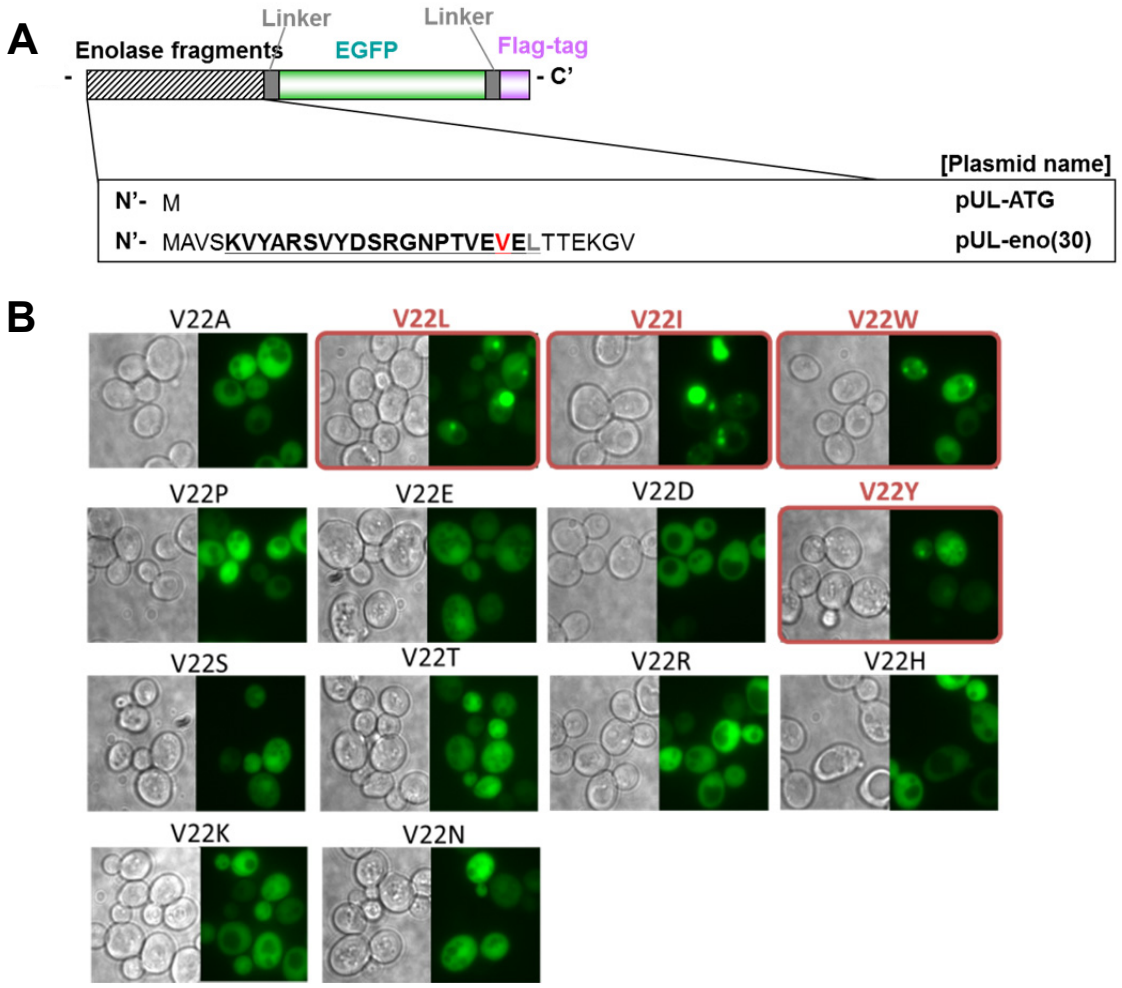

Fig. 5 Amino acid substitutions of Val22 residue. A: Illustration of pUL-eno(30) and the mutated residues. B: Fluorescence images. V22X: cells transformed with plasmid pUL-eno(30) V22X in which the Eno2p N-terminal (1–30) amino acid sequences with V22X substitution were conjugated with EGFP and a FLAG tag.

Conservation of the foci-forming ability

Conservation of the foci-forming ability of the N-terminal region was further investigated. The N-terminal region of Eno2p is conserved across species (Fig. 7A). In *Escherichia coli* enolase, although V22 was not conserved, the N-terminal region conserved the foci-forming ability. In contrast, in mouse β- and γ-enolase, the foci-forming ability was lost although V22 residues were conserved. Interestingly, mouse α-enolase retained the foci-forming ability (Fig. 7B). These results suggest that the foci-forming ability of the N-terminal region of Eno2p is conserved over species but is not always dependent on V22.

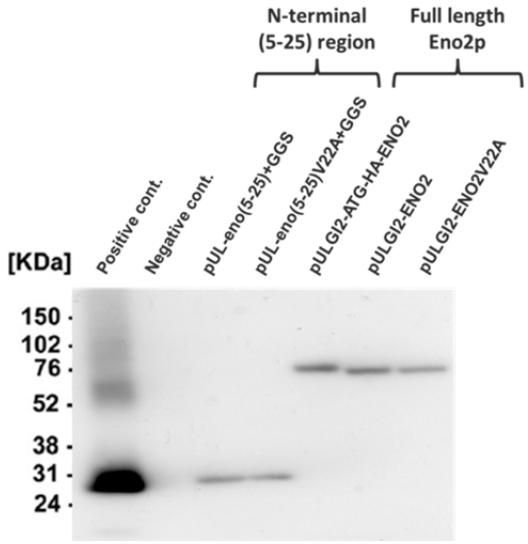

Fig. 6 Effects of V22A substitution on secretion of Eno2p. Positive cont.: secreted proteins from cells transformed with pULSG1C. Negative cont.: secreted proteins from cells transformed with pULI1. pUL-X: secreted proteins from cells transformed with pUL-X plasmids.

Discussion

Val 22 and foci forming (5-25) amino acid residues is located in the N-terminal beta-hairpin forming region in Eno2p (Fig. 8). Amino acids V, I, L, Y, and W, which supported the foci-forming ability at amino acid 22 in the N terminus, have also been reported to be important in stacking of β-hairpin structures of tau proteins (Margittai and Langen 2006). Accordingly, the three-dimensional structure of the N-terminal Eno2p region might be important in forming foci. Spatial rearrangement of the specific amino acid sequence of Eno2p may promote the spatial rearrangement of the whole protein (Fig. 9).

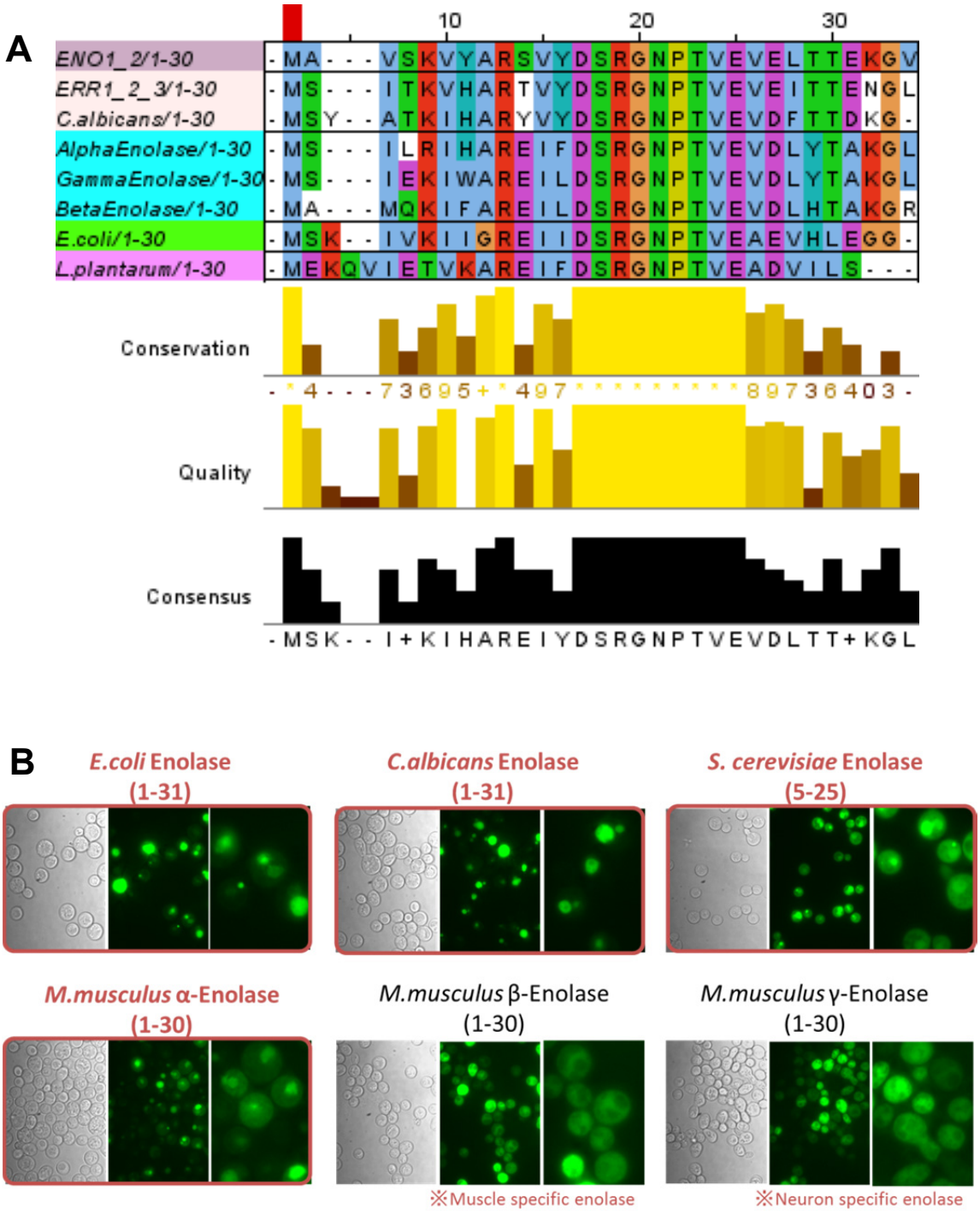

Fig. 7 Conservation of primary sequence and foci-forming properties od N-terminal region of enolases. A: Sequence alignment of N-terminal amino acids of Eno2p. B: Foci formation of N-terminal fragments of enolases conjugated with EGFP and a FLAG tag. Cells transformed with plasmids for producing N-terminal amino acid sequences of enolases conjugated with EGFP and a FLAG tag are shown.

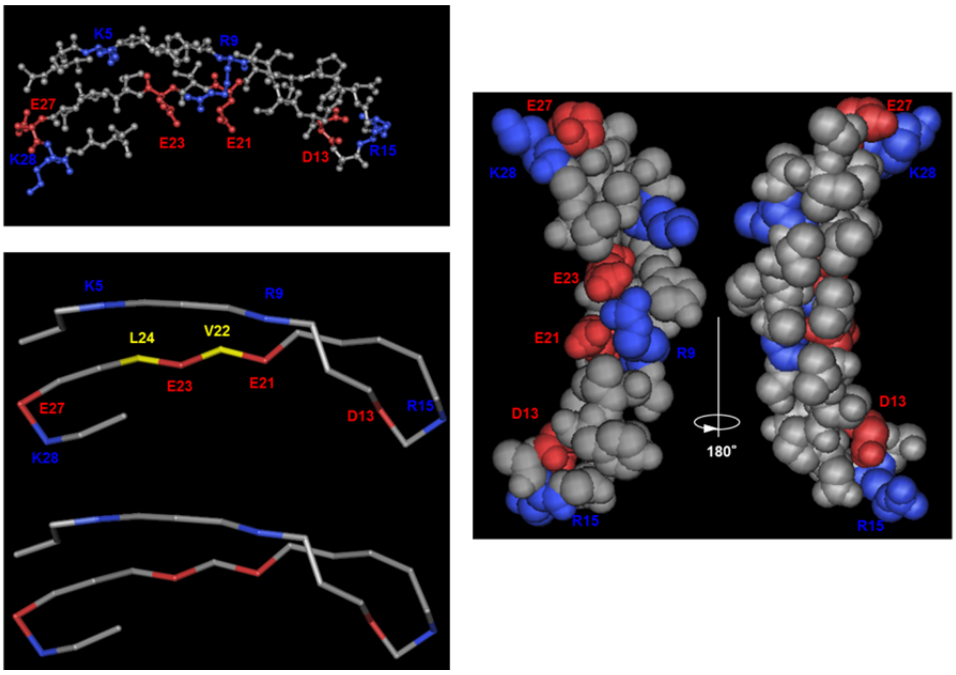

Fig. 8 Three-dimensional structures of N-terminal (1-30) region of Eno2p. Red: positively charged amino acid residues. Blue: negatively charged amino acid residues. Yellow: important amino acid residues for foci formation. PDB ID: 1one.

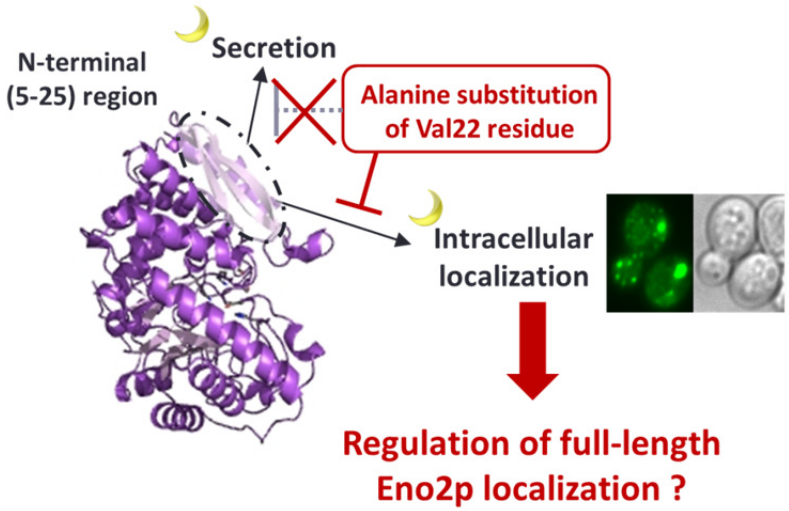

Fig. 9 Suggested roles of N-terminal region of Eno2p on unknown moonlighting functions. Sun: previously known function of moonlighting proteins. Moon: moonlighting functions. Dotted circle: suggested areas of proteins responsible for the function indicated by arrows.

Section 2 Discovery of foci-formation of full-length enolase under hypoxia

Discoveries of changes in localization of glycolytic enzymes including Eno2p, conjugated with EGFP, which are overproduced by plasmids in *S. cerevisiae* BY4741wt cells

S. cerevisiae B4741 wt strains transformed with plasmids for overexpressing proteins of glycolytic enzymes conjugated with EGFP and a FLAG-tag formed concentrated EGFP in static culture (Fig. 10).

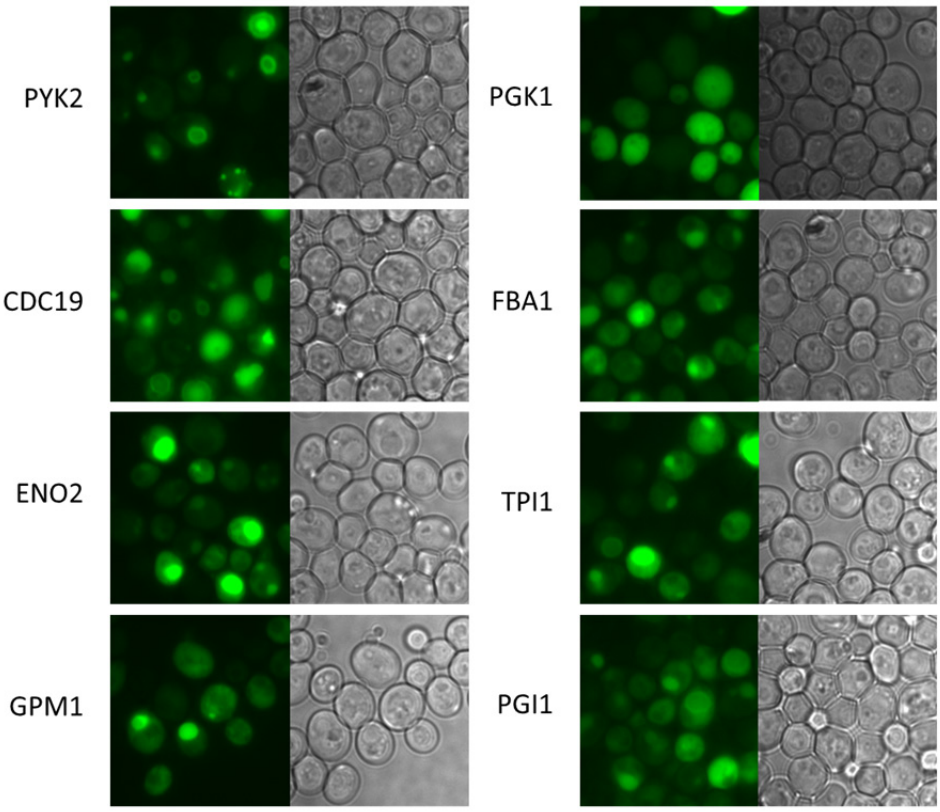

Fig. 10 Localization of EGFP fluorescence conjugated with glycolytic enzymes after static culture. Cells transformed with PULGI2-X plasmids are shown (X: each name represented in the figure).

Foci-formation of GFP-conjugated metabolic enzymes under hypoxia

Fermentation vials were used to culture cells under semi-anaerobic (hypoxic) conditions (Fig. 11). A GFP clone in which *ENO2* is fused with *GFP* (ENO2-GFP strain) formed foci under fermentative conditions after 6 h of culture in vials at 30°C (Fig. 11A). Foci formation by the glycolytic enzymes Cdc19p, Gpm1p, Pfk1p,Gpd1p, Ald4p, and Tdh3p under hypoxia was also observed (Fig. 11B).

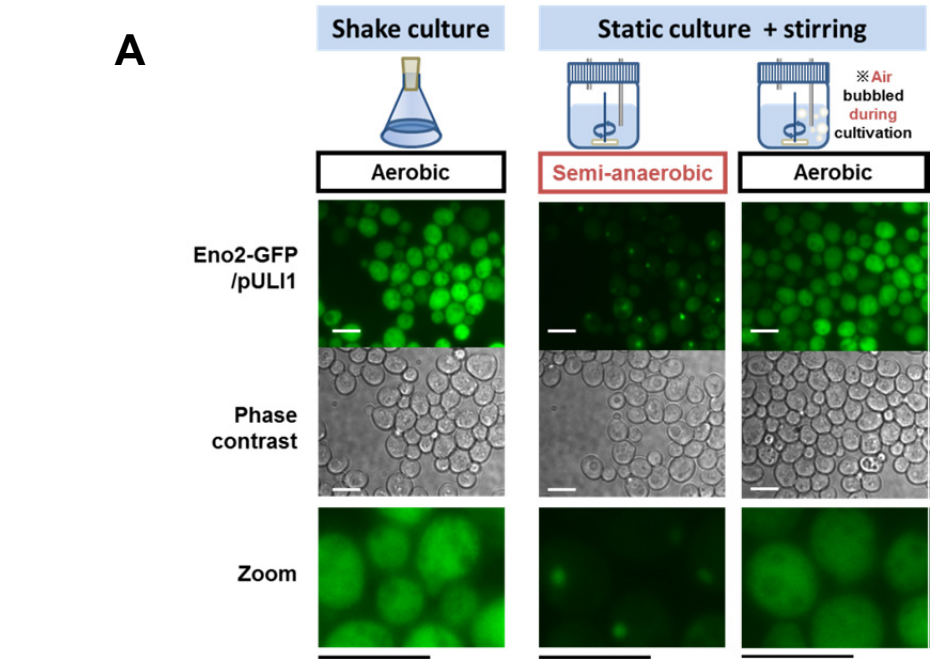
A
Shake culture
Static culture + stirring
※Air bubbled during cultivation
Aerobic
Semi-anaerobic
Aerobic
Eno2-GFP /pULI1
Phase contrast
Zoom

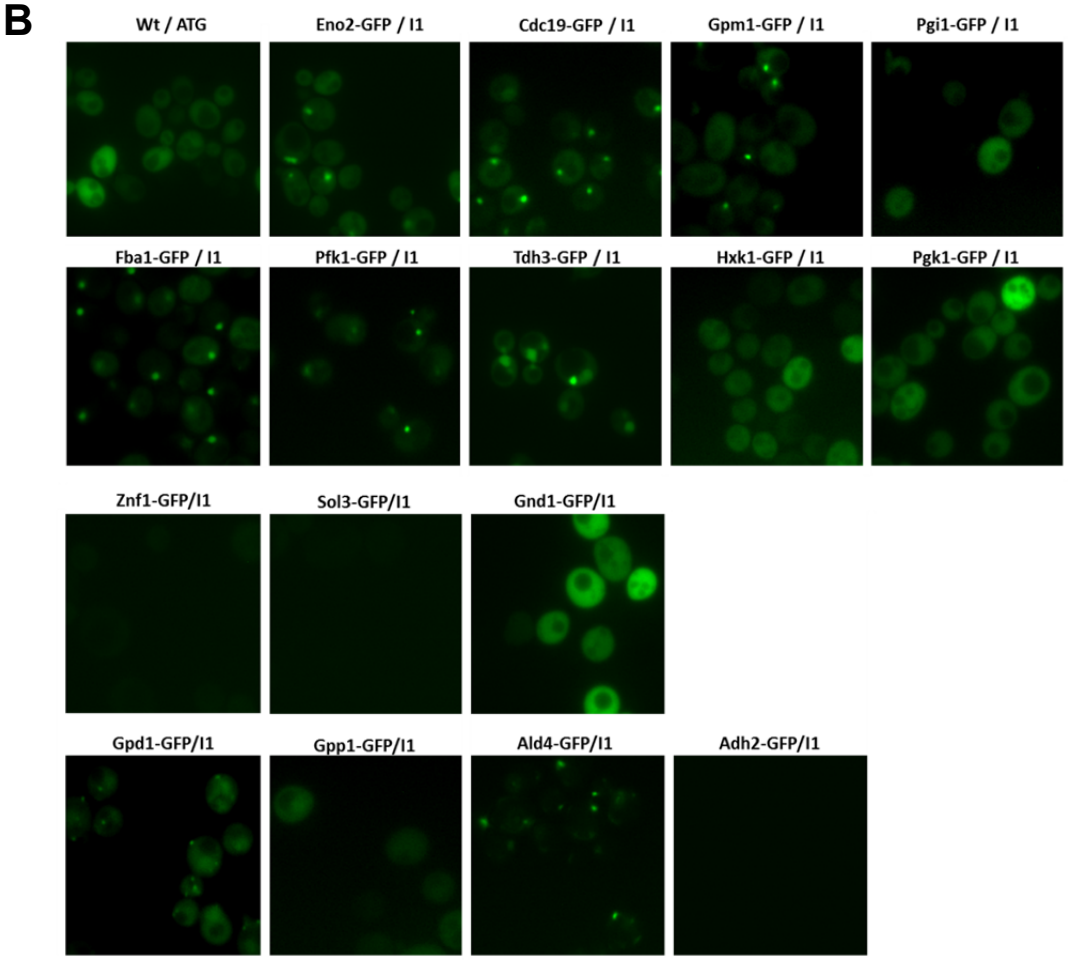
B
Wt / ATG
Eno2-GFP / I1
Cdc19-GFP / I1
Gpm1-GFP / I1
Pgi1-GFP / I1
Fba1-GFP / I1
Pfk1-GFP / I1
Tdh3-GFP / I1
Hxk1-GFP / I1
Pgk1-GFP / I1
Znf1-GFP/I1
Sol3-GFP/I1
Gnd1-GFP/I1
Gpd1-GFP/I1
Gpp1-GFP/I1
Ald4-GFP/I1
Adh2-GFP/I1

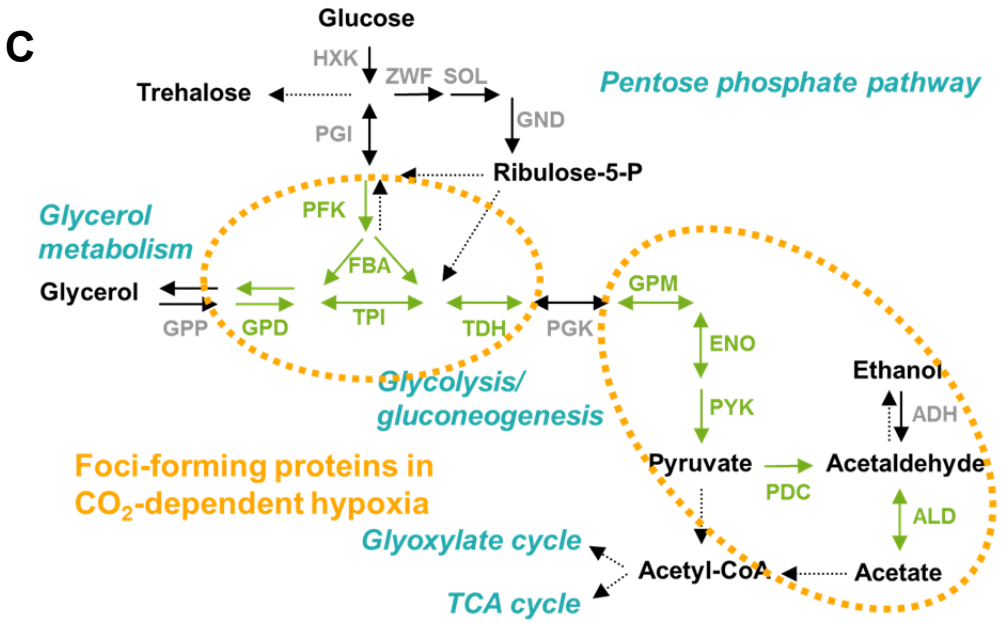

Fig. 11 Foci formation of glycolytic enzymes under hypoxia. A: Foci formation of ENO2-GFP strain under semi-anaerobic culture at 30°C. Bar = 10 μm. B: Foci formation of other metabolic enzymes. C: Summary of the foci-forming enzymes. Green letters indicate foci-formed proteins. Gray letters indicate investigated proteins that didn't form foci.

Time- and temperature-dependent foci formation of Eno2p-GFP

Foci formation of Eno2p was dependent on temperature and time. At 30°C, foci were formed after 6 h of semi-anaerobic cultivation, while in 37°C, foci were formed after 3 h of semi-anaerobic cultivation. At 25°C, interestingly, foci weren't formed after 12 h of semi-anaerobic culture (Fig. 12).

Measurements of pH and DO changes during the course of foci formation

During cultivation, pH did not fall below 5 in both CO_2-bubbled (Fig. 13A) and non-bubbled (Fig. 13B) vials. In CO_2-nonbubbled vials, DO decreased more rapidly at 37°C than at 30°C and 25°C, while in air-bubbled vials, DO remained at normoxic level after 8 h of cultivation (Fig. 13C). After 6 h of culture in vials at 30°C, the color of resazurin added to media was still pink, indicating there were some amount of oxygen in the vial (Fig. 13D).

Inhibition of foci formation by V22A substitution of Eno2p-GFP

After 12 h of culture in vials at 30°C, the V22A mutant of ENO2-GFP (ENO2V22A-GFP strain) did not form foci (Fig. 14).

Colocalization of foci of GFP clones with foci formed by N-terminal (1-28) region of Eno2p

Fluorescent foci formed by DsRED-conjugated N-terminal Eno2p were colocalized with foci of the ENO2-GFP strain at 30°C after 6 h of fermentative culture (Fig. 15).

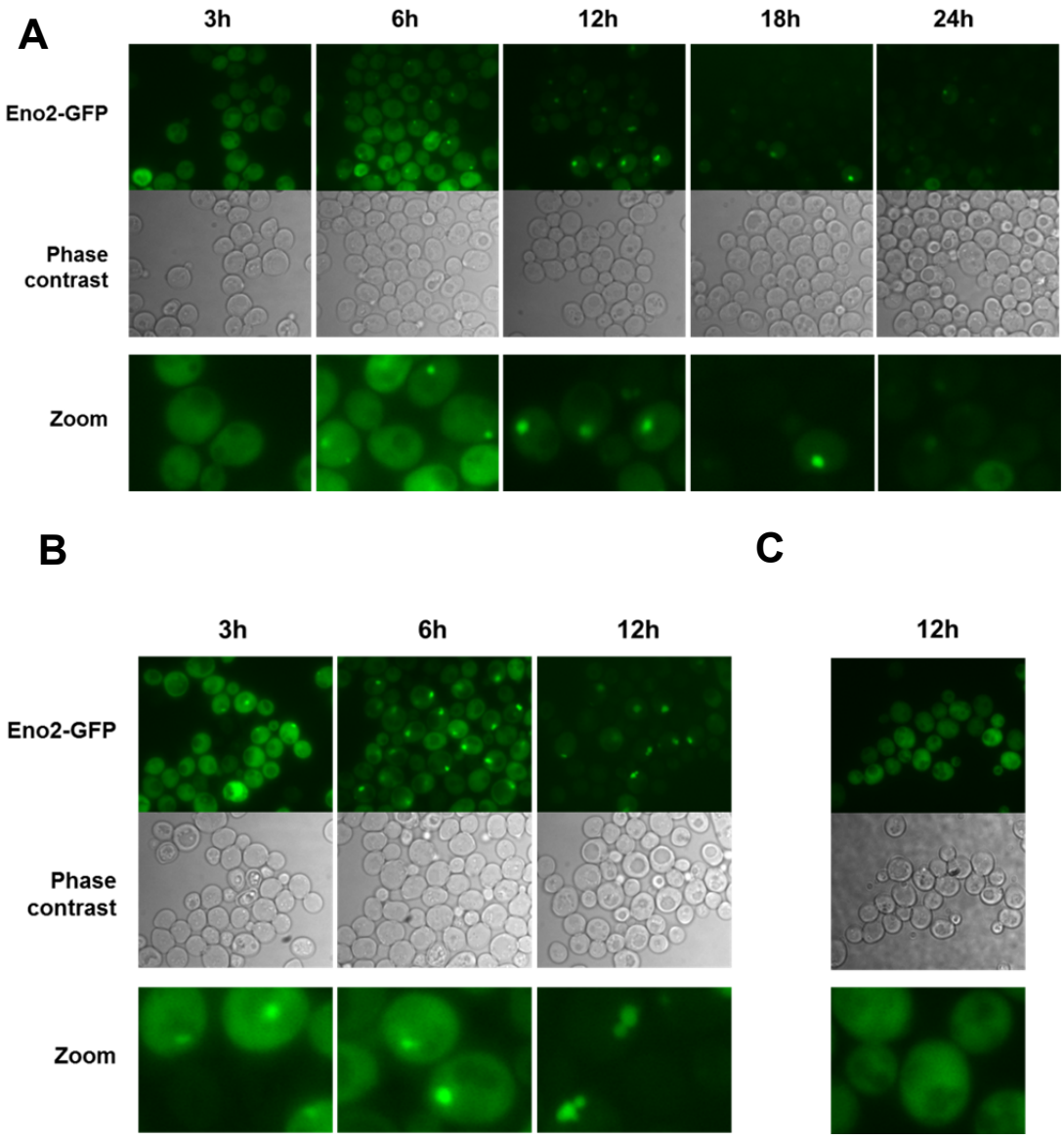

Fig. 12 Time-and temperature-dependent foci formation by Eno2p-GFP under hypoxia. Time-dependent foci formation of ENO2-GFP strain at indicated temperatures (A: 30°C, B: 37°C, and C: 25°C) are shown.

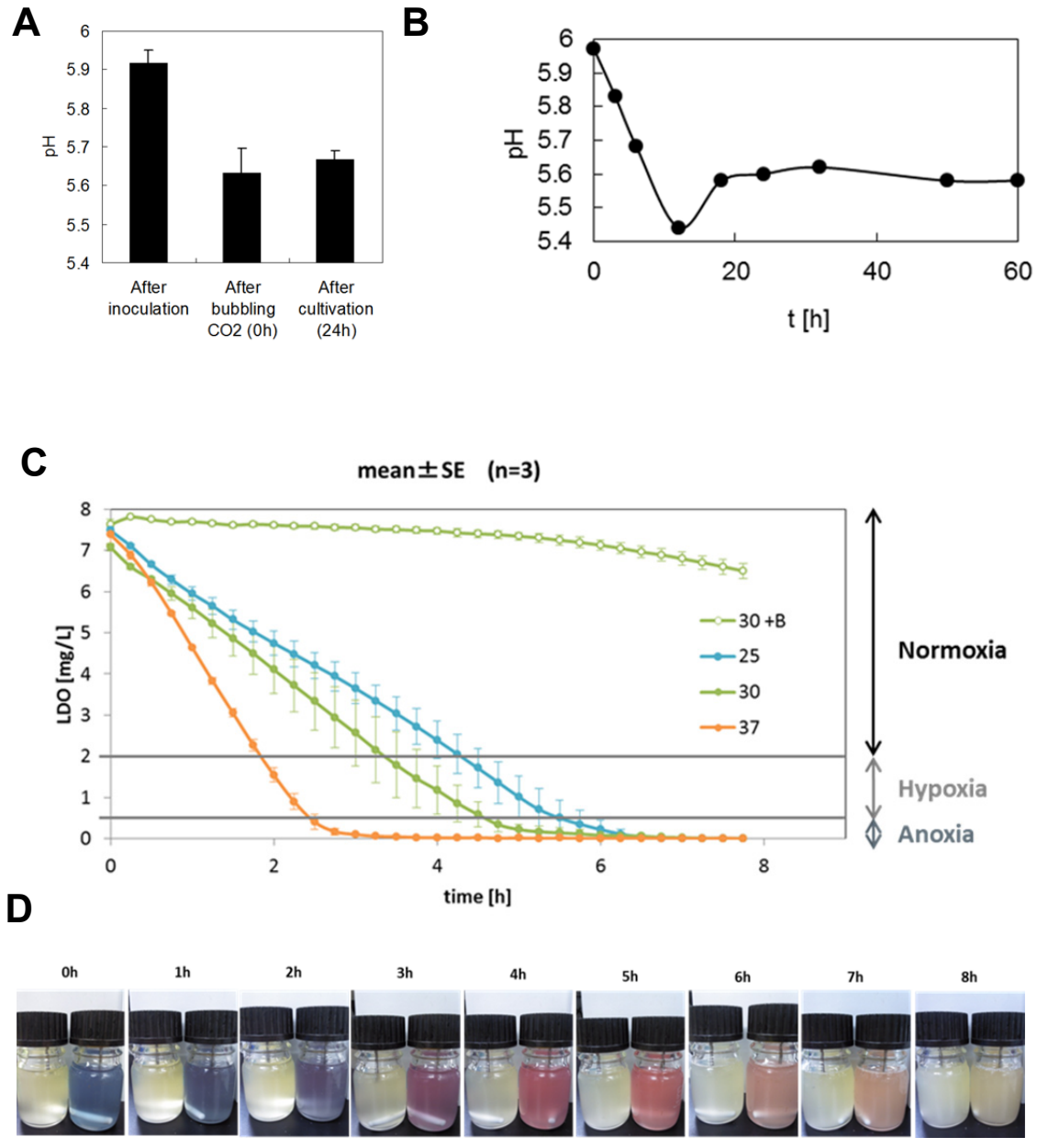

Fig. 13 pH and DO changes in the vials. A and B: changes in pH inside the culture vial with (A) or without (B) CO_2 bubbling before culture are shown. C: Time-and temperature-dependent DO changes without bubbling CO_2 before culture. D: DO changes represented by color changes of resazurin. Clear color shows anoxia.

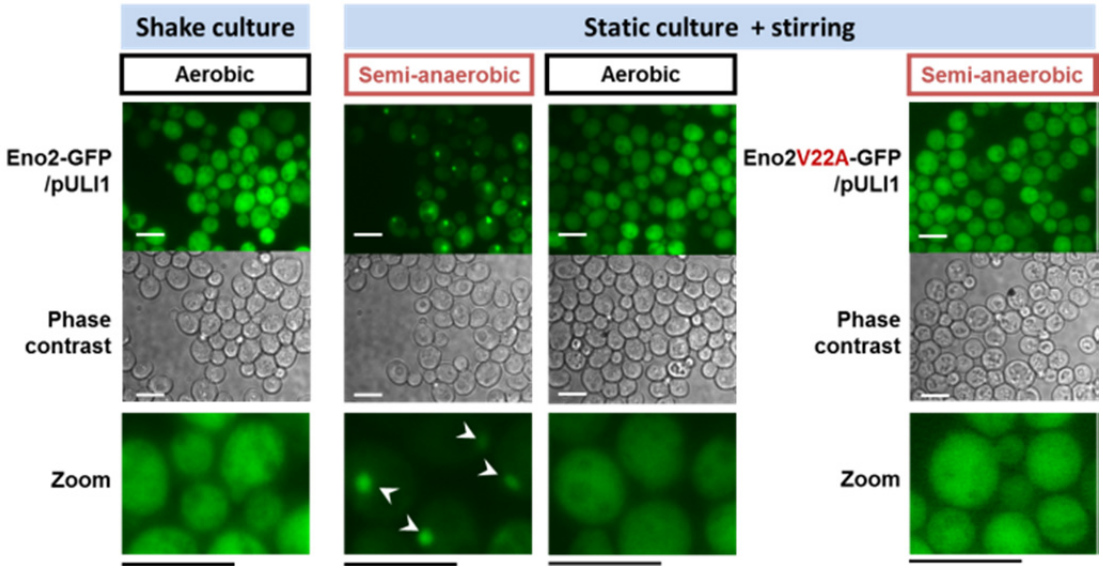

Fig. 14 Effects of substitution of Eno2p sequence on foci formation. Cells grown at 30°C in aerobic or anaerobic culture for 12 h. ENO2G: ENO2-GFP strain. eno2::ENO2V22A: V22A mutation introduced in *ENO2* sequence of ENO2-GFP strain. Bar = 10 μm.

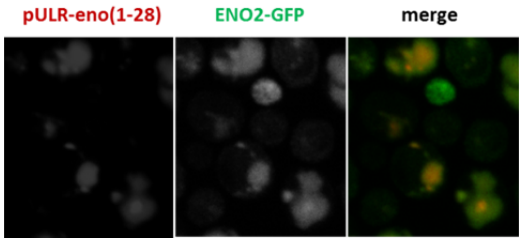

Fig. 15 Colocalization of the foci. N-terminal foci formation and (Red) and foci foemation of full length Eno2p (Green) are shown.

Discussion

Spatial rearrangement of glycolytic enzymes including Eno2p was detected for the first time in *S. cerevisiae* under hypoxic fermentation culture. The novel intercellular localization changes detected may enable glycolytic proteins to perform unknown moonlighting functions in response to specific environmental stimuli. Given that *S. cerevisiae* has many biological processes in common with other eukaryotic cells, these changes may be conserved over species. Regulation of several proteins participating sequentially in a metabolic pathway by spatial reorganization would be an important and effective method of regulating cellular processes. Colocalization of foci formed by full-length Eno2p-GFP and an N-terminal fragment fused with DsRED (Fig. 15) supported the speculation that

an N-terminal foci-forming region regulates spatial rearrangement of full-length Eno2p. I concluded that spatial rearrangement of the specific amino acid sequence of Eno2p promoted the spatial rearrangement of the whole protein. Screening peptide sequences would be a useful approach for discovering such amino acid sequences in other foci-forming proteins under hypoxia.

Section 3 Regulatory mechanisms of foci-formation of enolase

Results

Temperature-independent inhibition of foci formation by cycloheximide and rapamycin

Foci formation by Eno2p-GFP was inhibited by cycloheximide at 30°C and 37°C in semi-anaerobic culture (Fig. 16A). On application of a growth-inhibiting dose of farnesol, an inhibitor of the cAMP, PKA, and MAPK signaling pathways in *C. albicans* (Sato et al. 2004, Rhome et al. 2009, Cho et al. 2010, Deveau et al. 2010) and a mitochondrial ROS generator (Machida et al. 1998) and growth inhibitor (Machida et al. 1999) in *S. cerevisiae*, foci formation was conserved (Fig. 16B). In contrast, rapamycin at a growth-inhibiting dose inhibited foci formation at 37°C (Fig. 16B, C). These results suggest the DO-independent participation of both *de novo* protein synthesis and TORC1-dependent regulation at 37°C in foci formation.

Identification of *SNF1* as a regulator of foci formation at 30°C

To determine the signaling pathway regulating foci formation, knockout mutations of genes participating in signaling pathways, namely *HOG1* (MAPK pathway), *SCH9* (PI3K-AKT pathway), and *SNF1* (SNF1/AMPK pathway) were introduced into the ENO2-GFP strain. In semi-anaerobic culture, foci formation by the ENO2-GFP strain without *SNF1* (Δ*SNF1* ENO2-GFP strain) was inhibited at 30°C, while the other strains formed foci (Fig. 17A, B). To assess the involvement of Upc2p, which is a known regulator of hypoxia-responding transcription factor in yeast *C. albicans* (Synnott et al. 2010) and *S. cerevisiae* (Siso et al. 2012), a *UPC2* knockout mutation was introduced in the same manner. Foci formation was not inhibited, suggesting no involvement of Upc2p in foci formation under hypoxia (Fig. 17A). At 37°C in semi-anaerobic culture, the Δ*SNF1* ENO2-GFP strain formed foci (Fig. 17C). A strain with plasmid-reintegrated *SNF1* regained the foci-forming ability under semi-anaerobic culture at 30°C (Fig. 17D), showing the participation of *SNF1* in foci formation at 30°C. These results suggested that foci were formed at 30°C in response to hypoxia by participation of SNF1/AMPK. In general, the optimum temperature for cultivating the *S. cerevisiae* BY4741 strain is 30°C. We accordingly focused on foci formation induced at 30°C under hypoxia and by involvement of SNF1/AMPK.

Involvement of mitochondrial ROS production in foci formation

The involvement of mitochondrial ROS production, which is known to activate AMPK, was investigated using mitochondrial inhibitors and an antioxidant (Fig. 18A). The mitochondrial uncoupler carbonyl cyanide *m*-chlorophenylhydrazone (CCCP) inhibited foci formation, indicating mitochondrial involvement (Fig. 18B). Oligomycin A and antimycin A, inhibitors of mitochondrial ATPase and complex III, respectively, also inhibited foci formation. The antioxidant

N-acetyl-$_L$-cysteine (NAC) inhibited foci formation, indicating the involvement of mitochondrial ROS release to the cytoplasm under hypoxia (Fig.18C).

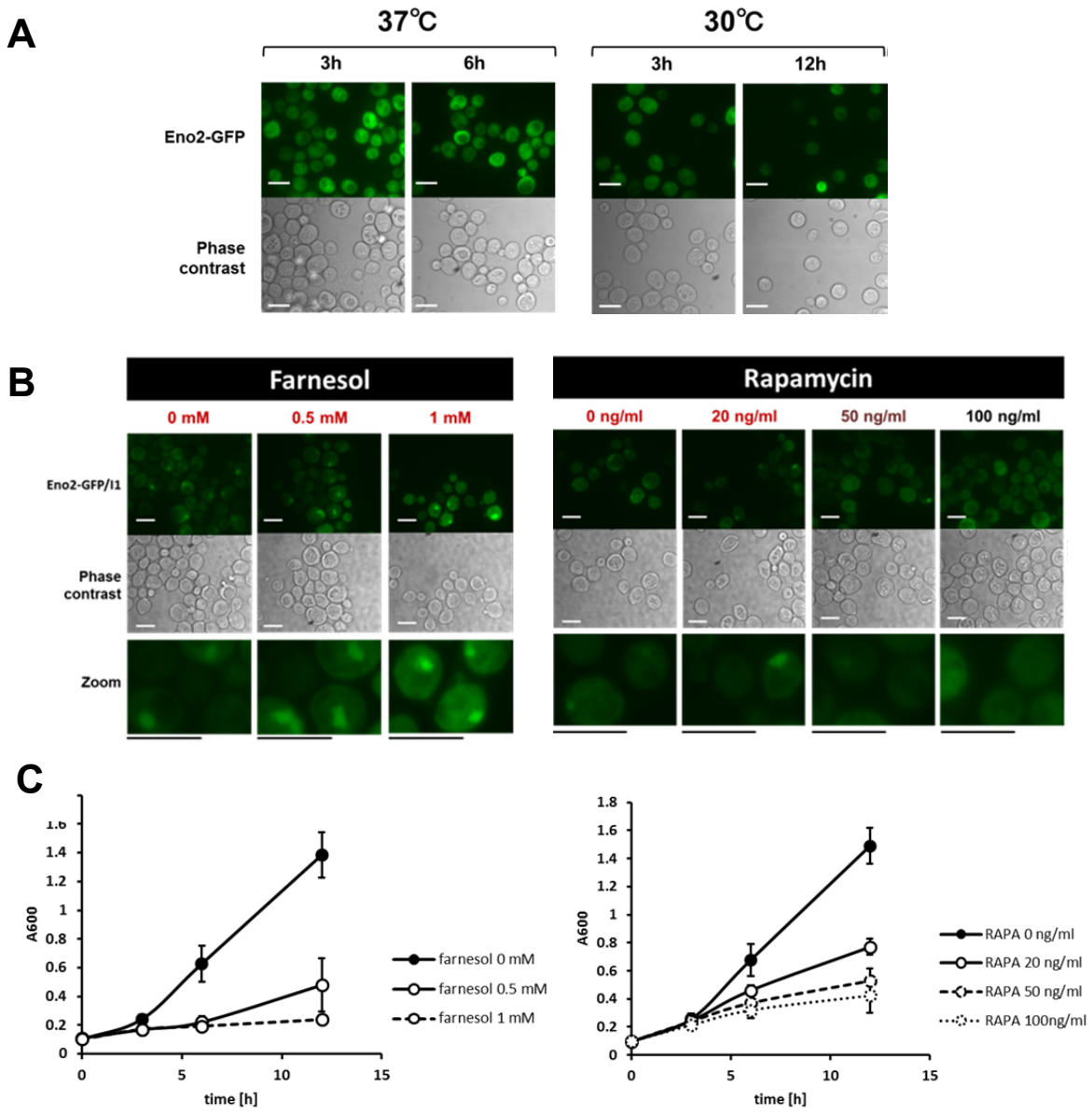

Fig. 16 Inhibition of foci formation by Eno2p with cycloheximide and rapamycin. A: Inhibition by the addition of cycloheximide and B: rapamycin. C: Growth inhibition by the addition of rapamycin and farnesol. For A, after 3 or 6 h of cultivation at indicated temperatures, ENO2-GFP cells transformed with PULI1 were observed. Each media contains cycloheximide. For B: After 12 h of semi-anaerobic culture at 37°C containing farnesol or rapamycin at indicated dose, cells were harvested and observed. Growth curves show A600 of media containing indicated doses of reagents. RAPA: rapamycin. Bar = 10 μm.

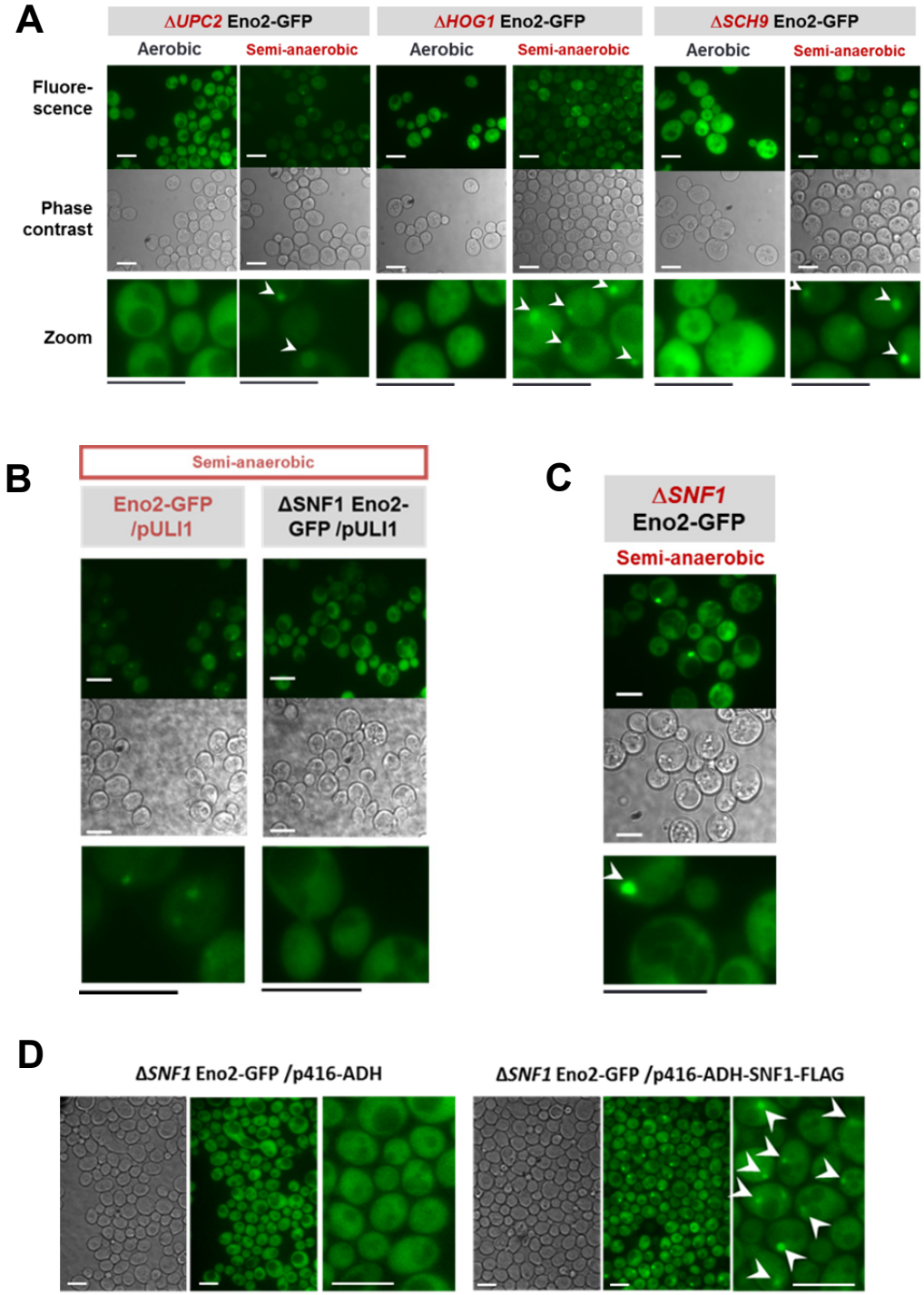

Fig. 17 Foci formation and its dependency on *SNF1*. A: ENO2-GFP strains with or without *HOG1* or *UPC2* knockout mutation. B: ENO2-GFP strains with or without *SNF1* knockout mutation. Each strain contains plasmid pULI1 or indicated plasmid. C:Foci formation by *SNF1* knockout mutant at 37°C. D: Plasmid reintegration of *SNF1*. Bar = 10 μm.

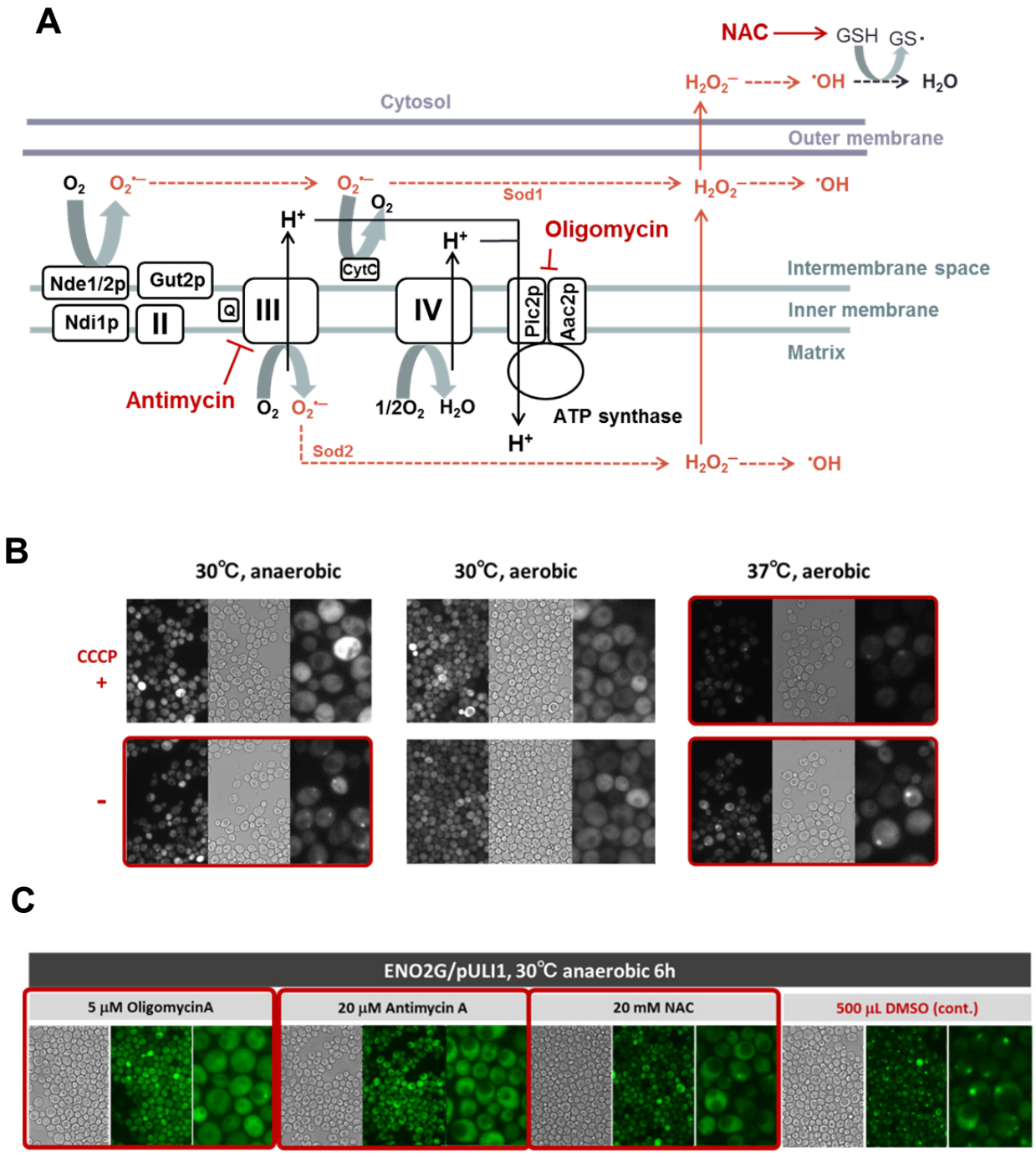

Fig. 18 Inhibition of foci formation by antioxidant and inhibitors for mitochondrial ROS production at 30°C A: Schematic illustration of inhibiting ROS produced by mitochondria (modified from Harrero et al. 2008 and Clémençon 2012). B: Inhibition by CCCP. C: Inhibition of foci formation by adding mitochondrial inhibitors and antioxidant.

Discussion

Temperature-independent inhibition of foci formation by cycloheximide suggested that *de novo* protein synthesis is an important factor, in addition to regulation by the signaling pathway. Although inhibition of foci formation by rapamycin was temperature independent, the doses of rapamycin added to cells that allowed inhibition of foci formation inhibited cell growth. This suggests that regulation by TORC1 occurs before *de novo* protein synthesis. However, TORC1 incorporation is important, given that foci formation was not inhibited when farnesol was added at a growth-inhibiting dose. The finding that *HOG1* and *SCH9* knockout failed to inhibit foci formation is reasonable, given that farnesol is reported to be an inhibitor of the MAPK and PKC/Akt pathways in the pathogenic fungus *C. albicans* (Synnott et al. 2010).

Inhibition of foci formation by *SNF1* knockout was unexpected, given that the SNF1/AMPK pathway is known to be activated by a glucose-limiting state in which glycolytic enzymes are downregulated. However, the inhibition of foci formation by mitochondria inhibitors and antioxidant supported SNF1/AMPK involvement in hypoxia-responsive foci formation. Foci formation was strongly dependent on heat and decreased DO in culture media. These results suggest that foci formation by Eno2p was dependent on more than one pathway. Although AMPK is known to inhibit the TOR pathway (Hardie 2011), there are some instances in which both the AMPK and TOR pathways regulate cell physiology (Hardie 2011). For example, in *S. cerevisiae*, both Snf1p and TORC1 have been suggested to have roles in regulation of fatty acids by unknown mechanisms (Zhang et al. 2011). The unknown regulatory mechanisms for these two pathways await discovery by future studies.

Section 4 The effects of foci on cellular carbon metabolism

Foci formation of plasmid-reintroduced Eno2p-EGFP-FLAG in BY4741Δ*ENO2* cells

To detect proteins involved in foci formation, an *ENO2* knockout (Δ*ENO2*) strain and plasmids for production of recombinant Eno2p-EGFP-FLAG protein or its V22A mutant (Eno2V22Ap-EGFP-FLAG) were prepared. The fluorescence intensities of Δ*ENO2* strains producing recombinant proteins were similar to those of the ENO2-GFP strain in aerobic culture (Fig. 19A). After 12 h of semi-anaerobic culture, the Eno2p-EGFP-FLAG protein formed foci (Fig. 19B).

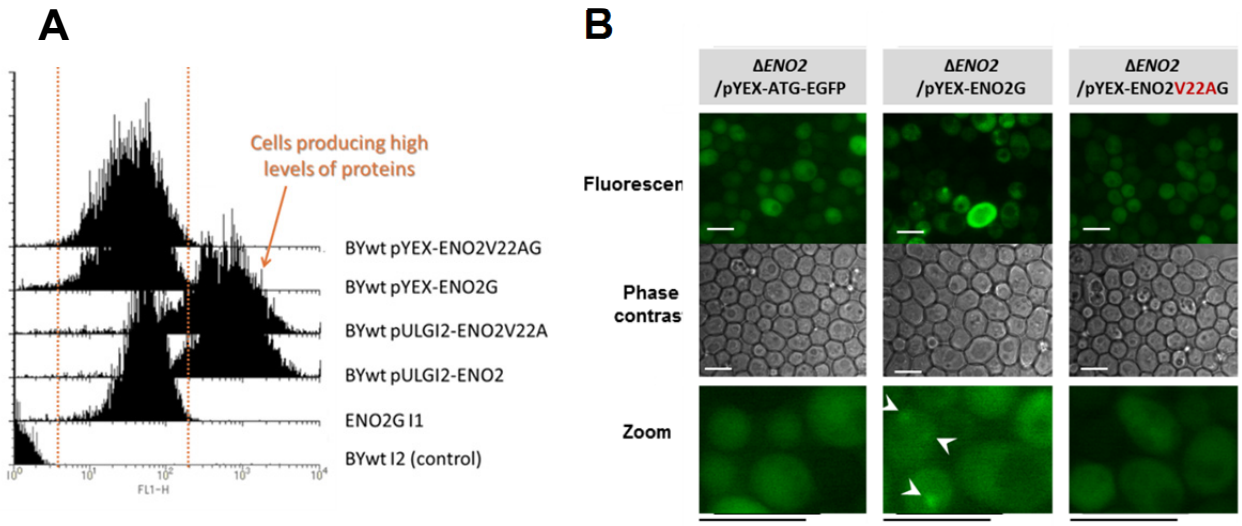

Fig. 19 foci formation of plasmid-reintroduced Eno2p-EGFP under hypoxia. A: Fluorescence intensities of each strain measured by FACS. B: Foci formation of plasmid-reintroduced Eno2p-EGFP in Δ*ENO2* strains. Bar = 10 μm.

Detection of coimmunoprecipitated proteins with foci-forming Eno2p

To investigate proteins associating with foci-forming Eno2p, Eno2p-EGFP-FLAG and Eno2V22Ap-EGFP-FLAG proteins were immunoprecipitated and identified by LC/MS/MS (Fig. 20A). As a result, 80 proteins including 43 metabolic proteins were detected in proteins coimmunoprecipitated with Eno2p-EGFP-FLAG (Fig. 20B). Of these, two proteins, Shm2p and Ade5,7p, were detected only in the proteins coimmunoprecipitated with Eno2p-EGFP-FLAG (Fig. 20C).

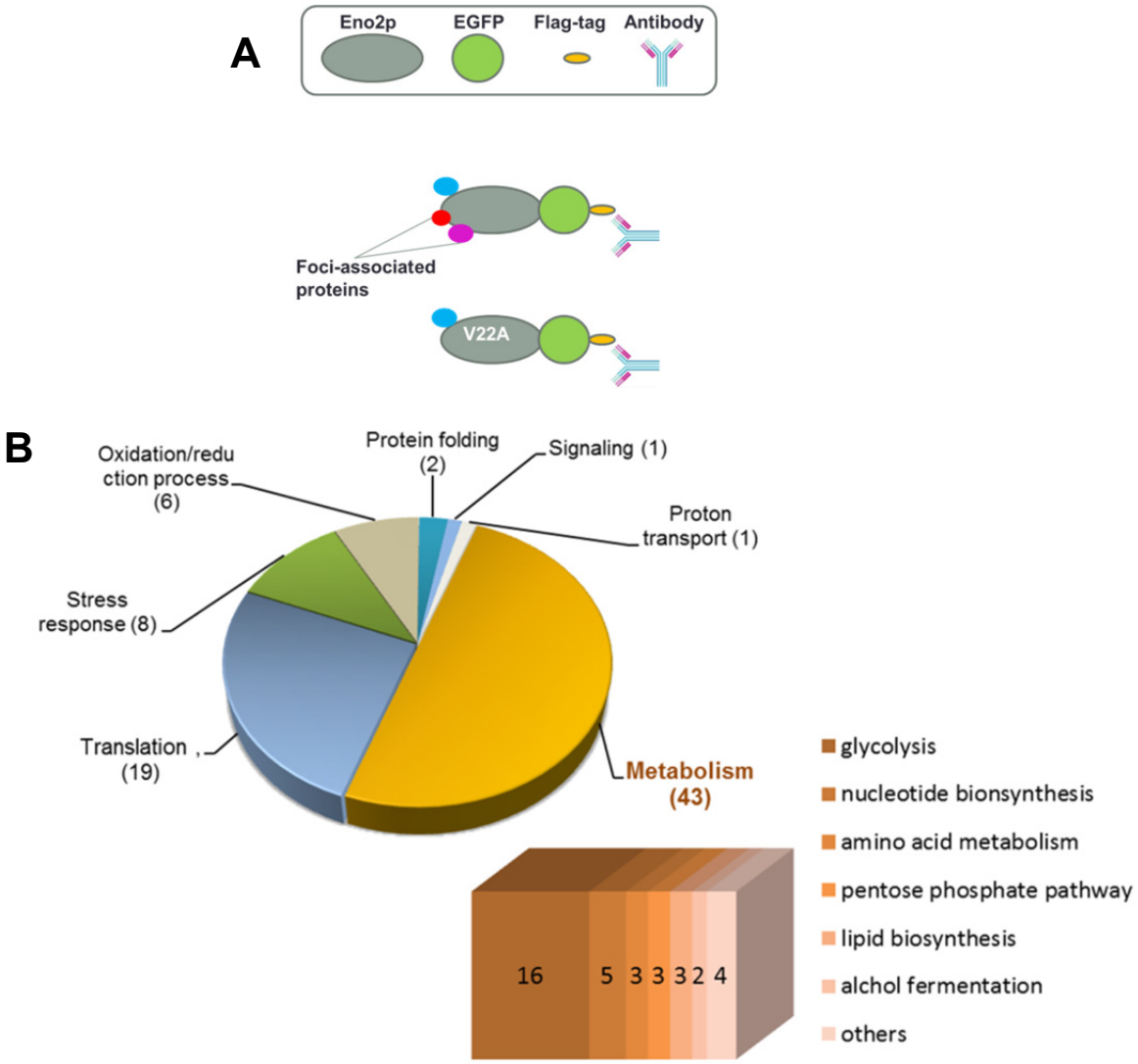

C

					Eno2p-EGFP-FLAG			Eno2V22AG-EGFP-FLAG		
Accession		# AAs	MW [kDa]	calc. pI	Coverage	# PSM	# Peptides	Coverage	# PSM	# Peptides
YLR058C	SHM2	469	52.2	7.43	9.17	7	3		N.D.	
YGL234W	ADE5,7	802	86.0	5.27	5.36	3	3		N.D.	

Fig. 20 Immunoprecipitation and identification of foci-associated proteins. A: Strategy for identifying foci-forming Eno2p-associated proteins. B: Overview of identified proteins (identified peptide number of ENO2-EGFP-FLAG-associated proteins ≥ 3). C: Examples of proteins detected by focused proteomic analysis. Eno2p-EGFP-FLAG: proteins detected by coimmunoprecipitation with Eno2p-EGFP-FLAG protein. Eno2V22Ap-EGFP-FLAG: proteins detected by coimmunoprecipitation with Eno2V22Ap-EGFP-FLAG protein. SHM2: *S. cerevisiae* gene encoding cytosolic serine hydroxymethyltransferase. ADE5,7: *S. cerevisiae* gene encoding bifunctional enzyme of the *de novo* purine nucleotide biosynthetic pathway, which contains aminoimidazole ribotide synthetase and glycinamide ribotide synthetase activities.

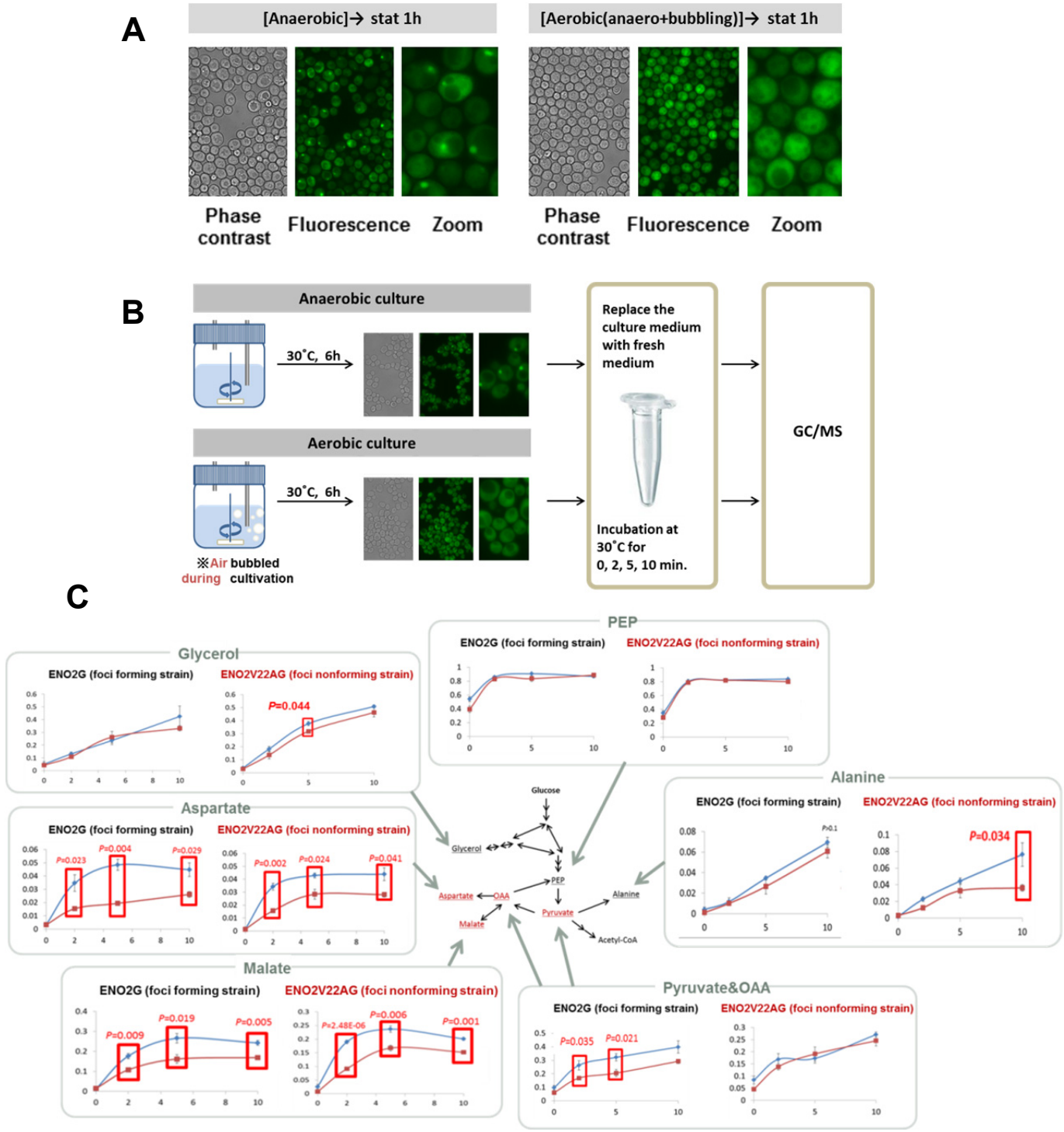

Fig. 21 Changes in carbon metabolic pathway of foci-carrying cells. A: Retention of the foci under aerobic culture. B: Scheme for measurement of incorporated ^{13}C in metabolites. C: Incorporation of ^{13}C derived from glucose into metabolites of foci forming and nonforming cells. Red line: metabolites extracted from cells after aerobic culture. Blue line: metabolites extracted from cells after anaerobic culture. Red line: metabolites extracted from cells after aerobic culture. Blue line: metabolites extracted from cells after anaerobic culture.

Investigation of the effects of foci-inhibiting mutations in hypoxia-treated cells on the carbon metabolic pathway by metabolic turnover analysis

In the ENO2-GFP strain, after semi-anaerobic culture for 6 h, foci were retained following 24 h of aerobic culture in fresh media (Fig. 21A). To investigate the effects of foci on cellular carbon metabolism, metabolic turnover analysis using [U-^{13}C]-glucose after semi-anaerobic (foci-forming condition) or aerobic (foci-non-forming condition) culture was measured using the ENO2-GFP and ENO2V22A-GFP strains (Fig. 21B). The ratio of ^{13}C-containing pyruvate and oxaloacetate were higher in foci-forming than in foci-non-forming cells after 2 and 5 min of intake (Fig. 21C). For glycerol and alanine, in the ENO2V22A-GFP strain, the ratios of 13C-containing metabolites were slightly higher in cells under anaerobic culture, whereas the ratio remained unchanged in the ENO2-GFP strain. These results suggested that cells carrying foci accelerated the incorporation of glucose-derived ^{13}C into pyruvate and oxaloacetate and preferentially produced aspartate and malate, rather than glycerol or alanine, from pyruvate.

Discussion

The organism's ability to switch the carbon metabolic pathway is considered important for controlling energy flow and synthesis of cellular components. Given that the glycolytic pathway has many branches connected to various metabolic pathways including nucleotide, amino acid, and lipid synthesis and energy production, effective use of carbon sources according to cellular needs in various situations is expected to be extremely important in the struggle for survival. Regulation of the carbon metabolic pathway has been reported to be accomplished by transcriptional regulation of various regulators (Daran-Lapujade et al. 2004). With respect to switching the carbon metabolic pathway in proliferating mammalian cells, p53 is known to target the TP53-induced glycolysis and apoptosis regulator and synthesis of cytochrome c oxidase, leading to glycolysis inhibition and a shift to oxidative phosphorylation (Bensaad et al. 2006, Matoba et al. 2006, Jones and Thompson 2009). It has not been reported that the central carbon metabolic pathway could be regulated by spatial reorganization or association of glycolytic enzymes.

Foci formation by Eno2p and other glycolytic enzymes conjugated with GFP under hypoxia (Fig. 5, S5) suggests the formation of a compartment of glycolytic enzymes in the cytosol. As predicted by a simulation study of glycolytic flux, under foci-forming conditions, incorporation of glucose-derived ^{13}C into pyruvate and oxaloacetate was accelerated. Inhibition of foci formation by introduction of the V22A mutation canceled out the effect, demonstrating the participation of foci formation by Eno2p in controlling carbon metabolism. Moreover, the increased ratio of ^{13}C-containing glycerol and alanine in foci-non-forming cells suggest that foci are needed to accelerate a specific branch of glycolysis. Thus, these results support a hypothesis that under

hypoxia, certain glycolytic enzymes are spatially reorganized to alter the carbon metabolic pathway. Fluxes and concentrations of metabolites in glycolysis are rapid and small, especially in reactions catalyzed by Eno2p, although Eno2p is one of the most abundant proteins in the cell. However, changing the amount of Eno2p seems to have no significant effect, as indicated by results in *E. coli* (Usui et al. 2012). Under hypoxia in *S. cerevisiae*, the amounts of Eno2p and other glycolytic enzymes reportedly increased significantly (de Groot et al. 2007). Controlling protein concentrations would be a reasonable and effective method to switch the carbon metabolic pathway.

In addition to the hypoxic state, higher temperatures of 37°C induced foci formation by Eno2p. The association of temperature and the hypoxic state in inducing foci formation remains unclear. The finding that foci formation at 37°C was inhibited by the addition of cycloheximide or rapamycin but not by *SNF1* knockout mutation suggests that there are two ways of regulation: by oxygen concentration and by temperature increase. Postmas et al recently reported that glycolytic flux increases in fermenting *S. cerevisiae* at 38°C (Postmus et al. 2012). They showed that increased activity of glycolytic enzymes did not correlate with protein abundance and suggested the contribution of post-translational regulation to enzyme activity. Foci formation by glycolytic enzymes is a seemingly efficient method of regulating glycolytic enzymes post-translationally.

The important amino acid residues or domains for foci formation by each enzyme could be determined in the manner we have demonstrated for Eno2p. Control of the carbon metabolic pathway in proliferating cells is an important issue. Eno2p and other glycolytic enzymes are overproduced in tumor cells in which the glycolysis rate is increased. If spatial reorganization of glycolytic enzymes occurs in mammalian cells, the results and methods demonstrated in this study could contribute to the control of carbon metabolism in proliferating cells including tumor cells.

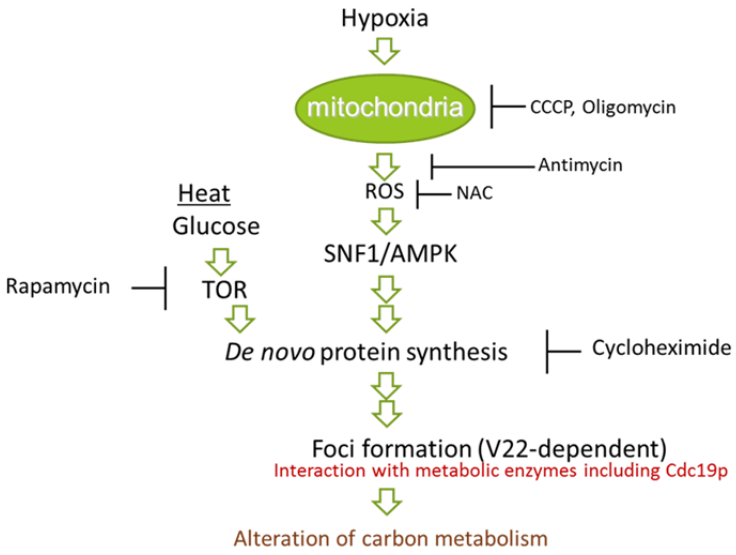

Fig. 22 Schematic illustration of the proposed regulation and the biological role of foci formation

Summary

Shifting metabolic pathways by forming protein complexes is an attractive strategy. In *Saccharomyces cerevisiae*, we found that glycolytic enzymes, including enolase (Eno2p), conjugated with GFP formed cellular foci under hypoxia. Foci formation by Eno2p was inhibited temperature independently by the addition of cycloheximide or rapamycin or by single alanine substitution of the Val22 residue. Using mitochondrial inhibitors and an antioxidant, mitochondrial ROS production was shown to participate in foci formation at 30°C. Foci formation was also inhibited at 30°C by an *SNF1* knockout mutation. Foci were observed in the cell after reoxygenation. Metabolic turnover analysis revealed that [U-^{13}C]-glucose was assimilated into pyruvate and oxaloacetate in shorter time in foci-forming than in -non-forming cells. These results suggest that under hypoxia, *S. cerevisiae* senses mitochondrial ROS by activating SNF1/AMPK and spatially reorganizes some metabolic enzymes in the cytosol via *de novo* protein synthesis, thereby contributing to an altered carbon metabolic pathway (Fig. 22).

References

1. Agbor TA, Cheong A, Comerford KM, Scholz CC, Bruning U, Clarke A, Cummins EP, Cagney G, Taylor CT (2011) Small ubiquitin-related modifier (SUMO)-1 promotes glycolysis in hypoxia. J. Biol. Chem. 286:4718-4726.
2. An S, Kumar R, Sheets ED, Benkovic SJ (2008) Reversible compartmentalization of de novo purine biosynthetic complexes in living cells. Science 320:103-106.
3. An S, Kyoung M, Allen JJ, Shokat KM, Benkovic SJ (2010) Dynamic regulation of a metabolic multi-enzyme complex by protein kinase CK2. J. Biol. Chem. 285:11093-11099.
4. Aoki W, Ueda T, Tatsukami Y, Kitahara N, Morisaka H, Kuroda K, Ueda M (2012) Time-course proteomic profile of Candida albicans during adaptation to a fetal serum. FEMS Immunol. Med. Microbiol. in press.
5. Bensaad K, Tsuruta A, Selak MA, Vidal MN, Nakano K, Bartrons R, Gottlieb E, Vousden KH (2006) TIGAR, a p53-inducible regulator of glycolysis and apoptosis. Cell 126:107-120.
6. Cho T, Nagao J, Imayoshi R, Kaminishi H, Aoyama T, Nakayama H (2010) Quorum sensing and morphological regulation in the pathogenetic fungus *Candida albicans*. J. Oral Biosci. 52:233-239.
7. Clémençon B (2012) Yeast Mitochondrial Interactosome Model: Metabolon Membrane Proteins Complex Involved in the Channeling of ADP/ATP. Int. J. Mol. Sci. 13:1858-1885.
8. Crighton D, Wilkinson S, O'Prey J, Syed N, Smith P, Harrison PR, Gasco M, Garrone O, Crook T, Ryan KM (2006) DRAM, a p53-induced modulator of autophagy, is critical for apoptosis. Cell 126:121-134.

9. Daran-Lapujade P, Jansen ML, Daran JM, van Gulik W, de Winde JH, Pronk JT (2004) Role of transcriptional regulation in controlling fluxes in central carbon metabolism of *Saccharomyces cerevisiae*. A chemostat culture study. J. Biol. Chem. 279:9125-9138.
10. de Groot MJ, Daran-Lapujade P, van Breukelen B, Knijnenburg TA, de Hulster EA, Reinders MJ, Pronk JT, Heck AJ, Slijper M (2007) Quantitative proteomics and transcriptomics of anaerobic and aerobic yeast cultures reveals post-transcriptional regulation of key cellular processes. Microbiol. 153:3864-3878.
11. Deveau A, Piispanen AE, Jackson AA, Hogan DA (2010) Farnesol induces hydrogen peroxide resistance in *Candida albicans* yeast by inhibiting the Ras-cyclic AMP signaling pathway. Eukaryot. Cell 9:569-577.
12. Feala JD, Coquin L, Zhou D, Haddad GG, Paternostro G, McCulloch AD (2009) Metabolism as means for hypoxia adaptation: metabolic profiling and flux balance analysis. BMC Syst. Biol. 3:91.
13. Frezza C, Zheng L, Tennant DA, Papkovsky DB, Hedley BA, Kalna G, Watson DG, Gottlieb E (2011) Metabolic profiling of hypoxic cells revealed a catabolic signature required for cell survival. PLoS One 6:e24411.
14. Green DR, Chipuk JE (2006) p53 and metabolism: Inside the TIGAR. Cell 126:30-32
15. Hardie DG (2011) AMP-activated protein kinase: an energy sensor that regulates all aspects of cell function. Genes Dev. 25:1895-1908.
16. Herrero E, Ros J, Bellí G, Cabiscol E (2008) Redox control and oxidative stress in yeast cells. Biochim. Biophys. Acta. 1780:1217-1235.
17. Huh WK, Falvo JV, Gerke LC, Carroll AS, Howson RW, Weissman JS, O'Shea EK (2003) Global analysis of protein localization in budding yeast. Nature 425:686-691.
18. Ingerson-Mahar M, Briegel A, Werner JN, Jensen GJ, Gitai Z (2010) The metabolic enzyme CTP synthase forms cytoskeletal filaments. Nat. Cell. Biol. 12:739-746.
19. Jeffery CJ (1999) Moonlighting proteins. Trends Biochem. Sci. 24:8-11.
20. Jones RG, Thompson CB (2009) Tumor suppressors and cell metabolism: a recipe for cancer growth. Genes Dev. 23:537-548.
21. Katahira S, Mizuike A, Fukuda H, Kondo A (2006) Ethanol fermentation from lignocellulosic hydrolysate by a recombinant xylose- and cellooligosaccharide-assimilating yeast strain. Appl. Microbiol. Biotechnol. 72:1136-1143.
22. Kizaka-Kondoh S, Inoue M, Harada H, Hiraoka M (2003) Tumor hypoxia: a target for selective cancer therapy. Cancer Sci. 94:1021-1028.
23. Machida K, Tanaka T, Fujita K, Taniguchi M (1998) Farnesol-induced generation of reactive oxygen species via indirect inhibition of the mitochondrial electron transport chain in the yeast *Saccharomyces cerevisiae*. J. Bacteriol. 180:4460-4465.

24. Machida K, Tanaka T, Yano Y, Otani S, Taniguchi M (1999) Farnesol-induced growth inhibition in *Saccharomyces cerevisiae* by a cell cycle mechanism. Microbiology 145 (Pt 2):293-299.
25. Margittai M, Langen R (2006) Side chain-dependent stacking modulates tau filament structure. J. Biol. Chem. 281:37820-37827.
26. Mashego MR, van Gulik WM, Vinke JL, Heijnen JJ (2003) Critical evaluation of sampling techniques for residual glucose determination in carbon-limited chemostat culture of *Saccharomyces cerevisiae*. Biotechnol. Bioeng. 83:395-399.
27. Margittai M, Langen R (2006) Side chain-dependent stacking modulates tau filament structure. J. Biol. Chem. 281:37820-37827.
28. Matsui K, Kuroda K, Ueda M (2009) Creation of a novel peptide endowing yeasts with acid tolerance using yeast cell-surface engineering. Appl. Microbiol. Biotechnol. 82:105-113.
29. Nanchen A, Fuhrer T, Sauer U (2007) Determination of metabolic flux ratios from 13C-experiments and gas chromatography-mass spectrometry data: protocol and principles. Methods Mol. Biol. 358:177-197.
30. Noree C, Sato BK, Broyer RM, Wilhelm JE (2010) Identification of novel filament-forming proteins in Saccharomyces cerevisiae and Drosophila melanogaster. J. Cell Biol. 190:541-551.
31. Postmus J, Aardema R, de Koning LJ, de Koster CG, Brul S, Smits GJ (2012) Isoenzyme expression changes in response to high temperature determine the metabolic regulation of increased glycolytic flux in yeast. FEMS Yeast Res. 12:571-581.
32. Rhome R, Del Poeta M (2009) Lipid signaling in pathogenic fungi. Annu. Rev. Microbiol. 63:119-131.
33. Sato T, Watanabe T, Mikami T, Matsumoto T (2004) Farnesol, a morphogenetic autoregulatory substance in the dimorphic fungus *Candida albicans*, inhibits hyphae growth through suppression of a mitogen-activated protein kinase cascade. Biol. Pharm. Bull. 27:751-752.
34. Semenza GL (2004) Intratumoral hypoxia, radiation resistance, and HIF-1. Cancer Cell 5:405-406.
35. Siso MI, Becerra M, Maceiras ML, Vazquez AV, Cerdan ME (2012) The yeast hypoxic responses, resources for new biotechnological opportunities. Biotechnol. Lett. 34:2161-2173.
36. Synnott JM, Guida A, Mulhern-Haughey S, Higgins DG, Butler G (2010) Regulation of the hypoxic response in *Candida albicans*. Eukaryot. Cell 9:1734-1746.
37. Tsugawa H, Bamba T, Shinohara M, Nishiumi S, Yoshida M, Fukusaki E (2011) Practical non-targeted gas chromatography/mass spectrometry-based metabolomics platform for metabolic phenotype analysis. J. Biosci. Bioeng. 112:292-298.
38. Usui Y, Hirasawa T, Furusawa C, Shirai T, Yamamoto N, Mori H, Shimizu H (2012) Investigating the effects of perturbations to pgi and eno gene expression on central carbon metabolism in Escherichia coli using (13)C metabolic flux analysis. Microbial Cell Fact. 11:87.

39. Zhang J, Vaga S, Chumnanpuen P, Kumar R, Vemuri GN, Aebersold R, Nielsen J (2011) Mapping the interaction of Snf1 with TORC1 in *Saccharomyces cerevisiae*. Mol. Syst. Biol. 7:545.

CHAPTER III

Development of a novel method and an instrument to validate intracellular roles of extracellular moonlighting proteins

Introduction

Secretion and surface localization of enolase have been found (see Chapter I). Yet, the roles and the mechanisms of function of secreted or surface-localized enolase in *S. cerevisiae* are not known. To uncover these, the system for experimental re-construction and investigation of cell-cell interaction by designed proteins should be developed. Here, the concept of a novel co-cultivation based method that is to observe changes of cells when co-cultivated with genetically-modified (GM) cells to produce effector proteins arose. While enolase is known to localize cellular surface of many organisms, the mechanisms of surface localization is not known. Therefore, well-known proteins that bind cellular surface should be selected to construct the model system.

Previously, Bosma et al. (2006) developed a method to display recombinant proteins on the non-GM gram-positive bacterial cell surface. They used the bacterial LysM domain (Pfam accession number PF01476) as a microbial-surfacebinding domain and non-GM gram-positive bacterial cells named gram-positive enhancer matrix particles as scaffolds to generate a non-GM vaccine (Bosma et al. 2006; van Roosmalen et al. 2006). However, the method includes chemical pretreatment of non-GM cells. The treatment kills bacteria, and it was impossible to investigate living bacterial functions such as multiple metabolic pathways and mobility. To use various native functions of bacteria, there is a need to develop a non-GM display system of living cells without chemical pretreatment. On the other hand, our system is different from previously reported system in the following points: this is a non-GM display system for living microorganisms without chemical pretreatment, and we used the lectin module, which is present in a broad range of species, as a binding module.

The C-type lectin-like domain (CTLD, InterPro entry accession number IPR16186) and LysM domain are cell wall-recognition domains, but their three-dimensional structures and determined binding substrates are different. The LysM domain has a distinctive αββα fold and has no similarity to other carbohydrate-binding modules (Bateman and Bycroft 2000). The fold includes a shallow groove formed by two helixes and two loops (Ohnuma et al. 2008). The groove has a cluster of hydrophobic residues, and by the participation of the groove, the LysM domain binds β-1,4-linked N-acetylglucosamine (chitin) oligosaccharides ((GlcNAc)n) (Ohnuma et al. 2008). LysM can recognize fungal cell wall (Wan et al. 2008) and bacterial cell wall peptidoglycans and the Nod receptor to initiate nodulation in the case of Rhizobium (Radutoiu et al. 2007). CTLD has a double-loop structure on both sides of antiparallel β-sheet (Zelensky and Gready 2005) to form a carbohydrate-binding site called the SPD (surfactant protein D) cleft (Hallman and Haataja 2006).

The cleft involves hydrophobic residues and has a Ca^{2+}-binding site. At this site, CTLD binds to various mono- and oligosaccharides or carbohydrate chains in a Ca^{2+}-dependent manner. In this study, we constructed a non-GM display system using one of the microbial-surface-binding domains, CTLD from human surfactant protein D (SP-D, Protein Data Bank accession number 1PWB), without chemical treatment.

Figure 1 shows a model of a newly constructed system to investigate intercellular roles of moonlighting proteins. In this model system termed the "molecular sniping and shooting method (MSSM)," target proteins fused with the yeast-cell-surface-binding motif are produced in GM yeast and secreted. The mechanism for the protein-targeting system to bind proteins to the co-cultivated non-GM yeast surface is based on the property of the binding motif and cell-surface carbohydrates. GM and non-GM yeasts were co-cultivated using a filter-membrane-separated reactor for rapid detection of the "sniping and shooting" effect. Secreted fusion proteins are diffused in the culture medium, through the filter membrane, and bind to target cellular surfaces. In this system, GM cells were named as sniper cells, and non-GM cells as target cells.

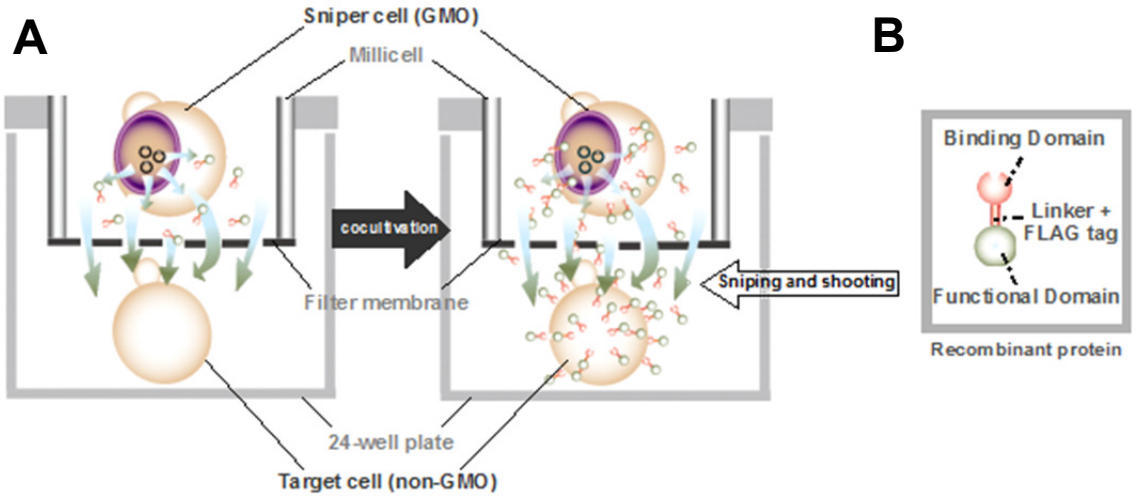

Fig. 1 Scheme of molecular sniping and shooting method (MSSM) A: Surface modified non-GMOs are constructed as follows: non-GMOs were cocultivated with GM yeasts, which produce recombinant proteins with the "binding domain" and "functional domain", the "sniping and shooting" domain on the surface of non-GMOs. B: The interactions between recombinant proteins and the surface of non-GMOs are based on the molecular recognition activity of lectins. In spite of cocultivation of non-GMOs and GM yeasts, there are no contaminations, because, in the cultivation chamber (Millicell), they are separated by the special membrane filter. The pore size of the membrane is 0.4 μm and it allows recombinant proteins to pass through, but not large cells like yeasts. Sniper cell: GM sniper cells which secrete recombinant proteins. Target cell: non-GM target cells which receive recombinant proteins.

Materials and methods

Strains and media

Escherichia coli DH5α [F^-, *endA1*, *hsdR17* (r_{K-} ; m_{K+}), *supE44*, *thi-1*, λ^-, *rec A1*, *gyrA96*, Δ*lacU169* (*φ80lacZΔM15*)] was used both as a host for recombinant DNA manipulation and as a target cell. *Saccharomyces cerevisiae* strain MT8-1 [*MATa*, *ade*, *his3*, *leu2*, *trp1*, *ura3*] (Tajima et al. 1985) was used to produce recombinant proteins. *S. cerevisiae* strain BY4741 [*MATa*, *his3-1*, *leu2*, *met15*, *ura3*], BY4741ΔCYC8 [*MATa*, *his3-1*, *leu2*, *met15*, *ura3*, Δ*CYC8*] (Conlan et al. 1999), and *Candida albicans* NBRC1594 were used as target cells for targeting recombinant proteins. *S. cerevisiae* BY4741 and BY4741Δ*CYC8* were obtained from Euroscarf. *E. coli* was grown in Luria–Bertani medium (1% (*w/v*) tryptone, 0.5% (*w/v*) yeast extract, 0.5% (*w/v*) sodium chloride, and 0.1% (*w/v*) ampicillin). Yeast was grown either in yeast peptone dextrose (YPD) medium (1% (*w/v*) yeast extract, 2% (*w/v*) polypeptone, and 2% (*w/v*) glucose) or SD-W (synthetic dextrose−tryptophan) medium (0.67% (*w/v*) yeast nitrogen base without amino acids, 2% (*w/v*) glucose, 0.002% adenine sulfate, 0.002% $_L$-histidine-HCl, 0.003% $_L$-leucine, and 0.002% uracil).

Plasmid construction and yeast transformation

Two expression vectors, pSDLn4 and pSDLc4, were designed for the N-terminal-free type and C-terminal-free type of enhanced green fluorescent protein (EGFP) for display, respectively. In short, human-placenta-cDNAderived CTLD and glucoamylase secretion signal-EGFPFLAG domains were inserted to the multicloning site of pWGP3 (Takahashi et al. 2001).

All polymerase chain reaction (PCR) amplifications were carried out using KOD-Plus-DNA polymerase (Toyobo, Osaka, Japan). Table 1 shows the used primers. EGFP sequence was amplified from pEGFP (Takara Bio, Otsu, Japan) using primers (see in Table 1) EGYL-F(*Bgl* II) and EGY-R(*Sal* I). Amplified EGFP sequence was ligated into the plasmid pMWFD (Kuroda and Ueda 2005) using the *Bgl* II and *Sal* I sites. The resulting plasmid was named pKGD1C. EGFP-FLAG-α-agglutinin sequence was amplified from pKGD1C using primers EGFP-F(*Xho* I) and *Kpn*I-R(AG). Amplified EGFP-FLAG-α-agglutinin sequence was ligated into the plasmid pCAS1 (Shibasaki et al. 2001) using the *Xho* I and *Kpn* I sites. The resulting plasmid was named pKGD2. Glucoamylase secretion signal, EGFP, and FLAG sequences were amplified from pKGD2 using primers (see in Table 1) EGFPF1 and EGFPR1-1 (for pSDLn4) or EGFPF1 and EGFPR1-2 (for pSDLc4). The CTLD sequence was amplified from human placenta cDNA (BioChain Institute, CA, USA) by PCR using the primer pairs SP-DF2-1 and SPD2RXKEX2Bgl20712 (for pSDLn4), and SP-DF2-2 and SP-DtaaRXKEX2 (for pSDLc4). To construct pSDLn4 and pSDLc4, amplified EGFP fragments were ligated into the multicopy expression plasmid pWGP3 using the *Kpn* I and *BamH* I sites. The resulting plasmid was cleaved with *Mlu* I and *BamH* I (for pSDLn4) or *Bgl* II and *Xho* I (for pSDLc4) and ligated with the CTLD fragment using the restriction sites *Mlu* I and *BamH* I,

or *Bgl* II and *Xho* I, respectively. All amplification products were purified, and their sequences were confirmed by DNA sequencing. The resulting plasmids pSDLn4, pSDLc4, and pWGP3 (control) were introduced into *S. cerevisiae* by the lithium acetate method (Ito et al. 1983). Transformed cells were inoculated on the SD-W plates for 2 days at 30°C.

Table 1 Primers used in Chapter III

Plasmid	Name of primer	Sequence
pKGD1C	EGYL-F(*Bgl* II)	5'-GATCCCAGATCTGGTGGATCTGGTGGCGTGAGCAAGGGCGAGGAGCTGTTCAC-3'
	EGY-R(*Sal*I)	5'-GCGGCCGTCGACCTTGTACAGCTCGTCCATGCCGAGAGTGATC-3'
pKGD2	EGFP-F(*Xho*I)	5'-TCGACCTCGAGGTGGATCTGGTGGCGTGAGCAAG-3'
	*Kpn*I-R(AG)	5'-AAAAAGGTACCTTTGATTATGTTCTTTCTATTTGAATGAGATATGAG-3'
pSDLn4	SP-DF2-1	5'-CGACGCGTGTGGGGGAGAAGATTTTCAA-3'
	SPD2RXKEX2Bgl20712	5'-CCGCTCGAGAGAACTCGCAGACCACAAGACTCTTTTCTCCACAAGCCCTGTCATTC CACTTGCCATTGGTGAATATCTCCACAC-3'
	EGFPF1	5'- CGGGGTACCATGCAACTGTTCAATTTGCC-3'
	EGFPR1-1	5'-CGCGGATCCACCAGCGGCCGCACCACGCGTCGAACCTCCAGCCTTGTCATCGTCA TCCTTGTAATCAGATCCACCCTTGTACAGCTCGTCCAT-3'
pSDLc4	SP-DF2-2	5'-GGAAGATCTCTGTGGGGGAGAAGATTTTCAA-3'
	SP-DtaaRXKEX2	5'-CGCGGATCCTTAGAACTCGCAGACCACAAGACTCTTTTCTCCAC-3'
	EGFPF1	5'- CGGGGTACCATGCAACTGTTCAATTTGCC-3'
	EGFPR1-2	5'-CGCGGATCCACCAGCGGCCGCATTAATTTAACGCGTCCATGGCGAACCTCCAGCC TTGTCATCGTCATCCTTGTAATCAGATCCACCCTTGTACAGCTC-3'

Fluorescence-activated cell sorting analysis

Because cocultivation was performed in small scale (using 24-well plate and cell culture insert, total volume was 1 ml), we used cell sorter to quantify EGFP transfer from GM cells to non-GM cells. The transformants were grown in 10 ml of preculture medium (SD-W containing 0.5% (*w/v*) casamino acids (SDC-W)) for 28 h at 30°C with shaking. Cell cultures were then inoculated into 100 ml of the main culture medium (SDC-W) at A600 of 0.01 and incubated at 30°C with shaking. After 24, 48, and 96 h, cells were collected and centrifuged in 1.5 ml tubes at 10,000×*g* for 1 min. Cell pellets were collected and washed with 500 µl of phosphate-buffered saline (PBS; 137 mM NaCl, 8.1 mM Na_2PO_4, 2.68 mM KCl, 1.47 mM KH_2PO_4, pH 7.4, Nippon Gene, Tokyo, Japan) and centrifuged in the same conditions. Obtained cell pellets were suspended in PBS and measured immediately with a cell sorter (JSAN, Bay Bioscience, Kobe, Japan) using the detection channel FLT1 (535DF45). In each case, the fluorescence of 40,000 cells was acquired.

For quantification of target cells prepared by MSSM, 10 µl samples of each co-cultivation medium were collected into 5 ml polystyrene tubes (Becton, Dickinson and Company, NJ, USA) and stored on ice. PBS (1 ml) was added to each sample. After 5 min of sonication using an ultrasonic washing machine (VS-25, VELVO-CLEAR, Osaka, Japan) at 40 kHz and room temperature, 10,000 cells were immediately analyzed using a cell sorter. The percentage of cells with high fluorescence intensity was calculated with respect to the total number of cells. Sonication was carried out to

separate aggregated cells (Kon et al. 2005), which facilitates cell sorting.

For re-cultivation of cells, 20 μl samples of each co-cultivation medium were collected into 5 ml polystyrene tubes, and 1 ml of PBS was added to each sample. After 5 min of sonication (40 kHz at room temperature), 10,000 cells were immediately analyzed using a cell sorter and 1,000 cells with a high fluorescence intensity were sorted and spread onto agar medium as described below. Cell viability was calculated by counting colonies formed on the plate. Colonies were also used for colony PCR as described below.

Cocultivation of GM and non-GM cells using membrane filter

To transfer fluorescence from GM cells to non-GM cells as they grow in the medium in which these cells are separated by a filter membrane, GM and non-GM cells were co-cultivated as follows. Non-GM cells (cells with the receptor as target cells) were inoculated into each well of a 24-well plate at 6.5×10^5 cells in a volume of 200 μl. A cell culture insert, Millicell (hanging type, membrane filter with a pore size of 0.4 μm; Millipore, Billerica, USA, see Fig. 1) was set into each well, then GM cells (cells with releasing function as sniper cells) were inoculated into Millicell for 1.3×10^6 cells in a volume of 600 μl. In the case of the BY4741Δ*CYC8* strain, 200 μl of SDC-W was added into Millicell after 65 h of cocultivation. As a control, non-GM cells were inoculated into 24-well plates as target cells: in this case, Millicell was not inserted into the wells. After co-cultivation at 30°C with shaking at 1,200 rpm, cells were harvested, and in each sample, fluorescence intensity was measured using a cell sorter. For microscopic observation, yeast cells were washed with PBS twice and observed by fluorescence microscopy.

Sodium dodecyl sulfate polyacrylamide gel electrophoresis and Western blotting of GM cell lysates and supernatants

Yeast cells transformed with pSDLn4 and pSDLc4 were grown in 100 ml of SDC-W medium for 2 days after pre-culture. Cells were then collected by centrifugation at 20,000×*g* for 20 min at 4°C. Supernatants were filtrated using 0.2 μm Steradisc (Kurabo, Osaka, Japan) and concentrated by ultrafiltration using Microcon YM-30 filters (Millipore). Cell pellets were washed with 50 ml of 50 mM Tris–HCl (pH 7.8) containing 5 mM ethylenediamine tetraacetic acid and 8 M urea twice and centrifuged under the same condition. Cells were homogenized using glass beads (3,000 rpm at 4°C for 1 min, twice). Super natants were collected by centrifugation at 20,000×*g* for 20 min at 4°C. After filtration using a 0.2-μm Steradisc, lysates were concentrated by ultrafiltration using Microcon YM-30 filters. Concentrated supernatants were analyzed by sodium dodecyl sulfate polyacrylamide gel electrophoresis (SDS-PAGE) using PAGEL 5–20% gradient gel (Atto, Tokyo, Japan) and by Western blotting. For Western blotting, an anti-flag antibody conjugated with horseradish peroxidase was used at a volume of 1:1,000.

Blue native-PAGE of GM cell lysates

Yeast cells transformed with pSDLn4, pSDLc4, and pWGP3 were subjected to the glass bead method as described above. Using supernatants obtained, blue-native PAGE (BN-PAGE) was performed as previously reported (Wittig et al. 2006) with native PAGETM 4–16% bis–Tris gel (Invitrogen, CA, USA).

Results

Production of EGFP fusion proteins by GM yeast

The plasmids pSDLn4 and pSDLc4 for the N-terminal- and C-terminal-free display of EGFP (Fig. 2) were constructed, respectively. Growth-phase-related production of the EGFP-fusion protein was observed by fluorescence microscopy and fluorescence-activated cell sorting (FACS) analysis (Fig. 3). In the early growth phase, yeast cells transformed with pSDLn4, pSDLc4, and pWGP3 (control) did not show any fluorescence. In the stationary phase, yeast cells transformed with pSDLn4 and pSDLc4 showed green fluorescence inside and in the periphery of each cell. Observed fluorescence indicates the EGFP fusion proteins on the way of secretion from GM sniper yeasts. FACS analysis showed a marked change in subcellular fluorescence intensity. SDS-PAGE and Western blotting also showed the production of FLAG-conjugated recombinant proteins. These results demonstrated the production of EGFP fusion proteins from GM sniper yeasts and suggested the secretion of these proteins from cells.

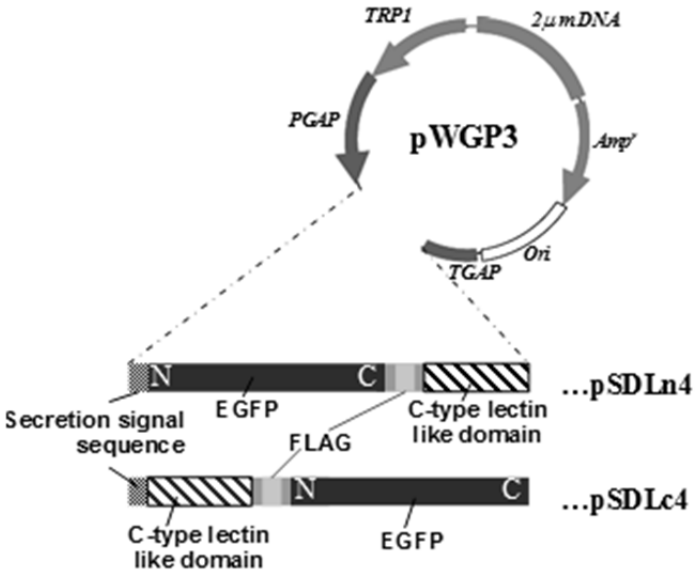

Fig. 2 Plasmids constructed in this study for MSSM Plasmids pSDLn4 and pSDLc4 were constructed for N-terminal-free and C-terminal-free EGFP surface display of non-GMO, respectively. In accompany with the secretion signal sequence, EGFP fragment was fused to N- or C-terminal of CTLD. Between EGFP fragment and CTLD was a FLAG-tag for immunodetetion. pWGP3 as control was used as the cassette vector in which the constructs were introduced. PGAP: GAPDH promoter, TGAP: GAP terminator

Transfer of EGFP fluorescence from GM sniper yeast to non-GM target cells in co-cultivation

To investigate the targeting of recombinant EGFP proteins fromGMsniper to non-GM target yeast cells, we cocultivated GMsniper and non-GMtarget cells usingMillicell (Millipore) as shown in Fig. 1. After cocultivation using 24-well plates and the Millicell system, BY4741Δ*CYC8*, one of the target cells, showed a marked increase in fluorescence intensity, as determined by FACS analysis (Fig. 4). Observation under a fluorescence microscope confirmed the green fluorescence on the surface of BY4741Δ*CYC8* strain cells examined, a shown in Fig. 4. There was no increase in fluorescence intensity on other examined strains. These results suggest that the specific display of recombinant EGFP on target yeast cells (in this case, BY4741Δ*CYC8*) succeeded. The target yeast cell represents a specific state of non-GM cells (Conlan et al. 1999). To evaluate whether the recombinant EGFP forms were trimers, BN-PAGE and Western blotting were performed (Fig. 3). BN-PAGE analysis showed that the fusion protein produced by GM sniper yeast cells was a monomer, judging from the result of SDS-PAGE.

Confirmation of survival of targeted cells after treatment with MSSM

MSSM alters properties of living cells without genetic modifications. This is the difference of MSSM from previous methods involving chemical treatments (Bosma et al. 2006). Therefore, cells used for MSSM should survive after cocultivation. We confirmed that cells were alive after treatment with MSSM by sorting and seeding 1×10^3 cells onto agar medium and calculating their viability. As a result, the pSDLc4-transformant and BY4741Δ*CYC8* both survived on the SDC-W agar medium. Almost all the BY4741Δ*CYC8* cells formed colonies. For each colony, colony PCR was performed to confirm that there were no plasmids in non-GM target cells. It was proved that GM target cells survived and did not contain plasmids. On YPD medium, the average viability of BY4741ΔCYC8 after 4 days of co-cultivation was 51.6% (n=3) when compared to the viability of cells before co-cultivation.

Specificity of CTLD produced by GM sniper cells

We investigated whether other strains can be target cells besides the specific BY4741Δ*CYC8* strain. We examined changes of fluorescence intensity in the *S. cerevisiae* BY4741 and MT8-1 strains and *C. albicans* after targeting with MSSM. After 1, 2, and 4 days of co-cultivation, all the strains showed nearly no transfer of fluorescence (Fig. 5).

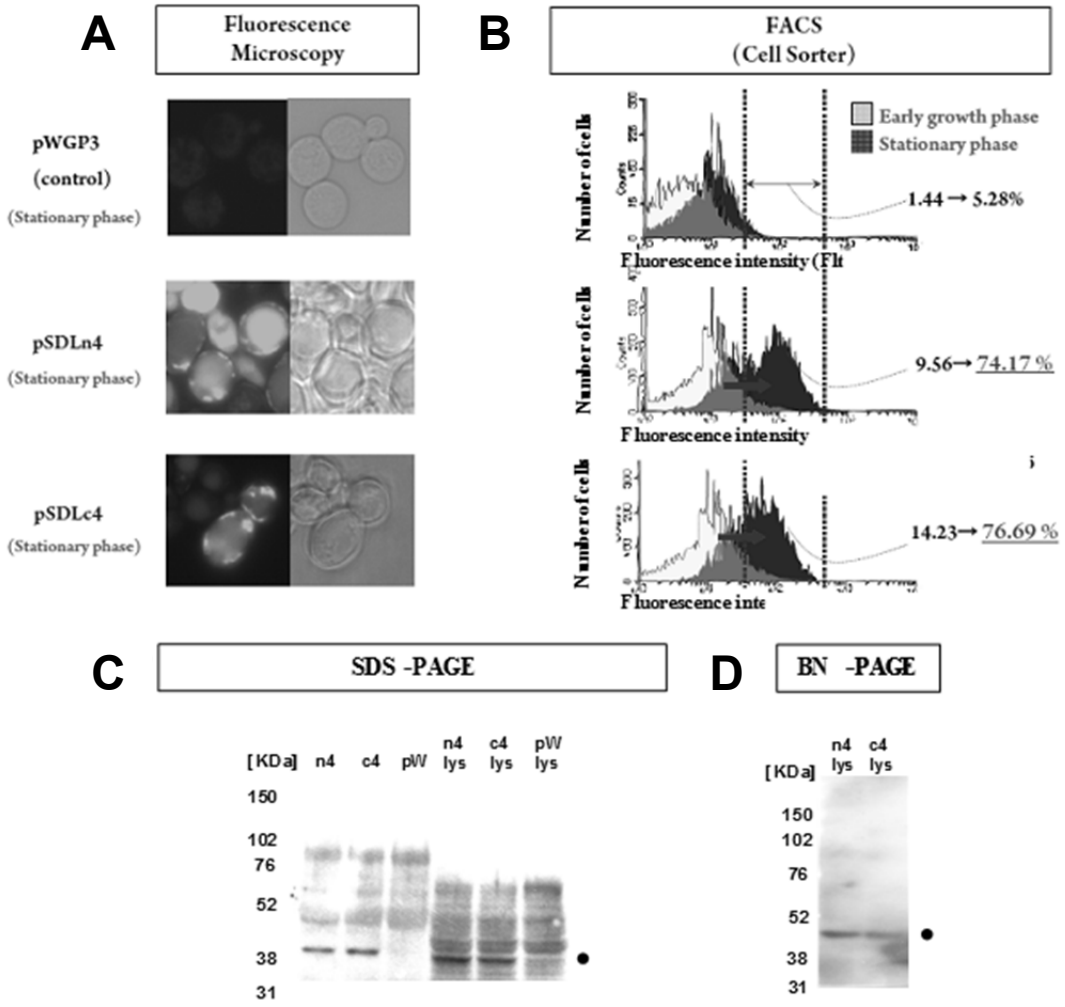

Fig. 3 Recombinant fusion proteins produced and secreted from GM sniper cells Phase contrast and fluorescence observation is shown (A). In fluorescence microscopy (Right), yeast cells transformed with pSDLn4 and pSDLc4 showed green fluorescence inside and in the periphery of the cells, while yeast cells transformed with pWGP3 showed no fluorescence. In FACS analysis (B) showed that from early growth phase (white area) to stationary phase (gray area), yeast cells transformed with pSDLn4 and pSDLc4 showed marked change of fluorescence intensity and subcellular localization. At stationary phase, as the percentage of cells with high (> 28) fluorescence intensity (% Total cells) was 5.28 %, 74.2 %, 76.7 % (At early growth phase, the percentage was 1.44 %, 9.65 %, 14.2 %) for yeast cells transformed with pWGP3, pSDLn4, and pSDLc4, respectively. SDS-PAGE (C, Western blotting) and BN-PAGE (D, Western blotting): yeast cells transformed with pWGP3 (pW), pSDLn4 (n4), and pSDLc4 (c4) were homogenized, and lysates (lys) and supernatant of culture medium, in C, were analyzed by Western blotting. Samples from yeast cells transformed with pSDLn4 and pSDLc4 showed each single band. Closed circle indicates the observed band of fusion proteins. Mr standard markers (Full range rainbow marker; GE Healthcare, Stockholm, Sweden) were used. n4/ c4/ pW: supernatants, n4 lys/ c4 lys/ pW lys: lysates

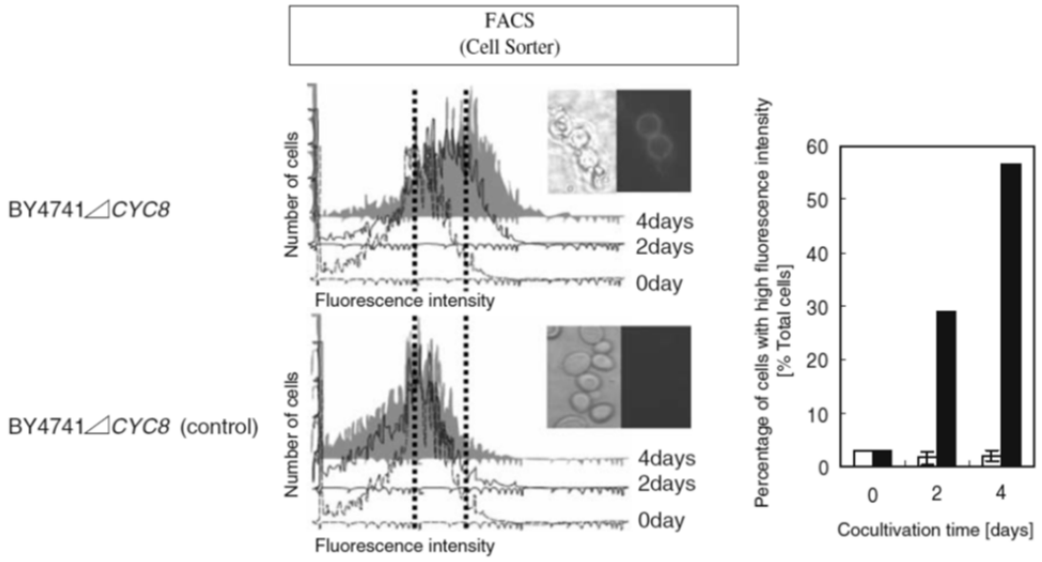

Fig. 4 Demonstration of transfer of recombinant proteins to non-GM S. cerevisiae BY4741ΔCYC8 target cells from GM sniper cells After 0, 2, and 4 days of co-cultivation with GM sniper cells, non-GM target cells (*S. cerevisiae* BY4741Δ*CYC8*) was analyzed using the cell sorter. As a control, the same strain was cultivated in 24-well plate. After 2 and 4 days, co-cultivated non-GM yeast showed marked shift of fluorescence intensity. The percent total cells defined in Fig. 3 that showed over 28 of fluorescence intensity increased from 2 to 4 days. By fluorescence microscopic observation, co-cultivated non-GM target yeast cells clearly showed green fluorescence on the surface of the cells (photos). Graph shows the presentation of percent total cells that exhibited fluorescence intensity >28 in each stage. White bars control, black bars co-cultivated BY4741Δ*CYC8*

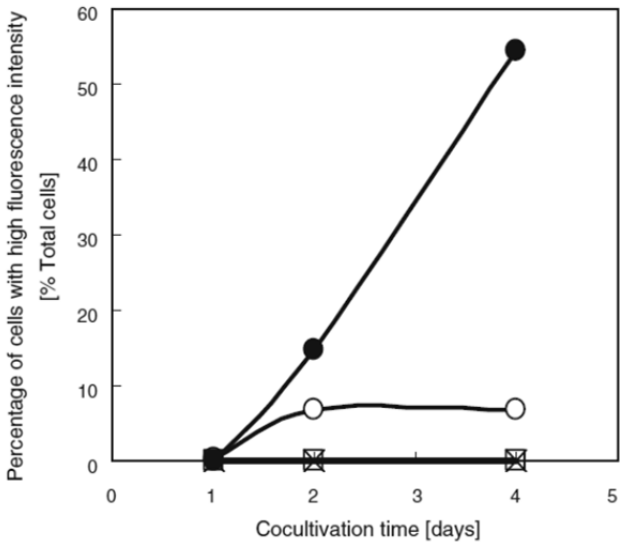

Fig. 5 Specificity of non-GM target cells as receiver cells *S. cerevisiae* MT8-1, BY4741, BY4741Δ*CYC8* strains, and *C. albicans* were co-cultivated with GM sniper cells. As a control, the same strain was cultivated in 24-well plate. After 1, 2, and 4 days, co-cultivated cells and control cells were analyzed using the cell sorter. The average count of percent total cells that showed fluorescence intensity (>28) were represented. Percent total cell count of control cells was subtracted from each count. Open circle *S. cerevisiae* MT8-1, closed circle *S. cerevisiae* BY4741ΔCYC8, open square C. albicans, X S. cerevisiae BY4741

Development of a novel instrument for large-scale co-cultivation

Instruments for large-scale co-cultivation of microbes were developed with aids of Sanki-seiki and Geo support. The instrument has two compartments that are separated by filter membranes, which arrow proteins and small molecules to pass through but not cells (Fig. 6).

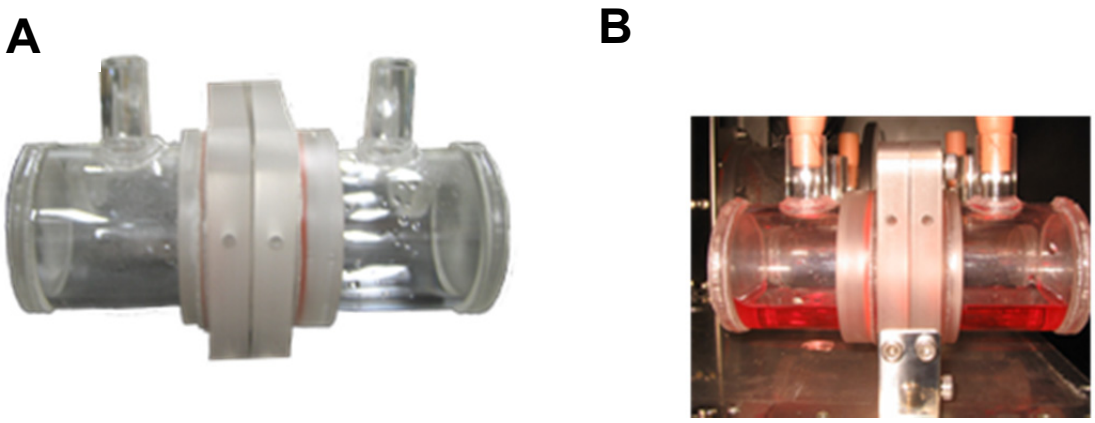

Fig. 6 Development of a novel instrument for large-scale co-cultivation

Discussion

The targeting of the recombinant protein from GM sniper to living non-GM target cells using a novel co-cultivation system with a membrane filter was demonstrated. The protein targeting system was designated as the molecular sniping and shooting method (MSSM). MSSM has the following features: it allows analysis of two different strains in co-cultivation state separately and simultaneously; and it allows production of non-GM target cells with the ability derived from functional recombinant proteins without self-production in a living state.

In MSSM, non-GM target strains showed a marked increase in fluorescence intensity, which indicates the recombinant fusion proteins were produced and secreted by GM sniper cells to non-GM target cells in the filter membrane-separated reactor (Fig. 4). These results indicate that fusion proteins produced by GM sniper cells were specifically targeted on the surface of non-GM target cells. The co-cultivation test showed that *S. cerevisiae* MT8-1 strain hardly binds the constructed fusion proteins on its surface. Therefore, *S. cerevisiae* MT8-1 cells were suitable as GM sniper yeast cells in the present study.

BN-PAGE analysis showed that the constructed fusion protein was a monomer. The fusion protein contains the CTLD of human SP-D, which was reported to have no binding activity in the monomer state; it is required to be a trimmer to exhibit binding ability to lipopolysaccharides and

phospholipids (Kishore et al. 1996) and bacteria (Eda et al. 1997). However, interestingly, our fusion proteins bound to its ligand in the monomer state. The observation that C. albicans (previously reported suitable strain for SP-D) showed no change in the fluorescence intensity (Fig. 5) also suggests that CTLD used in MSSM exhibited the interesting change of property of its binding target.

Summary

A novel method was developed to coat living wt cells with functional recombinant proteins. First, I prepared yeast cells to secrete constructed proteins that have two domains: a functional domain and a binding domain that recognizes other cells. Second, I co-cultivated recombinant protein-secreting cells and wt cells that share and co-utilize the medium containing recombinant using a filter-membrane-separated cultivation reactor. Engineered yeast cells secreted enhanced green fluorescent protein (EGFP) fusion proteins to culture medium. After co-cultivation, EGFP fusion proteins were targeted to *Saccharomyces cerevisiae* BY4741Δ*CYC8* cell surface. In addition, I participated in developing novel culture devises for large scale co-cultivation.

References

1. Allen MJ, Voelker DR, Mason RJ (2001) Interactions of surfactant proteins A and D with *Saccharomyces cerevisiae* and *Aspergillus fumigatus*. Infect. Immun. 69:2037-2044.
2. Bateman A, Bycroft M (2000) The structure of a LysM domain from *E. coli* membrane-bound lytic murein transglycosylase D (MltD). J. Mol. Biol. 299:1113-1119.
3. Bosma T, Kanninga R, Neef J, Audouy SA, van Roosmalen ML, Steen A, Buist G, Kok J, Kuipers OP, Robillard G, Leenhouts K (2006) Novel surface display system for proteins on nongenetically modified gram-positive bacteria. Appl. Environ. Microbiol. 72:880-889.
4. Clark H, Reid K (2003) The potential of recombinant surfactant protein D therapy to reduce inflammation in neonatal chronic lung disease, cystic fibrosis, and emphysema. Arch. Dis. Child .88:981-984.
5. Conlan RS, Gounalaki N, Hatzis P, Tzamarias D (1999) The Tup1-Cyc8 protein complex can shift from a transcriptional co-repressor to a transcriptional co-activator. J. Biol. Chem. 274:205-210.
6. Eda S, Suzuki Y, Kawai T, Ohtani K, Kase T, Fujinaga Y, Sakamoto T, Kurimura T, Wakamiya N (1997) Structure of a truncated human surfactant protein D is less effective in agglutinating bacteria than the native structure and fails to inhibit haemagglutination by influenza A virus. Biochem. J. 323:393-399.
7. Georgiou G, Stathopoulos C, Daugherty PS, Nayak AR, Iverson BL, Curtiss R 3rd (1997) Display of heterologous proteins on the surface of microorganisms: from the screening of

combinatorial libraries to live recombinant vaccines. Nat. Biotechnol. 15:29-34.

8. Hallman M, Haataja R (2006) Surfactant protein polymorphisms and neonatal lung disease. Semin. Perinatol. 30:350-361.
9. Hug K (2008) Genetically modified organisms: do the benefits outweigh the risks? Medicina (Kaunas) 44:87-99.
10. Ito H, Fukuda Y, Murata K, Kimura A (1983) Transformation of intact yeast cells treated with alkali cations. J. Bacteriol. 153:163-168.
11. Jose J (2006) Autodisplay: efficient bacterial surface display of recombinant proteins. Appl. Microbiol. Biotechnol. 69:607-614.
12. Khaw TS, Katakura Y, Ninomiya K,Moukamnerd C, Kondo A, Ueda M, Shioya S (2007) Enhancement of ethanol production by promoting surface contact between starch granules and arming yeast in direct ethanol fermentation. J. Biosci. Bioeng. 103:95-97.
13. Kishore U, Wang JY, Hoppe HJ, Reid KB (1996) The alpha-helical neck region of human lung surfactant protein D is essential for the binding of the carbohydrate recognition domains to lipopolysaccharides and phospholipids. Biochem. J. 318:505-511.
14. Kon T, Nakakura S, Mitsubayashi K (2005) Intracellular analysis of Saccharomyces cerevisiae using CLSM after ultrasonic treatments. Nanomedicine 1:159-163.
15. Kondo A, Ueda M (2004) Yeast cell-surface display — applications of molecular display. Appl. Microbiol. Biotechnol. 64:28-40.
16. Kuroda K, Ueda M (2003) Bioadsorption of cadmium ion by cell surface-engineered yeasts displaying metallothionein and hexa-His. Appl. Microbiol. Biotechnol. 63:182-186.
17. Kuroda K, Ueda M (2005) Effective display of metallothionein tandem repeats on the bioadsorption of cadmium ion. Appl. Microbiol. Biotechnol. 70:458-463.
18. Kuzmenko AI, Wu H, McCormack FK (2006) Pulmonary collectins selectively permeabilize model bacterial membranes containing rough lipopolysaccharide. Biochemistry 45:2679-2685.
19. Meschi J, Crouch EC, Skolnik P, Yahya K, Holmskov U, Leth-Larsen R, Tornoe I, Tecle T, White MR, Hartshorn KL (2005) Surfactant protein D binds to human immunodeficiency virus (HIV) envelope protein gp120 and inhibits HIV replication. J. Gen. Virol. 86:3097-3107.
20. Modlich U, Bohne J, Schmidt M, von Kalle C, Knoss S, Schambach A, Baum C (2006) Cell-culture assays reveal the importance of retroviral vector design for insertional genotoxicity. Blood 108:2545-2553.
21. Ohnuma T, Onaga S, Murata K, Taira T, Katoh E (2008) LysM domains from *Pteris ryukyuensis* chitinase-A: a stability study and characterization of the chitin-binding site. J. Biol. Chem. 283:5178-5187.
22. Palaniyar N, Clark H, Nadesalingam J, Shin MJ, Hawgood S, Reid KB (2005) Innate immune collectin surfactant protein D enhances the clearance of DNA by macrophages and minimizes

anti-DNA antibody generation. J. Immunol. 174:7352-7358.

23. Radutoiu S, Madsen LH, Madsen EB, Jurkiewicz A, Fukai E, Quistgaard EM, Albrektsen AS, James EK, Thirup S, Stougaard J (2007) LysM domains mediate lipochitin-oligosaccharide recognition and Nfr genes extend the symbiotic host range. EMBO J. 26:3923-3935.
24. Samuelson P, Gunneriusson E, Nygren PA, Stahl S (2002) Display of proteins on bacteria. J. Biotechnol. 96:129-154.
25. Schreuder MP, Mooren AT, Toschka HY, Verrips CT, Klis FM (1996) Immobilizing proteins on the surface of yeast cells. Trends Biotechnol. 14:115-120.
26. Shibasaki S, Ueda M, Iizuka T, Hirayama M, Ikeda Y, Kamasawa N, Osumi M, Tanaka A (2001) Quantitative evaluation of the enhanced green fluorescent protein displayed on the cell surface of *Saccharomyces cerevisiae* by fluorometric and confocal laser scanning microscopic analyses. Appl. Microbiol. Biotechnol. 55:471-475.
27. Shigechi H, Uyama K, Fujita Y, Matsumoto T, Ueda M, Tanaka A, Fukuda H, Kondo A (2002) Efficient ethanol production from starch through development of novel flocculent yeast strains displaying glucoamylase and co-displaying or secreting α-amylase. J. Mol. Catal. B. Enzym. 17:179-187.
28. Shiraga S, Ueda M, Takahashi S, Tanaka A (2002) Construction of the combinatorial library of *Rhizopus oryzae* lipase mutated in the lid domain by displaying on yeast cell surface. J. Mol. Catal. 17:167-173.
29. Smith GP (1985) Filamentous fusion phage: novel expression vectors that display cloned antigens on the virion surface. Science 228:1315-1317.
30. Stratford M (1992) Yeast flocculation: reconciliation of physiological and genetic viewpoints. Yeast 8:25-38.
31. Tajima M, Nogi Y, Fukasawa T (1985) Primary structure of the *Saccharomyces cerevisiae* GAL7 gene. Yeast 1:67-77.
32. Takahashi S, Ueda M, Tanaka A (2001) Function of the prosequence for in vivo folding and secretion of active *Rhizopus oryzae* lipase in *Saccharomyces cerevisiae*. Appl. Microbiol. Biotechnol. 55:454-462.
33. Tamaru Y, Ohtsuka M, Kato K, Manabe S, Kuroda K, Sanada M, Ueda M (2006) Application of the arming system for the expression of the 380R antigen from red sea bream iridovirus (RSIV) on the surface of yeast cells: a first step for the development of an oral vaccine. Biotechnol. Prog. 22:949-953.
34. Ueda M, Tanaka A (2000) Cell surface engineering of yeast: construction of arming yeast with biocatalyst. J. Biosci. Bioeng. 90:125-136.
35. Ueda M, Murai T, Shibasaki Y, Kamasawa N, Osumi M, Tanaka A (1998) Molecular breeding of polysaccharide-utilizing yeast cells by cell surface engineering. Ann. NY. Acad. Sci.

864:528-537.

36. Van Roosmalen ML, Kanninga R, El Khattabi M, Neef J, Audouy S, Bosma T, Kuipers A, Post E, Steen A, Kok J, Buist G, Kuipers OP, Robillard G, Leenhouts K (2006) Mucosal vaccine delivery of antigens tightly bound to an adjuvant particle made from foodgrade bacteria. Methods 38:144-149.
37. Van Rozendaal BA, van Spriel AB, van De Winkel JG, Haagsman HP (2000) Role of pulmonary surfactant protein D in innate defense against Candida albicans. J. Infect. Dis. 182:917-922.
38. Wadle A, Mischo A, Imig J, Wullner B, Hensel D, Watzig K, Neumann F, Kubuschok B, Schmidt W, Old LJ, Pfreundschuh M, Renner C (2005) Serological identification of breast cancerrelated antigens from a Saccharomyces cerevisiae surface display library. Int. J. Cancer 117:104-113.
39. Wan J, Zhang XC, Neece D, Ramonell KM, Clough S, Kim SY, Stacey MG, Stacey G (2008) A LysM receptor-like kinase plays a critical role in chitin signaling and fungal resistance in *Arabidopsis*. Plant Cell 20:471-481.
40. Wittig I, Braun HP, Schagger H (2006) Blue native PAGE. Nat. Protoc. 1:418-428.
41. Wu CH, Mulchandani A, Chen W (2008) Versatile microbial surfacedisplay for environmental remediation and biofuels production. Trends. Microbiol. 16:181-188.
42. Zelensky AN, Gready JE (2005) The C-type lectin-like domain superfamily. FEBS J. 272:6179-6217.

GENERAL CONCLUSION

The present study was conducted to reveal the molecular basis of the moonlighting protein enolase, particularly focusing on mechanisms regulating inter- and intracellular localization.

In chapter I, the Eno2p secretion pathway was investigated. It was revealed for the first time that Eno2p was secreted via a SNARE protein Tlg2p-driven unknown secretion pathway. In the study, the N-terminal amino acid region of Eno2p was found to be secreted while forming foci in the cell. The results suggested that the N-terminal region of Eno2p may be the region regulating Eno2p localization.

In chapter II, the first N-terminal foci-forming region was investigated in detail. It was found that the (5–25)-amino acid region was sufficient for foci formation. In addition, alanine substitution of the V22 residue was found to inhibit foci formation. Next, the correlation between the foci and localization of full-length Eno2p was investigated. Full-length Eno2p was found to form foci under hypoxia. Because V22 substitution to alanine diminished the foci-forming property of full-length Eno2p and both foci formed by the N-terminal region and full-length Eno2p colocalized, localization change in Eno2p is suggested to be regulated by the N-terminal region. Furthermore, the mechanisms and biological effects of the foci were investigated. Foci formation under hypoxia was regulated by the sensing pathway of mitochondrial ROS production. Moreover, the correlation between the changes in the metabolic pathway and foci formation in the cell suggests the role of the foci as a metabolic regulator. The universality of the sensing and glycolytic pathways suggests that foci formation is a conserved way of regulating cellular physiology.

In chapter III, novel methods and instruments for investigating extracellular roles of moonlighting proteins were prepared. Using these, the unknown functions of secreted enolase in *Saccharomyces cerevisiae* will be revealed.

In summary, the findings of present study suggest that the spatial reorganization of proteins regulates cellular physiology.

ACKNOWLEDGEMENTS

This thesis is submitted by the author to Kyoto University for the Doctor degree of Agriculture. The studies presented here have been carried out under the direction of Professor Mitsuyoshi Ueda in the Laboratory of Biomacromolecular Chemistry, Division of Applied Life Sciences, Graduate School of Agriculture, Kyoto University.

I would like to express my sincere gratitude to Professor Dr. Mitsuyoshi Ueda for his continuous guidance, patience, and encouragements. I am deeply grateful to Associate Professor Dr. Kouichi Kuroda for his support, guidance, understanding and encouragements throughout my laboratory life. I am also deeply grateful to Assistant Professor Dr. Hironobu Morisaka for his understanding, encouragements, continuous support and collaborations. I would like to express my sincere appreciation to Secretory Fukuko Suzuki to her understanding, patience and kindhearted support throughout my laboratory life. My deep appreciation goes to all the present and past members of Prof. Ueda's laboratory for their constant encouragement and support throughout this work.

I am deeply grateful to Dr. Masahiro Takagi, Professor of Japan Advanced Institute of Science and Technology, for his guidance, helpful collaboration, and warmhearted encouragements. I also thank all the members of Prof. Takagi's laboratory for their kindness supports.

I am also deeply grateful to Yasuhiro Sato of Carl Zeiss Microscopy Co., Ltd for his continuous and patient technical supports, helpful collaboration, and warm encouragements.

I would like to sincerely thank Dr. Hiro-o Hamaguchi, former Professor of Tokyo University and current Professor of Waseda University, for his kindness support, discussions, and encouragements on this work. I would like to thank Dr. Chikao Onogi and Taiga Wada of Prof. Hamaguchi's laboratory, for their technical supports and thoughtful discussions related to this work.

I would like to gratefully thank Dr. Wataru Fujibuchi, Professor of Kyoto University, for his continuous warm encouragements and thoughtful discussions on this work.

I gratefully acknowledge Dr. Hiroshi Harada, Principal Investigator of Group of Radiation and Tumor Biology, Career-Path Promotion Unit for Young Life Scientists, Kyoto University, for his suggestions and productive discussions on cell physiology under hypoxia.

I would like to sincerely thank Dr. Eiichiro Fukusaki, Professor of Osaka University for his thoughtful suggestions and helpful discussions on metabolic analysis, and continuous warm encouragements.

I would like to thank Dr. Randy Schekman at University of California, Berkeley, for providing the RSY282 (*sec23-1*) strain.

I acknowledge The JSPS Research Fellowships for Young Scientists [09J02920] from the Japan Society for the Promotion of Sciences.

Finally, I would like to sincerely thank my parents and brothers, Jirou, Futaba, Takurou, and Akira, for their deep understanding, continuous encouragements, and supports.

PUBLICATION

CHAPTER I

Miura, N., Kirino, A., Endo, S., Morisaka, H., Kuroda, K., Takagi, M., and Ueda, M.

Tracing putative trafficking of glycolytic enzyme enolase via SNARE-driven unconventional secretion

Eukaryot. Cell. **11**, 1075-1082 (2012)

CHAPTER II

Miura, N., Shinohara, M., Tatsukami, Y., Sato, Y., Morisaka, H., Kuroda, K., and Ueda, M.

Spatial reorganization of yeast enolase to switch carbon metabolic pathway under hypoxia

Submitted

CHAPTER III

Miura, N., Aoki, W., Tokumoto, N., Kuroda, K., and Ueda, M.

Cell surface modification for non-GMO without chemical treatment by novel GMO-coupled and -separated cocultivation method

Appl. Microbiol. Biotechnol. **82**, 293-301 (2009)

Other publications

In English

Shinya, R., Takeuchi, Y., Miura, N., Kuroda, K., Ueda, M., and Futai, K.

Surface coat proteins of the pine wood nematode, *Bursaphelenchus xylophilus*: profiles of stage and isolate-specific characters

Nematology, **11**, 429-438 (2009)

Aoki, W., Kitahara, N., Miura, N., Morisaka, H., Yamamoto, Y., Kuroda, K., and Ueda, M.

Comprehensive characterization of secreted aspartic proteases encoded by a virulence gene family in *Candida albicans*

J. Biochem., **150**, 431-438 (2011)

Aoki, W., Kitahara, N., Miura, N., Morisaka, H., Kuroda, K., and Ueda, M.

Profiling of adhesive properties of the agglutinin-like sequence (ALS) protein family, a virulent attribute of *Candida albicans*

FEMS Immunol. Med. Microbiol., **65**, 121-124 (2012)

Aoki, W., Kitahara, N., Miura, N., Morisaka, H., Yamamoto, Y., Kuroda, K., and Ueda, M.
Candida albicans Possesses Sap7 as a Pepstatin A-Insensitive Secreted Aspartic Protease
PLoS One, **7**, e32513 (2012)

Aoki, W., Kitahara, N., Miura, N., Morisaka, H., Kuroda, K., and Ueda, M.
Design of a novel antimicrobial peptide activated by virulent proteases
Chemical Biology & Drug Design, 80: 725–733 (2012)

Fushimi, T., Miura, N., Shintani, H., Tsunoda, H., Kuroda, K., and Ueda, M.
Mutant firefly luciferases with improved specific activity and dATP discrimination constructed by yeast cell surface engineering
Appl. Microbiol. Biotechnol., in press (doi: 10.1007/s00253-012-4467-4)

In Japanese

◆総説

黒田浩一、三浦夏子、植田充美, 『バイオマスデザインに向けた植物育種の新発想』, 「BIOINDUSTRY」, 25(4), 20-24 (2008)

黒田浩一、三浦夏子,『金属イオン吸着・回収に向けた細胞表層デザインと吸着分子の創製』, 「日本生物工学会誌」, 86(6), 280-282 (2008)

◆書籍

三浦夏子、林絵理、植田充美, 「シングルセル解析の最前線」(神原秀記・松永是・植田充美監修),『変異タンパク質およびタンパク質ドメインを用いた short RNA の回収、分離技術（p. 142-148)』シーエムシー出版, 2010.